TÉCNICO LISBOA

Biomechanical Analysis of Subjects after Surgical Repair of the Achilles Tendon

Marisa Isabel Clemente da Silva

Thesis to obtain the Master of Science Degree in

Biomedical Technologies

Supervisors: Prof. Miguel Pedro Tavares da Silva
Dr. Manuel Cassiano Neves

Examination Committee

Chairperson: Prof. Patrícia Margarida Piedade Figueiredo
Supervisor: Prof. Miguel Pedro Tavares da Silva
Members of the Committee: Prof. João Eurico da Fonseca
Prof. João Miguel Raposo Sanches

June 2014

Agradecimentos

Ao Professor Miguel Tavares da Silva pelo seu empenho na unidade curricular de Biomecatrónica, a qual desencadeou a minha motivação para o desenvolvimento deste trabalho, bem como a ajuda e esforço concedido como orientador científico no seu desenvolvimento.

Ao Dr. Manuel Cassiano Neves pelo empenho, ajuda e esforço concedido como orientador científico e clínico e pelo encaminhamento dos doentes por ele assistidos no Hospital CUF Descobertas para a avaliação no laboratório.

Ao Dr. João Vide pelo seu empenho e esforço concedido através do seu conhecimento científico e clínico.

Ao Sérgio Gonçalves e Tiago Malaquias por toda a paciência, por todo o apoio dado no laboratório nomeadamente nas aquisições dos dados e pelas tantas conversas e discussões.

Aos meus amigos e familiares, nomeadamente ao Carlos Sapateiro, à Luísa Clemente, à Cristiana Clemente, à Sandra Galiza e à Maria Costa pela disponibilidade em se submeterem às aquisições.

Aos meus amigos pelas palavras de conforto nas horas de maior desânimo, por nunca me deixaram desistir, e pelo apoio e compreensão nos momentos de ausência no decorrer da realização deste trabalho.

À minha família, em especial aos meus pais e às minhas avós pela oportunidade que me deram em continuar os meus estudos e ao meu irmão por apoiar-me sempre e nunca me deixar desistir.

Resumo

O estudo do movimento humano tem despertado bastante interesse ao longo dos tempos, na comunidade médica e científica. Este interesse permitiu o desenvolvimento de novas técnicas de análise. As metodologias multicorpo são um exemplo disso e permitiram o desenvolvimento de ajudas técnicas (ortóteses e próteses) mais personalizadas e o estudo dos impactos de determinada intervenção cirúrgica, nomeadamente as cirurgias ortopédicas.

Este trabalho foi desenvolvido com o intuito de se estudar os padrões da marcha em indivíduos que sofreram uma ruptura no tendão de Aquiles e se submeteram a uma intervenção cirúrgica. O interesse neste trabalho surgiu devido ao facto de existirem poucos estudos efectuados ou dados relativos aos indivíduos que sofrerem uma ruptura deste tipo e que reproduzam os padrões da marcha dos mesmos. Desta forma, foi necessário desenvolver um protocolo de análise em ambiente laboratorial que permitisse obter diversos parâmetros cinéticos, cinemáticos, espaciais/temporais e de activações musculares. Foram realizadas um conjunto de rotinas que permitiram automatizar e optimizar o processamento dos dados. Este estudo, que considerou indivíduos sem patologia e com patologia, foi elaborado recorrendo a metodologias multicorpo com coordenadas relativas, através do programa de simulação OpenSim. Os resultados obtidos apresentam consistência com a literatura. São exemplos dos resultados a diminuição do perímetro muscular no membro lesionado, a diferença nos valores e na distribuição das forças e pressões e a diferença dos momentos articulares no pé.

Palavras-Chave: Sistemas Multicorpo, Análise de Marcha, Tendão de Aquiles, Cinética, Cinemática, Activações Musculares

Abstract

The study of human movement has been subject of a great interest by the medical and scientific community. It was through this interest that new methods of study/analysis in these two areas arose. Dynamic multibody systems are an example of these methods and have enabled the development of more personalized orthoses and prostheses and pre-study of the impacts of some surgeries (orthopedic surgery).

This work was developed in order to study the gait patterns of subjects after surgical repair of a ruptured Achilles tendon. This study is relevant as there are not many data reported in this area. Thus, it was necessary to develop an analysis protocol in laboratory environment that allows to obtain several biomechanical parameters (kinetics, kinematics, spatial/temporal and muscle activations). A set of routines that allow to setup data processing were performed. This study considered pathological and non-pathological subjects and was carried out using the dynamic multibody systems of relative coordinates, using the OpenSim simulation program. These results showed consistency with the literature. For example, the distribution of plantar pressure differ between the two groups and the moment in some articulations of the foot is lower when compared to the same moment in the control group.

Keywords: Multibody Dynamic System, Gait Analysis, Achilles tendon, Kinetics, Kinematics and Muscle Activations

Contents

Agradecimentos III
Resumo V
Abstract VII
Keywords VII
List of Figures XIII
List of Tables XV
List of Graphs XVII
Glossary XXI
List of Symbols XXIII
Chapter I 1
1. Introduction 1
1.1 Motivation 2
1.2 Objectives 3
1.3 Literature Review 3
1.4 Main Contributions 4
1.5 Structure and Organization 5
Chapter II 7
2. Anatomy 7
2.1 Skeletal System – Thigh, Leg and Foot 7
2.2 Muscular System – Thigh, Leg and Foot 8
2.3 Foot Joints 10
2.3.1 Ankle or Talocrural Joint 11
2.3.2 Talocalcaneal or Subtalar Joint 12
2.3.3 Metatarsophalangeal Joints 12
2.3.4 Motions of the Ankle, Subtalar and Metatarsophalangeal Joints 12
2.3.5 Achilles tendon 12
2.3.6 Ruptures of Achilles tendon and surgery techniques of repair Achilles tendon 13
3. Human Gait 15
3.1 Definitions and Terminology 15
3.1.1 Spatial Terminology 15
3.1.2 Terminology associated with gait 17
3.1.3 Movements 17

3.2 Gait Cycle 18
3.3 Theories of Human Walking 20
3.3.1 Theory of inverted pendulum 20
3.3.2 Theory of six gait determinants 20
3.4 Plantar Pressure 21
3.4.1 Foot alignment vs. arch type of foot and Centre of Pressure 21
3.4.2 Pressure Distribution 22
3.5 Gait Cycle and Achilles tendon 22
3.5.1 Motion of limbs and articulations 23
3.5.2 Gait Cycle and muscles related to the Achilles tendon 23
Chapter IV 27
4. Multibody Dynamic Systems 27
4.1 Multibody Systems 27
4.1.1 Kinematic Analysis of Multibody Systems 29
4.1.2 Dynamic Analysis of Multibody Systems 30
4.2 OpenSim Software 30
4.2.1 Multibody Dynamic Systems in OpenSim 31
4.2.1.1 Inverse Kinematics in OpenSim 32
4.2.1.2 Inverse Dynamics in OpenSim 33
4.2.1.3 Computed Muscle Control 33
Chapter V 35
5. Model and Protocol Definition 35
5.1 Questionnaires 35
5.2 Model Definition 36
5.3 Acquisition Protocol 37
5.4 Data Treatment Protocol 40
5.4.1 Data Treatment using QTM 40
5.4.2 Preparing the OpenSim input files 40
5.4.3 Data Treatment using OpenSim 41
5.4.4 Data Treatment using Footscan 42
5.4.5 Data Treatment using GAITRite 43
5.4.6 Data Treatment using ANOVA 43
Chapter VI 45
6 Results 45

6.1 Presentation of Results 45
6.2 Discussion of Results 47
6.2.1 Questionnaires 47
6.2.2 Measured Results 47
6.2.3 Time-Distance Parameters 48
6.2.3.1 ANOVA Results 49
6.2.4 Plantar Pressure Results 49
6.2.4.1 ANOVA results 53
6.3 Kinematic Results 53
6.3.1 Static GRF 54
6.3.2 Dynamic GRF 55
6.3.3 Kinematic Data 56
6.3.3.1 Gait Cycle Analysis – one stride 56
6.3.3.2 IK Analysis – healthy foot vs injured foot 59
6.3.3.3 IK Analysis – Patients vs Control Group 65
6.3.4 Dynamic Analysis 69
6.3.4.1 ID Analysis – Healthy Foot vs. Injured Foot 69
6.3.4.2 ID Analysis – Patients vs Control Group 72
6.3.4.3 CMC – Patients 76
Chapter VII 87
7 Conclusions and Future Developments 87
7.1 Conclusion 87
7.2 Future Developments 89
References 91
Appendix 94
Appendix I – Clinical rating system for the ankle and hind foot – AOFAS Score 94
Appendix II – SF-v36 95
Appendix III – Static Images of Plantar Pressures of patients 97
Appendix IV – Graphs of Control Group 98
IK Graphs of Control Group 98
ID Graphs of Control Group 98
CMC Graphs of Control Group 99

List of Figures

Figure 2.1 – Muscles of the leg (Gray, 2013). 8
Figure 2.2 – Right Foot Muscles: Superficial Muscles (a), Deep Muscles (b) (Seeley et al., 2008). 9
Figure 2.3 – Foot Joints in top view and lateral view. 11
Figure 2.4 – Posterior View of ankle joint (Hall, 2003). 11
Figure 2.5 – Revolute joint (Seeley et al., 2008) 11
Figure 2.6 – Ellipsoid joint (Seeley et al., 2008). 12
Figure 2.7 – Achilles tendon anatomy (Seeley et al., 2008). 13
Figure 3.1 – Spatial Reference (Seeley et al., 2008). 16
Figure 3.2 – Anatomical Reference Position (Gray, 2013). 16
Figure 3.3 – Time distance parameters (Vaughan et al., 1999). 17
Figure 3.4 – Most Referenced Movements in this work (Completo & Fonseca, 2011). 18
Figure 3.5 – (a) The sequence of normal gait cycle and (b) The events of the gait (Vaughan et al., 1999) 19
Figure 3.6 – 3rd Gait Determinant – Knee Flexion during Stance Phase (Saunders et al., 1953). 20
Figure 3.7 – 4th and 5th Foot, Ankle and Knee Mechanisms (Herr, 2009). 21
Figure 3.8 – 7th Gait Determinant (Herr, 2009). 21
Figure 4.1 – Schematic representation of a generic multibody system (Flores et al., 2008). 27
Figure 4.2 – Relative coordinates (Silva, 2012). 28
Figure 4.3 – Inputs and outputs of IK in OpenSim. 32
Figure 4.4 – Inputs and outputs files of ID in OpenSim. 33
Figure 4.5 – Generic Hill-Type muscle model. 33
Figure 4.6 – Inputs and outputs files of Control Muscle Control in OpenSim. 34
Figure 5.1 – Musculoskeletal model defined in OpenSim (Frontal View, Lateral View and Posterior View) used in the analyses. 36
Figure 5.2 Schematic Representation of the foot segments. 37
Figure 5.3 – Spatial arrangement of cameras in LBL. 38
Figure 5.4 – Location of the markers in subject's body. 39
Figure 5.5 – Flow-Chart summarizing the data treatment. 40
Figure 5.6 – Axes Convention (a) OpenSim, (b) AMTI and (c) Cameras. 41
Figure 5.7 – Force progression in the two foot segments. 41
Figure 5.8 – Flow-Chart summarizing the data treatment in OpenSim. 42
Figure 5.9 – Flow-Chart summarizing the data treatment in Footscan. 42
Figure 5.10 – Regions Division of the left foot and the right foot by footscan. 43
Figure 5.11 – Flow-Chart summarizing the data treatment in GAITRite. 43

List of Tables

Table 2.1 – Description of the external muscles of the foot – ANTERIOR COMPARTIMENT (Esperança Pina 2010; Seeley et al. 2008). 9
Table 2.2 – Description of the external muscles of the foot – LATERAL COMPARTIMENT 9
Table 2.3 – Description of the external muscles of the foot – POSTERIOR COMPARTIMENT (Esperança Pina 2010; Seeley et al. 2008). 10
Table 2.4 – Description of the internal muscles of the foot (Esperança Pina 2010; Seeley et al. 2008). 10
Table 2.5 – Motions of Joints (Hall 2003). 12
Table 3.0.1 – Summary of phases of gait cycle and accompanying motions of lower limb joints (Rodgers 1988) 23
Table 5.1 – Anatomical segments of the model defined, and corresponding rigid bodies. 37
Table 5.2 – Markers List. 39
Table 6.1 – Data of Control Group. 45
Table 6.2 – Data of Patients. 46
Table 6.3 – Results of questionnaire – AOFAS score and SF-36v2. 47
Table 6.4 – Perimeter of Leg. 47
Table 6.5 – Articular Movements – Dorsiflexion and Plantar flexion. 48
Table 6.6 – Time-Distance Parameters of Control Group. 48
Table 6.7 – Time-Distance Parameters of Patients. 49
Table 6.8 – ANOVA: single factor of velocity. 49
Table 6.9 – Foot characteristics. 50
Table 6.10 – Subtalar Angle and Foot Axis Angle. 50
Table 6.11 – Minimum and Maximum Force Normalized of Control Group (N/kg). 51
Table 6.12 – Minimum and Maximum Plantar Pressure of Control Group (N/cm^2). 51
Table 6.13 – Minimum and Maximum Pressure of patients (N/cm^2). 52
Table 6.14 – Minimum and Maximum Force of patients (N/kg). 52
Table 6.15 – ANOVA: single factor of Maximum Force. 53
Table 6.16 – ANOVA: single factor of Minimum Force. 53
Table 6.17 – ANOVA: single factor of Maximum Pressure. 53
Table 6.18 – ANOVA: single factor of Minimum Pressure. 53
Table 6.19 – Static GRF of Control Group (*could not get this value). 54
Table 6.20 – Static GRF of Patients (*could not get this value). 54
Table 6.21 – Hip flexion angle (a) and Knee Angle (b) of patients. 65
Table 6.22 – Ankle Angle (a) and MTP angle (b) of patients. 65
Table 6.23 – Mechanical Power of Patients. 84
Table 6.24 – Force Muscle of Patients. 85
Table 7.1 – Summary table of what variables that showed significant changes. 89

List of Graphs

Graph 6.1 – GRF in sagittal plane of patient 1: Right Foot vs Injured Foot (a); 55
Graph 6.2 – GRF in sagittal plane of patient 3: Right Foot vs Injured Foot (a); 55
Graph 6.3 – GRF in sagittal plane of patient 5: Injured Foot vs Left Foot (a); 55
Graph 6.4 – GRF in sagittal plane of patient 7: Injured Foot vs Left Foot. 55
Graph 6.5 – Joint angles of patient 1: (a) Hip Flexion Angle, (b) Knee Angle, (c) Ankle Angle, (d) Subtalar Angle and (e) Metatarsophalangeal Angle for one stride. 56
Graph 6.6 – Joint angles of patient 2: (a) Hip Flexion Angle, (b) Knee Angle, (c) Ankle Angle, (d) Subtalar Angle and (e) Metatarsophalangeal Angle for one stride. 57
Graph 6.7 – Joint angles of patient 3: (a) Hip Flexion Angle, (b) Knee Angle, (c) Ankle Angle, (d) Subtalar Angle and (e) Metatarsophalangeal Angle for one stride. 57
Graph 6.8 – Joint angles of patient 4: (a) Hip Flexion Angle, (b) Knee Angle, (c) Ankle Angle, (d) Subtalar Angle and (e) Metatarsophalangeal Angle for one stride. 58
Graph 6.9 – Joint angles of patient 5: (a) Hip Flexion Angle, (b) Knee Angle, (c) Ankle Angle, (d) Subtalar Angle and (e) Metatarsophalangeal Angle for one stride. 58
Graph 6.10 – Joint angles of patient 6: (a) Hip Flexion Angle, (b) Knee Angle, (c) Ankle Angle, (d) Subtalar Angle and (e) Metatarsophalangeal Angle for one stride. 58
Graph 6.11 – Joint angles of patient 7: (a) Hip Flexion Angle, (b) Knee Angle, (c) Ankle Angle, (d) Subtalar Angle and (e) Metatarsophalangeal Angle for one stride. 59
Graph 6.12 – Intra-variability joint angles of patient 1: (a) Hip Flexion Angle, (b) Knee Angle, (c) Ankle Angle, (d) Subtalar Angle and (e) Metatarsophalangeal Angle. 60
Graph 6.13 – Intra-variability joint angles of patient 2: (a) Hip Flexion Angle, (b) Knee Angle, (c) Ankle Angle, (d) Subtalar Angle and (e) Metatarsophalangeal Angle. 61
Graph 6.14 – Intra-variability joint angles of patient 3: (a) Hip Flexion Angle, (b) Knee Angle, (c) Ankle Angle, (d) Subtalar Angle and (e) Metatarsophalangeal Angle. 62
Graph 6.15 – Intra-variability joint angles of patient 4: (a) Hip Flexion Angle, (b) Knee Angle, (c) Ankle Angle, (d) Subtalar Angle and (e) Metatarsophalangeal Angle. 62
Graph 6.16 – Intra-variability joint angles of patient 5: (a) Hip Flexion Angle, (b) Knee Angle, (c) Ankle Angle, (d) Subtalar Angle and (e) Metatarsophalangeal Angle. 63
Graph 6.17 – Intra-variability joint angles of patient 6: (a) Hip Flexion Angle, (b) Knee Angle, (c) Ankle Angle, (d) Subtalar Angle and (e) Metatarsophalangeal Angle. 64
Graph 6.18 – Intra-variability joint angles of patient 7: (a) Hip Flexion Angle, (b) Knee Angle, (c) Ankle Angle, (d) Subtalar Angle and (e) Metatarsophalangeal Angle. 64
Graph 6.19 – Control Group vs patient 1: (a) Hip Flexion Angle, (b) Knee Angle, (c) Ankle Angle, (d) Subtalar Angle and (e) Metatarsophalangeal Angle. 66
Graph 6.20 Control group vs. Patient 2: (a) Hip Flexion Angle, (b) Knee Angle, (c) Ankle Angle, (d) Subtalar Angle and (e) Metatarsophalangeal Angle. 66
Graph 6.21 – Control group vs. Patient 3: (a) Hip Flexion Angle, (b) Knee Angle, (c) Ankle Angle, (d) Subtalar Angle and (e) Metatarsophalangeal Angle. 67

Graph 6.22 – Control group vs. Patient 5: (a) Hip Flexion Angle, (b) Knee Angle, (c) Ankle Angle, (d) Subtalar Angle and (e) Metatarsophalangeal Angle. 67
Graph 6.23 – Control group vs. Patient 6: (a) Hip Flexion Angle, (b) Knee Angle, (c) Ankle Angle, (d) Subtalar Angle and (e) Metatarsophalangeal Angle. 68
Graph 6.24 – Control group vs. Patient 7: (a) Hip Flexion Angle, (b) Knee Angle, (c) Ankle Angle, (d) Subtalar Angle and (e) Metatarsophalangeal Angle. 68
Graph 6.25 – Intra-variability moment of patient 1: (a) Hip Flexion Moment, (b) Knee Moment, (c) Ankle Moment, (d) Subtalar Moment and (e) Metatarsophalangeal Moment 70
Graph 6.26 – Intra-variability moment of patient 2: (a) Hip Flexion Moment, (b) Knee Moment, (c) Ankle Moment, (d) Subtalar Moment and (e) Metatarsophalangeal Moment. 70
Graph 6.27 – Intra-variability moment of patient 3: (a) Hip Flexion Moment, (b) Knee Moment, (c) Ankle Moment, (d) Subtalar Moment and (e) Metatarsophalangeal Moment. 71
Graph 6.28 – Intra-variability moment of patient 5: (a) Hip Flexion Moment, (b) Knee Moment, (c) Ankle Moment, (d) Subtalar Moment and (e) Metatarsophalangeal Moment. 71
Graph 6.29 – Intra-variability moment of patient 6: (a) Hip Flexion Moment, (b) Knee Moment, (c) Ankle Moment, (d) Subtalar Moment and (e) Metatarsophalangeal Moment. 72
Graph 6.30 – Intra-variability moment of patient 7: (a) Hip Flexion Moment, (b) Knee Moment, (c) Ankle Moment, (d) Subtalar Moment and (e) Metatarsophalangeal Moment. 72
Graph 6.31 – Moment of patient 1 vs Control Group: (a) Hip Flexion Moment, (b) Knee Moment, (c) Ankle Moment, (d) Subtalar Moment and (e) Metatarsophalangeal Moment. 73
Graph 6.32 – Moment of patient 2 vs Control Group: (a) Hip Flexion Moment, (b) Knee Moment, (c) Ankle Moment, (d) Subtalar Moment and (e) Metatarsophalangeal Moment. 74
Graph 6.33 – Moment of patient 3 vs Control Group: (a) Hip Flexion Moment, (b) Knee Moment, (c) Ankle Moment, (d) Subtalar Moment and (e) Metatarsophalangeal Moment. 74
Graph 6.34 – Moment of patient 6 vs Control Group: (a) Hip Flexion Moment, (b) Knee Moment, (c) Ankle Moment, (d) Subtalar Moment and (e) Metatarsophalangeal Moment. 75
Graph 6.35 – Moment of patient 5 vs Control Group: (a) Hip Flexion Moment, (b) Knee Moment, (c) Ankle Moment, (d) Subtalar Moment and (e) Metatarsophalangeal Moment. 75
Graph 6.36 – Moment of patient 7 vs Control Group: (a) Hip Flexion Moment, (b) Knee Moment, (c) Ankle Moment, (d) Subtalar Moment and (e) Metatarsophalangeal Moment. 76
Graph 6.37 – Muscle Power of *Soleus* (a), *Medial Gastrocnemius* (b), *Lateral Gastrocnemius* (c), *Anterior Tibialis* (d) vs Gait Cycle of patient 1. 77
Graph 6.38 – Muscle Power of *Soleus* (a), *Medial Gastrocnemius* (b), *Lateral Gastrocnemius* (c), *Tibialis Anterior* (d) vs Gait Cycle of patient 2. 78
Graph 6.39 – Muscle Force of *Soleus* (a), *Medial Gastrocnemius* (b), *Lateral Gastrocnemius* (c), *Tibialis Anterior* (d) vs Gait Cycle of patient 2. 78
Graph 6.40 – Muscle Power of *Soleus* (a), *Medial Gastrocnemius* (b), *Lateral Gastrocnemius* (c), *Tibialis Anterior* (d) vs Gait Cycle of patient 3. 79
Graph 6.41 – Muscle Force of *Soleus* (a), *Medial Gastrocnemius* (b), *Lateral Gastrocnemius* (c), *Tibialis Anterior* (d) vs Gait Cycle of patient 3. 79

Graph 6.42 – Muscle Power of *Soleus* (a), *Medial Gastrocnemius* (b), *Lateral Gastrocnemius* (c), *Tibialis Anterior* (d) vs Gait Cycle of patient 4. 80
Graph 6.43 – Muscle Force of *Soleus* (a), *Medial Gastrocnemius* (b), *Lateral Gastrocnemius* (c), *Tibialis Anterior* (d) vs Gait Cycle of patient 4. 80
Graph 6.44 – Muscle Power of *Soleus* (a), *Medial Gastrocnemius* (b), *Lateral Gastrocnemius* (c), *Tibialis Anterior* (d) vs Gait Cycle of patient 5. 81
Graph 6.45 – Muscle Force of *Soleus* (a), *Medial Gastrocnemius* (b), *Lateral Gastrocnemius* (c), *Tibialis Anterior* (d) vs Gait Cycle of patient 5. 81
Graph 6.46 – Muscle Power of *Soleus* (a), *Medial Gastrocnemius* (b), *Lateral Gastrocnemius* (c), *Tibialis Anterior* (d) vs Gait Cycle of patient 6. 82
Graph 6.47 – Muscle Force of *Soleus* (a), *Medial Gastrocnemius* (b), *Lateral Gastrocnemius* (c), *Tibialis Anterior* (d) vs Gait Cycle of patient 6. 82
Graph 6.48 – Muscle Power of *Soleus* (a), *Medial Gastrocnemius* (b), *Lateral Gastrocnemius* (c), *Tibialis Anterior* vs Gait Cycle of patient 7..... 83
Graph 6.49 – Muscle Force of *Soleus* (a), *Medial Gastrocnemius* (b), *Lateral Gastrocnemius* (c), *Tibialis Anterior* (d) vs Gait Cycle of patient 7. 84

Glossary

3D – Three-dimensional;

ASIS – Anterior Superior Iliac Spine;

COM – Center Of Mass;

COP – Center of Pressure;

Cm – Centimeter;

CMC – Control Muscle Computed;

Cte – Constant;

FD – Forward Dynamics;

GRF – Ground Reaction Force;

HC – Heel Contact;

HO – Heel Off;

IC – Initial Contact;

ID – Inverse Dynamics;

IK – Inverse Kinematics;

IS – Initial Swing;

LBL – *Laboratório de Biomecânica de Lisboa;*

m – Meters;

Min – Minimum;

Max – Maximum;

PO – Push-Off;

PSIS – Posterior Superior Iliac Spine;

QTM – Qualysis Track Manager;

RRA – Reduce Residual Forces;

SO – Static Optimization;

SwP – Swing Phase;

TO – Toe-Off;

List of Symbols

F_x – Anterior-posterior component of GRF;

F_Y – Medial-lateral component of GRF;

F_z – Vertical component of GRF;

θ – Pennation angle;

$\boldsymbol{k}$ – Muscle Tension;

t – Time;

$\boldsymbol{P_J}$ – Mechanical Power;

$\boldsymbol{\omega}$ – Angular velocity;

n – Number of coordinates;

n_s – Total number of scleronomic constraints;

n_r – Total number of rheonomic constraints;

$\boldsymbol{\Phi_q}$ – Jacobian Matrix;

$\boldsymbol{q}$ – Vector of generalized coordinates;

$\dot{\boldsymbol{q}}$ – Vector with system velocities;

$\ddot{\boldsymbol{q}}$ – Vector with system accelerations;

$\boldsymbol{\Phi}$ – Kinematic Constraints Vector;

$\dot{\boldsymbol{\Phi}}$ – Velocity Constraints;

$\ddot{\boldsymbol{\Phi}}$ – Acceleration Constraints;

$e_{0,}e_{1,}e_{2,}, e_{3,}$ – Euler Parameters;

β – Angle between joints;

$\boldsymbol{M}$ – System Mass Matrix;

$\boldsymbol{g}$ – Vector of generalized force;

$\boldsymbol{\gamma}$ – Right-hand-side of the acceleration equation;

$\boldsymbol{\nu}$ – Right-hand-side of the velocity equation;

$\boldsymbol{\lambda}$ – Lagrange Multipliers;

x_i^{exp} – Experimental position of marker i;

$x_i(q)$ – Position of marker i on the model;

q_j^{exp} – Experimental value for coordinate j;

w_i – Marker i weight;

ω_j – Coordinate j weight;

$\boldsymbol{q}^*$ – Set of desired accelerations;

$\dot{\boldsymbol{q}}_{\boldsymbol{exp}}$ – Experimental-derived coordinates;

$\bar{x}$ – Mean;

σ – Standard Deviation;

Chapter I

1. Introduction

Over the last few years, the progress in the scientific knowledge of biomechanics has been remarkable. Biomechanics improve the knowledge related to the musculoskeletal system and there are several authors who reported gait analysis as the pattern of motion most studied up to now (Winter, 1991). The human gait takes innumerous definitions but in 2001, Whittle defined non-pathological or normal gait as a method of locomotion that involves both legs alternatively, and provides support and balance (Whittle, 2001). Although human movements seem quite simple, in reality, they assume a high degree of complexity that is related with the involvement of the musculoskeletal system and the central nervous system. Considering human gait it is characterized by a set of motions patterns which vary slightly from subject to subject but with parameters that tend to be preserved within subjects. These parameters are for instance the stride length, cadence and speed (Completo and Fonseca, 2011; Winter, 1991).

The improvements in this area allow the association of biomechanics with many medical areas, for example orthopedics. This association arose from the need that orthopedics have to define quantitatively what states qualitatively. In this area, the study of human gait is a concept that has developed primarily due to the need for perceiving and evaluating the normal and pathologic gait patterns and in the face of the results to implement better corrections, treatments or the design of new orthopedic products.

The gait analysis focuses essentially on four different areas classified as time-distance parameters, classical mechanics, pedobarography and electromyography analysis. The time-distance parameters provide the following information: time information, distance information and time-distance or combined information. The time information is, for example, the stride time, percentage of stance and swing phase; the distance information is the stride and step length and width; from the combination of both the velocity and cadence are obtained. Classical mechanics comprehends the kinematic and dynamic analysis of the movement. Kinematics studies the motion without considering

the forces inherent in its origin, such as the displacement of the members, the velocity and acceleration of the limbs and joints. Kinetics studies the forces, torques (or moments) and powers that are generated these motions. Electromyography focuses on the study of muscle activity, namely the amplitude, duration and frequency of the electrical signal during muscle contraction. And finally, pedobarography analysis comprehends the analysis of the pressure of the foot (Completo & Fonseca, 2011).

In order to proceed to a gait analysis there are several tools that allow the calculation of the variables previously presented. Examples of such tools are Inverse Kinematics/Dynamics and Forward Dynamics. In the case of Inverse Kinematics, IK, the position data is given as the input and then the velocity and the acceleration are calculated, using a proper algorithm. In the case of the Inverse Dynamics, ID, the joint moments are calculated considering the forces applied externally and the kinematic data. In case of Forward Dynamics, FD, the trajectories of the coordinates and their velocities are calculated from patterns of muscle activation/forces or joint net torques by solving the equations-of-motion of the system (Completo & Fonseca, 2011; Delp, Habib, & Seth, 2014; Winter, 1991).

In order to computationally to solve these methodologies various software like OpenSim, Visual 3D, SimMechanics, Apollo can be used (C-Motion, 2014; Delp et al., 2014; MathWorks, 2014b). These tools allow the modelling of the musculoskeletal system, and consequently to study it. For instance, these software can be applied in the study of the outcome of a surgical procedure. One of the most popular is OpenSim, since it user-friendly open-source software, which can be easily used either by surgeons or by researchers (Delp et al., 2014).

In this work, the results from subjects who have suffered a rupture of Achilles tendon and whose treatment focused on surgery and physical rehabilitation, will be the subjected to the evaluation of the kinetic, kinematic, plantar pressure and specific muscle patterns. These results will be compared with a control group with the objective of evaluating if there are or not associated changes in the human gait patterns of the targeted population.

1.1 Motivation

The clinical application of gait analysis has increasing, since it enables the improvement of the quality of life of the patient. Over time, this improvement was done through the emergence of new medical devices, such as prostheses and orthoses. Today, this improvement is also focused on the quantification of the effects that a treatment can cause or not in the patients.

Although the literature states that the incidence of Achilles tendon ruptures is unknown, Coughlim et al suggest that is less than 0.2%. Therefore, there is a great interest by the medical community in understanding the physical, biological and biomechanical effects of this rupture (Coughlim et al., 2007).

For this study there is a strong interest in the medical community trying to understand what effects a surgical treatment has on subject who suffered a ruptured of the Achilles tendon. Namely, if there are altered gait patterns, and if surgical treatment may or may not influence the results (Follak, Ganzer, and Merk, 2002). A simple search on the internet allows to understand that there are not so many studies on gait analysis that compare the types of surgery currently used. Mezzaroba et al, in 2012, conducted

a study that aimed the analysis of the results for percutaneous surgery, in particularly the Tenolig technique (Mezzaroba, Bortolato, Fancellu, Marcovich, & Valentini, 2012).

1.2 Objectives

The main objective of this work was to answer the questions that arose when defining it: What are the changes inherent in gait after the rupture of the Achilles tendon? Did the quality of life of subjects changed? Does the technique used for surgery interfere on the musculoskeletal biomechanics of subjects?

This work is essentially experimental and focus on the evaluation of the gait in subjects operated of the Achilles tendon through different surgical techniques. With the purpose of validity results obtained for the patients group, a control group of healthy subjects with no history of injury to the lower limb, were also evaluated.

The subjects were selected by *Hospital CUF Descobertas* and the acquisitions of data were carried out at the *Laboratório de Biomecânica de Lisboa*, LBL, of the Department of Mechanical Engineering at *Instituto Superior Técnico.* The collected data comprehends time-distance parameters, kinetic, kinematic and plantar pressure data that may be used to develop a database and would be evaluated having in accounted the main variables defined by orthopedist and by the researcher who executed the gait analysis. These data is then to be compared with a control group and the pattern values existing in the literature.

In order to achieve this objective, five major steps have to be considered. Firstly, it was necessary to obtain a protocol for clinical evaluation of seven subjects who have suffered a rupture of the Achilles tendon. Secondly, the protocol established for the gait analysis needed to be adapted, namely to the kinetic, kinematic data to automatically generate the input files of the software of analysis (OpenSim). Thirdly, it was necessary to determine which variables would be important and relevant for this study. Fourth, it was necessary evaluate seven patients and ten normal subjects for the control group. Then, after all analyzes were done, the results obtained were compared with the ones obtained for the controls to verify whether there are significant changes. These comparisons were made using analysis of subjects with intra variability, comparing non-injured with injured foot and also comparing with the control group.

1.3 Literature Review

Ruptures and treatments of the Achilles tendon have been documented since the time of Hippocrates, but just on 1633 the first description was published. However, just in recent times, the most effective type of treatment (surgery or just physical rehabilitation) has been discussed (Coughlim et al., 2007; Digest, 1997; Lynch, 2004).

The tendon lesions are frequent and these are normally due to the excessive practice of exercise (e.g. running with the wrong technique), the use of inappropriate footwear, a sudden activation of the tendon after a long period of inactivity or a traumatic injury during a sportive event (Follak et al., 2002).

These lesions can be unleashed by concomitant factors that can predispose a patient to Achilles tendon rupture, including systemic inflammatory arthritis (e.g. rheumatoid arthritis), endocrine dysfunction (e.g. renal failure) and bacterial infection. Kujala et al, in 1992, suggested that patients with certain blood types are more at risk for Achilles tendon rupture (Coughlim et al. 2007). These small lesions may become into inflammations of the tendon (tendinitis) or in the most severe cases into ruptures (Digest, 1997).

The rupture usually occurs 4cm to 6cm above the calcaneal insertion in hypovascular region but it can occur anywhere along the tendon's course and it can be partial or total. The ruptures in the middle portion occur most often (72% to 73%), distal ruptures occur less often (14% to 24%) and proximal ruptures are the least often to occur (4% to 14%). The symptoms include weakness, difficulty to walk, pain in heel and equilibrium lost. The violent stretching of the Achilles tendon can cause its rupture which is commonly treated by surgery (open or percutaneous) and the rehabilitation is slow (Costa, Kay, and Donell, 2005; Digest, 1997). According to patients evaluated in this work, the common feeling when the rupture of the Achilles tendon occurs, is that the subject was shot in these area, some even hear the sound of a click.

There are a few studies performed in the area of biomechanical analysis in Achilles tendon rupture. However, it is noteworthy the growing interest from the scientific and medical community in using biomechanical analysis to analyze what changes exist after an injury of this tendon.

In the few published studies we found that the majority is based on the comparison between the clinical analyses (orthopedic perspective) and biomechanical analysis results. Almost all of these studies focus in the analysis of gait but do not perform them all in the same study (focuses, in generally, only type of analysis), do not distinguish the type of surgery or treatment of rehabilitation, and do not compare the results obtained with the other one of a control group.

There are two important studies conducted in 2005, one conducted by Naim F. et al and other conducted by Kay D. et al. In the first one, only patients were considered and an isokinetic analysis was carried out (assessment of muscle force with the aid of a device at a constant speed). In the second one, in which a pedobarography analysis was performed, were studied 14 subjects with ruptured tendon and 15 which were evaluated with no problems (control group) that realized a pedobarography analysis.

It is not easy to conduct these studies because as these are time and can last from 12 weeks to 48 months and subjects do not always make themselves available for such analysis (Costa et al. 2005; F. and Simsek, 2005). In conclusion, Costa et al. stated that one type of analysis is not sufficient to validate the differences observed and the number of patients was not significant (Costa et al. 2005).

1.4 Main Contributions

The main contributions of this thesis are:

- The development of an experimental methodology of analysis of the human gait to be applied in LBL, that allows the study of the time-distance parameters, kinetic, kinematic, plantar pressure and muscle variables. This methodology includes a protocol for motion acquisition and a set of routines to process and analyze the obtained results;

- The production of the specific MATLAB® conversion scripts that are used to prepare the data obtained from the system in use in the LBL to be readily used by the OpenSim software, for the kinematic, dynamic and computed muscle control analysis;
- The appraisal whether or not changes in individuals with this condition occur and how much they are and the transference of this knowledge to the medical and scientific community.

1.5 Structure and Organization

The thesis is divided in seven chapters:

Chapter I – presents the motivation of the author in respect to the theme, the objectives that she proposes to achieve, a state of art over the main topics of the work and a brief resume of the main contributions;

Chapter II – covers the anatomical (osteology, myology and arthrology) and biomechanics aspects of the lower limbs, namely the leg and the foot. A brief explanation of the anatomy of the thigh, leg and foot, the Achilles tendon and its rupture and surgery techniques closes this chapter;

Chapter III – describes the human gait namely key words and concepts used in gait analysis;

Chapter IV – focuses on multibody dynamics, presenting the key concepts of multibody systems analysis with the OpenSim software;

Chapter V – presents the acquisition protocol, with some considerations about the model used, the markers' placement, as well as the cameras and force plates. Also the data treatment is also discussed here;

Chapter VI – presents the results obtained from plantar pressure analysis and inverse kinematics and dynamics, and their respective discussion;

Chapter VII – presents the most relevant conclusions of this work and possible future developments.

Chapter II

This work requires an understanding of the structure of musculoskeletal systems and its most relevant mechanical properties. In this chapter it is possible to review some of the key concepts of human anatomy.

2. Anatomy

2.1 Skeletal System – Thigh, Leg and Foot

The lower limb consists of three segments: thigh, leg and foot, which are interconnected by the knee joint, in the case of the thigh and lower leg, and by the ankle joint in the case of the leg and the foot.

The skeletal structure of the thigh consists in the femur bone which articulates with the top of the coxal bone at the hip joint, and with the tibia at the knee joint in the lower part. The lower leg is composed by two bones, the tibia which is located on the medial side and the fibula which is located laterally. Finally, the foot has a total of 26 bones, which are divided into three groups, the tarsus which has seven bones, the metatarsus with 5 bones (the metatarsals) and fingers formed by the phalanges. The ankle-foot complex presents six major joints: the ankle or talocrural joint, the intertarsal joint, the tarsometatarsal joint, the intermetatarsal joint, the metatarsophalangeal joint and the interphalangeal joint. The intertarsal joint includes the talocalcaneal-navicular joint, the calcaneal-cuboid joint, the subtalar or talocalcaneal joint, the cuneo-navicular joint, the cuboid-navicular joint, the intercuneiform joint and the cuneo-cuboid joint. In this work, the author will focus on the joints of the foot with greater emphasis are the ankle joint, the subtalar joint and the metatarsophalangeal joint, since are the ones with more relevancy for gait analysis (Esperança Pina 2010; Seeley, Stephens, and Tate 2008).

2.2 Muscular System – Thigh, Leg and Foot

There are several muscles that compose the lower limb apparatus and allow the execution of the movements related to the human gait. The classification of these muscles depends on their location. They are classified as internal, external, anterior-external, in the case of the hip, anterior or posterior in the case of thigh and leg, and intrinsic or extrinsic in the case of the foot.

The most relevant muscles crossing the hip joint and the thigh are the *Gluteus Maximus*, the *Gluteus Medius*, the *Gluteus Minimus*, the *Piriformis*, the *Obturador Internus* and *Externus*, the *Lower Gemellus* and the *Quadratus Femoris*. From the thigh muscles stand out the *Pectinius*, the *Adductor Longus*, the *Addutor Brevis* and the *Magnus Addutor*. The *Gracilis* is considered internal. From the posterior side, are part the *Bicipes Femoris*, the *Semitendinosus* and the *Semimembranosus*.

The most relevant muscles crossing the leg are the *Tibialis Anterior*, the *Extensor Hallucis Longus*, the *Extensor Digitoruium Longus* and the *Peronius Tertius* from anterior side. From the external side two muscles stand out: the *Peroneus Longus* and the *Peroneus Brevis*. Finally, the posterior side include the *Triceps Surae*, the *Plantaris*, the *Popliteus*, the *Flexor Digitorum Longus*, the *Tibialis Posterior* and the *Flexor Hallucis Longus*. They can be identified in the Figure 2.1.

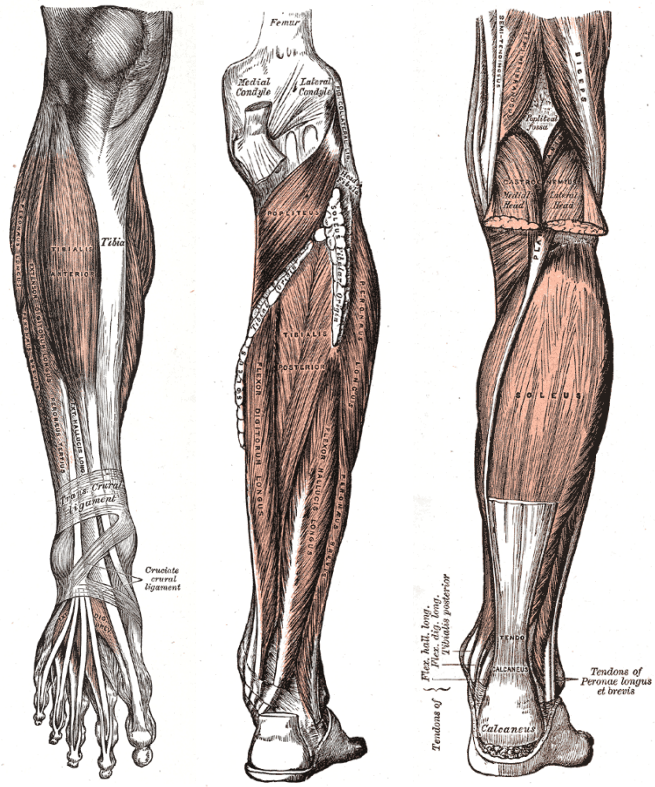

Figure 2.1 – Muscles of the leg (Gray, 2013)**.**

Concerning to the foot, there are several muscles that should be referred. In the dorsal group there is just the *Extensor Digitorum Brevis*. The group of the plantar muscles is divided into internal, external and middle portions of the foot. The *Adductor Hallucis*, the *Flexor Hallucis Brevis*, and the *Abductor Hallucis* belong to the internal group. In the external group, the *Abductor Digiti Minimi*, the *Flexor Digiti Minimi Brevis*, and finally the *Opponen Diggiti Minimi* can be found. In the middle group

there are part the *Flexor Digitorum Brevis*, the *Quadratus Plantae* and the *Musculorum Lumbricales*. Finally, in the *interosseous muscle* group the *Musculorum Interossei Plantares* and *Musculorum Interossei Dorsales*, and can be found as depicted in Figure 2.2.

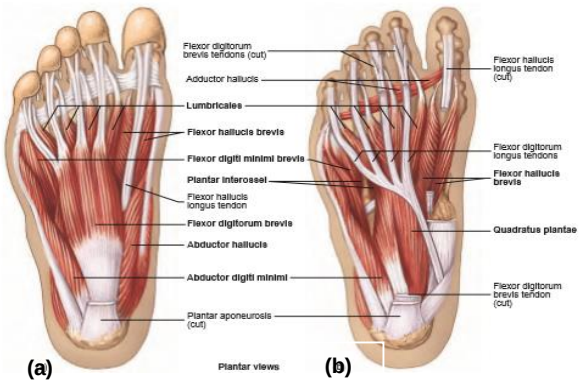

Figure 2.2 – Right Foot Muscles: Superficial Muscles (a), Deep Muscles (b) (Seeley et al., 2008)**.**

In the following tables the muscles of the leg and foot, mentioned above are presented together with the corresponding insertion and origin and major functions (view tables 2.1 to 2.3).

Table 2.1 – Description of the external muscles of the foot – ANTERIOR COMPARTIMENT (Esperança Pina, 2010; Seeley et al. 2008)**.**

Muscle	Origin	Insertion	Function
Extensor Digitorum Longus	Tibia and Fibula	Middle and distal phalanges of the four outer toes	Dorsiflexes, abducts and everts foot; extension the four lateral toes
Extensor Hallucis Longus	Fibula	Distal Phalange of the hallux	Extension hallux, dorsiflexes and inverts foot
Tibialis Anterior	Tibia	First metatarsal and first cuneiform	Dorsiflexes, adduces and inverts foot
Fibularis Tertitus	Fibula	Fifth metatarsal	Dorsiflexes, abducts and everts foot

Table 2.2 – Description of the external muscles of the foot – LATERAL COMPARTIMENT
(Esperança Pina, 2010; Seeley et al., 2008)**.**

Muscle	Origin	Insertion	Function
Fibularis Brevis	Fibula	Fifth metatarsal	Everts and abducts foot
Fibularis Longus	Fibula	Fifth metatarsal	Everts, abducts and plantarflexes foot

Table 2.3 – Description of the external muscles of the foot – POSTERIOR COMPARTIMENT (Esperança Pina, 2010; Seeley et al., 2008)**.**

Muscle	Origin	Insertion	Function
Gastrocnemius	Femur	Calcaneus by means of calcaneal (Achilles) tendon	Plantarflexes foot, adduces and inverts foot
Plantaris	Femur	Calcaneus by means of calcaneal (Achilles) tendon	Plantar Flexion and assist in Knee flexion
Soleus	Tibia and Fibula	Calcaneus by means of calcaneal (Achilles) tendon	Plantarflexes foot, adduces and inverts foot
Flexor Digitorum Longus	Tibia	Distal phalanges of the four lateral toes	Dorsiflexes four lateral toes and plantarflexes foot
Flexor Hallucis Longus	Fibula	Distal phalange of hallux	Dorsiflexes hallux and plantarflexes foot
Popliteus	Femur	Posterior tibia	Dorsiflexes and medially rotates leg
Tibialis posterior	Tibia and Fibula	Navicular, the three cuneiforms, Cuboid and Metatarsals (2-4)	Adduces/inverts foot and plantar flexor

In table 2.4 it is possible visualize the muscles of the leg and foot that causes movement in foot.

Table 2.4 – Description of the internal muscles of the foot (Esperança Pina, 2010; Seeley et al., 2008)**.**

Muscle	Origin	Insertion	Function
Abductor digiti minimi	Calcaneus	Proximal phalange of the fifth toe	Abducts and dorsiflexes fifth toe
Abductor Hallucis	Cuboid, Lateral Cuneiform, second and third metatarsals, three last metatarsophalangeal joints	Fused with *Flexor Hallucis Brevis* and *Flexor Hallucis Longus*	Abducts and dorsiflexes hallux
Adductor Hallucis	Calcaneus	Proximal phalange of hallux	Adduces and dorsiflexes hallux
Extensor Digitorum Brevis	Calcaneus	Proximal phalange of the hallux and three tendons fused with *Extensor Digitorum Longus*	Plantarflexes the proximal phalanges of the four lateral toes
Flexor Digiti Minimi Brevis	Fifth metatarsal	Proximal phalange of fifth toe	Dorsiflexes the proximal phalange of the fifth toe
Flexor Digitorum Brevis	Calcaneus	Medial phalanges of second to fifth toe	Dorsiflexes the lateral four toes
Flexor Hallucis Brevis	Cuboid and Lateral Cuneiform	Proximal phalange of the hallux and lateral Sesamoid	Dorsiflexes hallux
Dorsal Interossei	Metatarsals (3-5)	Proximal phalanges (3-5)	Dorsiflexes the proximal phalanges (3-5)
Plantar Interossei	Metatarsals	Proximal phalanges (2-4)	Dorsiflexes the proximal phalanges (2-4)
Lumbricales	*Flexor Digitorum Longus*	Extensor tendons of the four lateral toes	Dorsiflexes the proximal phalanges and plantarflexes the medial and distal phalanges
Quadratus Plantae	Calcaneus	Tendons of *Flexor Digitorum Longus*	Assists *Flexor Digitorum Longus*

2.3 Foot Joints

The foot is a complex skeletal system that comprises many joints: the calcaneo-cuboid, the ankle/talocrural joint, the subtalar/talocalcaneal joint, the talocalcaneo-navicular joint, the tarsometatarsal joint, intermetatarsal joint, the metatarsophalangeal joint, the interphalangeal joint, and their location can be view in Figure 2.3. In this work the most important joints that are considered are

the talocrural, subtalar and metatarsophalangeal joints since these are directly or indirectly affect the movement of the Achilles tendon (Hall, 2003).

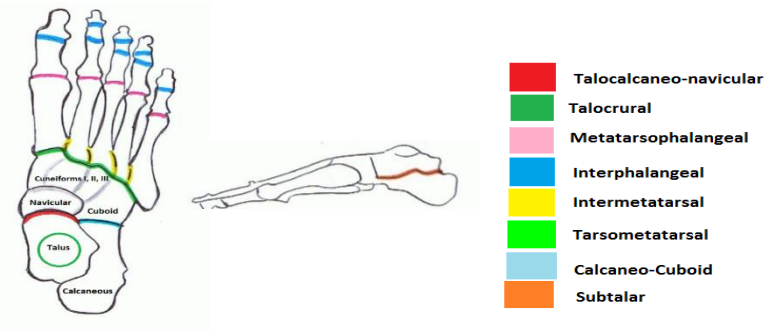

Figure 2.3 – Foot Joints in top view and lateral view.

2.3.1 Ankle or Talocrural Joint

The ankle joint, or talocrural joint, is the region where the leg and foot connect. This joint is composed by three bones: fibula, tibia and talus. The connection and the localization of these bones can be visualized in Figure 2.4. The ankle region includes the distal tibiofibular, tibiotalar and fibulotalar joints.

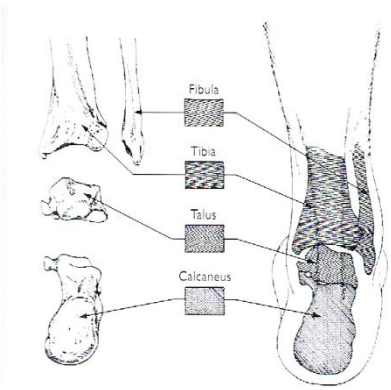

Figure 2.4 – Posterior View of ankle joint (Hall, 2003)**.**

Motion at the ankle occurs primarily in the sagittal plane, with the ankle functioning as a revolute joint with a moving axis of rotation during the stance phase of the gait. This type of joint – revolute – in the mechanical definition, has 1 degree of freedom a as shown in Figure 2.5. This joint promotes motions of plantar flexion and dorsiflexion of the foot (Leardini, O'Connor, Catani, & Giannini, 1999).

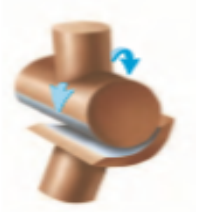

Figure 2.5 – Revolute joint (Seeley et al., 2008)

2.3.2 Talocalcaneal or Subtalar Joint

This joint is formed between the rear face of the calcaneus, the inner face of the talus and the upper face of calcaneus. It is a uniaxial or revolute joint (view Figure 2.5) which has 1 degree of freedom and promotes motions of eversion and inversion (Hall, 2003).

2.3.3 Metatarsophalangeal Joints

They are formed by the reception of the rounded heads of the metatarsal bones in shallow cavities on the ends of the first phalanges. In mechanical language it is considered an ellipsoid joint and allows movements of two plans, as shown in Figure 2.6 (Seeley et al., 2008).

Figure 2.6 – Ellipsoid joint (Seeley et al., 2008)**.**

2.3.4 Motions of the Ankle, Subtalar and Metatarsophalangeal Joints

The motion of rotation of the ankle joint occurs primarily in the sagittal plane during the stance phase of the gait. This joint assumes the flexion and extension that in the specific case of the foot are called plantar flexion and dorsiflexion. These movements depend on the position of the knee, and there are several ranges of values for these angles. Hall says that when the knee is in extension, it exist 10º of dorsiflexion and when it is flexed, approximately 30º. Furthermore, Nordin claims that the range of angular values, for dorsiflexion, is between 10º and 20º, and for plantar flexion between 40º and 55º (Hall, 2003; Nordin & Victor, 2001). The movements of the subtalar joint are essentially inversion and eversion and varies in the range of 2º to -2º. Finally the metatarsophalangeal joint performs the movements of dorsiflexion and plantar flexion (Coughlim et al., 2007). In the following table (Table 2.5), a summary of the movements made by the foot joints is represented.

Table 2.5 – Motions of Joints (Hall, 2003)**.**

Joint	Movements
Ankle	Dorsiflexion and Plantar Flexion
Subtalar	Eversion and Inversion
Metatarsophalangeal	Dorsiflexion and Plantar Flexion

2.3.5 Achilles tendon

A tendon is a fiber bundle of tissue which inserts the muscle to bone or it is intercalled between muscles mass. It assumes properties such as strength and flexibility but it does not confer elasticity. They are composed mainly of collagen fibers and contain few blood vessels. They are responsible for the transfer of force between muscle and bone, and for the generation of the movement of the joint.

The name of Achilles tendon is due the legendary Greek hero Achilles, who was only vulnerable in the Achilles tendon (Digest, 1997). It is also known as the calcaneus's tendon or the tendon of the posterior leg. In a simplified form it is the tendon that connects the leg muscles to the heel and it is formed by the superficial compartment of the calf muscles – *Gastrocnemius* and *Soleus* – and the *Plantaris*. The *Soleus* has the origin in fibula and tibia and its insertion is through the Achilles tendon to the calcaneus. The *Gastrocnemius* has the origin in the medial and lateral condyles of the femur and its insertion is through the Achilles tendon to the calcaneus. Lastly, *Plantaris* has origin in the femur and its insertion is through the Achilles tendon to the calcaneus. All these muscles provide essentially plantar flexion motion. The Figure 2.7 shows the muscles that constitute the Achilles tendon (Seeley et al., 2008).

This tendon is the most resistant of the human body, but is also the most susceptible to lesions because it crosses two joints: the knee and the ankle and acts as a viscoelastic material with rapid loading of the muscle–tendon unit. With the modulus of elasticity increasing, the tendon becomes a stiffer structure and is more prone to rupture.

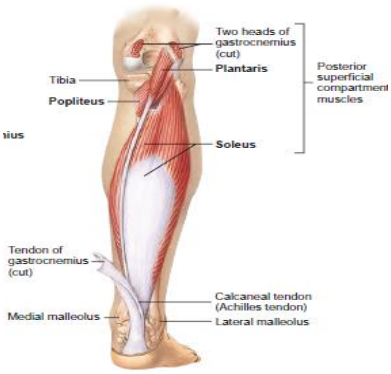

Figure 2.7 – Achilles tendon anatomy (Seeley et al., 2008)**.**

2.3.6 Ruptures of Achilles tendon and surgery techniques of repair Achilles tendon

The violent stretching of the Achilles tendon can cause its rupture which is commonly treated by surgery followed by a long rehabilitation period (Digest, 1997).

The diagnosis of Achilles tendon rupture is made by an orthopedist (physical tests) and confirmed with imaging techniques (usually radiographs and ultrasounds). The physical tests consist in inspection, palpation, motion and a provocative test. The first one evaluate if an increase of the ankle dorsiflexion associated with calf atrophy exist. The second one consists in palpation of the gap. The third consists in evaluating if the patient present a weakness during the realization of the ankle plantar flexion and the last one consists in the Thompson Test that check if a lack of plantar flexion exists when the calf is squeezed (Digest, 1997).

According to Khan et al. in 2004, there is some discussion involving the choice of the best treatment (surgical or non-surgical) and the best technique when the treatment is surgery (Coughlim et al., 2007; Digest, 1997; Khan, Fick, Brammar, Crawford, & Parker, 2004; Lynch, 2004).

Numerous surgical procedures have been proposed to repair the rupture of Achilles tendons. The basic goal of all surgical treatment is to restore the anatomic length of the *Triceps Surae* (*Gastrocnemius*

and Soleus) by approximating the ruptured tendon extremities. Essentially there are two techniques of surgery: the open and the percutaneous/mini-open surgery. The open is the conventional type, while the percutaneous consists on the repair of the tendon using the aid of several devices. In comparison, literature indicates that currently the most widely used is the percutaneous surgery, since it produces a lower tissue invasion and causes fewer side effects (Lynch, 2004). There are several surgical techniques. However, taking into account the work and experience of the orthopedic team who assisted the surgical repair in this work, only three percutaneous techniques will be mentioned. In the mini-open surgery there are essentially three types of techniques: the Tenolig®, the Achillon® and the Ma&Griffith®. The technique Ma&Griffith® requires making 6 to 8 small incisions in the proximal and distal side of the tendon stump to direct the suture through the incisions (Aes, Opin, & Verous, 2006). The Tenolig® technique consists in percutaneously introducing two harpoon sutures from the proximal region to the distal of each side of the tendon and crossing the place of rupture (Lansdaal et al., 2007). Finally, the Achillon® uses a device that is inserted in the proximal direction of the incision. The suture is made from the medial to the lateral side. The Achillon® device is then removed from the transverse incision leaving the suture within the proximal aspect of the tendon. These steps are then repeated for the distal stump of the tendon. The suture ends are then tied to their proximal and distal portions corresponding with the foot (Orr, McCriskin, & Dutton, 2013). In Figure 2.8 are present the steps of the Ma&Griffith® and the Tenolig® are presented, and the device used in the Achillon® technique.

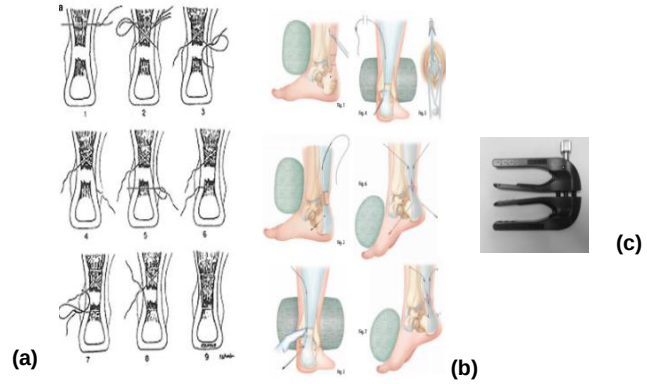

Figure 2.8 – Ma&Griffith technique steps (a); Tenolig technique steps (b); and Achillon instrument (c) (INTEGRA, 2010; Orthopedics, n.d.; Taglialavoro et al., 2011)**.**

Studies performed with patients that were subjected to these techniques show the existence of a reduced number of post-surgery complications. Moreover, most of these complications are easy to solve and usually do not affect the mobility of the patient. The usual complications, after a surgery, are a re-rupture (less common in surgery treatment than non-operative treatment), wound healing complications and *surae* nerve injury (Coughlim et al., 2007; Taglialavoro, Biz, Mastrangelo, & Aldegheri, 2011).

Chapter III

3. Human Gait

The human gait is, according to Winter in 1991, is one of the most studied motions in biomechanics. Although it is initially difficult to master, the movements associated to the gait, when they are acquired by the subject become unconscious despite the numerous factors that contribute to the triggering of the same (Completo & Fonseca, 2011; Winter, 1991). Whittle defined non-pathological or normal gait as a mode of locomotion that involves both legs alternately, and provides support and balance (Whittle, 2001).

In this chapter, the spatial terminology for inter-relation and joint motion will be briefly reviewed as well as a brief description of the major phases of human gait is provided.

3.1 Definitions and Terminology

3.1.1 Spatial Terminology

The definition of reference axis in spatial reference system varies from author to author. However, in order to standardize the communication and facilitate the understanding of the results obtained in the medical and scientific community, many researchers have adopted the terms direction of progression to define the X axis, lateral to define the Y axis and finally vertical to define the Z axis (Winter, 1991). However the notation of the axes used for processing and handling of data, in OpenSim software is different ($x=x_{OpenSim}$; $y=z_{OpenSim}$; $z=y_{OpenSim}$). For this reason in this work, the reference of axis, is made only with the names medio-lateral, anterior-posterior and horizontal plans. Susan Hall, in 2003, presented a definition for each of the plans:

- **Sagittal Plane (XOZ)**: is a vertical plane passing through the long axis that crosses the body, and that separates the body into right and left sides. Whatever is situated near this plane is called medial, and that it is way from the plane is called lateral;
- **Horizontal Plane (XOY)**: is a horizontal plane that cuts the body into superior and inferior halves;
- **Antero-Posterior or Frontal Plane (YOZ):** separating the body into anterior (frontal) and posterior (dorsal) sides (Hall, 2003; Seeley et al., 2008; Winter, 1991).

In Figure 3.1 shown below, the spatial representation of the above plans is represented.

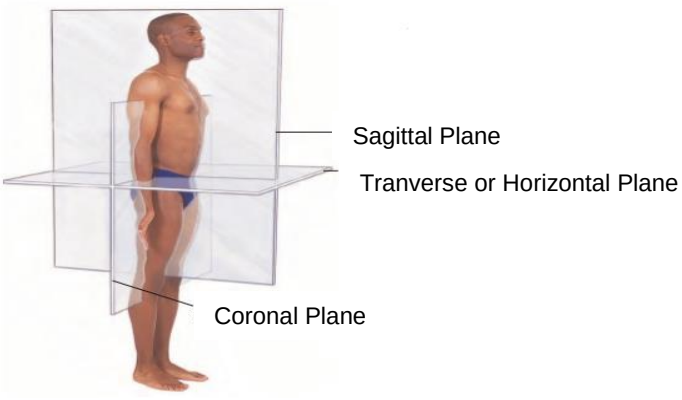

Figure 3.1 – Spatial Reference (Seeley et al., 2008)**.**

In order to define and better understand the plans described above is necessary to understand the definition of Anatomical Reference Position. In this position, the subject is upright, looking straight ahead, with the arms along the body position – slightly away from his body – and his palms towards the previous plan, as shown in Figure 3.2 presented below.

Figure 3.2 – Anatomical Reference Position (Gray, 2013)**.**

As gait analysis refers often to the acting of the limbs, it is necessary to define two important concepts:

- **Ipsilateral** – is used to describe the same side of the body;
- **Contralateral** – is used to describe the opposite side of the body (Gray, 2013; Seeley et al., 2008).

3.1.2 Terminology associated with gait

There are many terms associated with gait that are important to define so that one can better understand gait analysis, as for example, the step length, stride length, step width, stride time, foot angle, and can be viewed schematically in Figure 3.3.

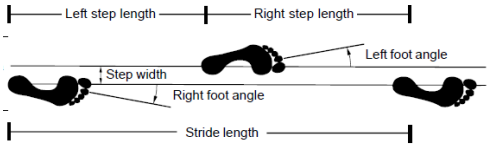

Figure 3.3 – Time distance parameters (Vaughan et al., 1999)**.**

- **Step Length:** is the horizontal distance measured between a determined point of a foot and the same point of the contralateral foot and represents the distance traveled forward by a single leg;
- **Step Width:** represents the mediolateral distance between the heels of the two feet;
- **Stride Length:** is the horizontal distance measured between a determined point of a foot and the same point of the same foot;
- **Foot Angle:** represents the angle of the rotation of the foot;
- **Stride Time:** is the time measured between a determined point of a foot and the same point of the same foot;
- **Step Time:** is the time measured between a determined point of a foot and the same point of the other foot;
- **Stance Time:** is the period of time in which the foot is on the ground expressed in seconds;
- **Swing Time:** is the period of time in which the foot is not in contact with the ground; **Cadence:** is the number of steps per unit of time;
- **Gait velocity:** is the average velocity along the plane of progression of the body (Vaughan, Davis, & O'Connor, 1999; Winter, 1991).

3.1.3 Movements

In case of movements, there are several perceptions for the same concept and for this reason it is very important to define them. In this thesis, the most important position is the anatomical reference position and motions associated with the lower limb, namely flexion, extension, plantar flexion, dorsiflexion, foot eversion/inversion and foot supination and pronation:

- **Plantar Flexion:** joint movement of the foot towards the bottom of the foot;
- **Dorsiflexion:** joint movement of the foot in the direction of the dorsal part of the foot;
- **Foot Eversion:** rotation of the calcaneus externally;
- **Foot Inversion:** rotation of the calcaneus internally;
- **Foot Supination:** movement of the sole of the foot on the medial direction;
- **Foot Pronation:** movement of the sole of the foot on the lateral direction;

These movements can be seen illustratively in Figure 3.4.

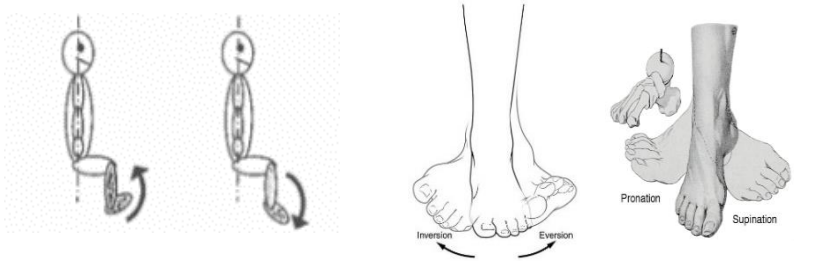

Dorsiflexion Plantar Flexion Inversion-Eversion Pronation-Supination

Figure 3.4 – Most Referenced Movements in this work (Completo & Fonseca, 2011)**.**

3.2 Gait Cycle

In simple terms, the human gait can be defined as the result from the balance between maintaining an erect posture and provide locomotion.

The human gait is influenced by musculoskeletal system, the muscle tone and the neurological system (Winter, 1991). Through joint action of all these factors it can be defined human gait as one sequence of events and reflexes more or less complex and that once learned becomes subconscious. Is through the multiple body segments that these move together varying amplitudes, velocities, accelerations, exerting forces and moments variables (Completo & Fonseca, 2011). There are several definitions for the gait cycle but Norkin, in 1992, defined it as a sequence of movements that occur between two successive contacts of the same foot with the ground and only one cycle is considered because it is assumed that all others are approximately equal. In order to be able for researchers to study in detail the gait, various gait cycle phases and sub-phases events were defined. Thus, it is considered that the gait cycle begins when the contact of the heel of the right foot with the ground occurs and ends when the contact of the heel of the right foot with the ground occurs again. The gait cycle is divided in two phases, the stance phase that takes approximately 60% of the cycle and the swing phase that takes the last 40% of the cycle (Vaughan et al., 1999). The stance phase occurs when the foot is in contact with the ground surface and the swing phase corresponds to the period in which the foot airborne, and ending when the heel contacts the ground again. There are several terms that are used to describe gait cycle when interaction of the foot with the ground exists. For the interaction of the foot with the ground, Winter sets two important concepts: the initial contact (IC), and heel contact (HC). The IC occurs at the instant of time in which the foot makes the first contact with the ground and in the case of non-pathological subjects is at this point that it is also given the HC. For the motion in which the foot leaves the ground it is important define the Toe-Off (TO), which represents at time which the foot is no longer in contact with the ground.

As there are various movements associated with these phases, the researchers decided divide the stance phase into three sub-phases in order to evaluate in detail all movements and the total gait cycle events. The sub-phases of stance phase are:

1. First Double Support: when both feet are in contact with the ground;

2. Single Limb Stance: when the contralateral foot is swinging through and only the right foot is in ground contact;
3. Second Double Support: when both feet are again in ground contact.

Traditionally the gait cycle has been divided into events (Stance phase: IC, Midstance, Terminal Stance and Pre-swing; Swing phase: Initial Swing (IS), Midswing and Terminal swing):

1. IC (0% to 2%): initiates the gait cycle and represents the point at which the body's centre of gravity is at its lowest position;
2. Weight Acceptance (0% to 10%): represents the period between IC and a maximum knee flexion during stance phase;
3. Midstance (10% to 30%): includes the foot flat (the time when the plantar surface of the foot touches the ground). Occurs when the swinging (contralateral) foot passes the stance foot and the body's centre of gravity is at its highest position;
4. Terminal Stance (30% to 50%): represents the time period between midstance and pre-swing;
5. Pre-swing or second double support (50% to 60%): begins with the IC of the contralateral foot and ends with TO of the ipsilateral foot;
6. Push-Off (PO): is the period of time when the lower limb is pushing away from the ground (powered plantar flexion);
7. Initial Swing (60% to 70%): beings as soon as the foot leaves the ground and the subject activates the hip flexor muscles to accelerate the leg forward;
8. Midswing (70% to 85%): occurs when the foot passes directly beneath the body, coincidental with midstance for the other foot;
9. Terminal Swing (85% to 100%): describes the action of the muscles as they slow the leg and stabilize the foot in preparation for the next heel strike.

In Figure 3.5 we can view all events patent in the gait cycle. The nomenclature refers to the right side of the body but the same occurs in left side too and in normal gait, the gait cycle is approximately symmetric.

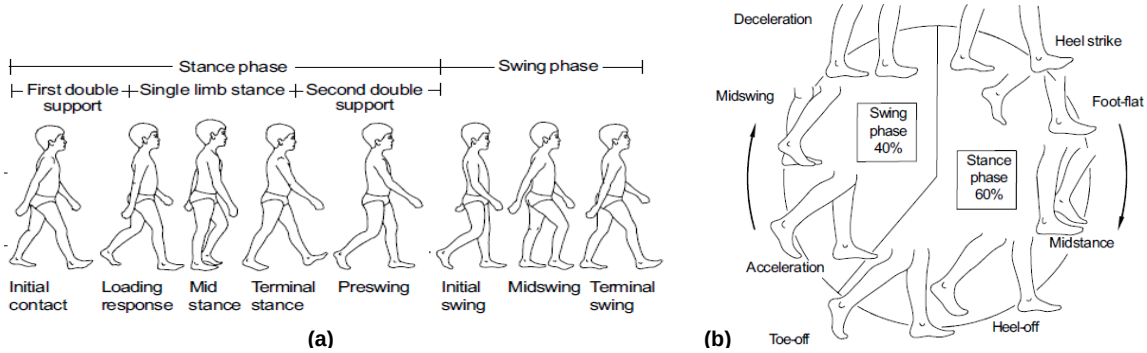

Figure 3.5 – (a) The sequence of normal gait cycle and (b) The events of the gait (Vaughan et al., 1999)**.**

3.3 Theories of Human Walking

Human movement is controlled by the Central Nervous System and musculoskeletal system. Thus the human gait can be considered a mechanism that once learned becomes unconscious. There are several theories that seek to explain human gait and for several years two of these theories have prevailed: the theory of inverted pendulum and the theory of the gait determinants (Kuo, 2007).

3.3.1 Theory of inverted pendulum

The theory of inverted pendulum was enunciated by Cavagna and Margaria, between the years 1963 and 1966. This theory proposes that the leg during the stance phase acts as an inverted pendulum, describing an arc and coexists with the theory of the six determinants of gait. In theory, there is a low energy consumption during the motion because this allows the system does not involve mechanical power to produce the arc of the leg (Kuo & Donelan, 2010).

3.3.2 Theory of six gait determinants

The theory of the gait determinants was enunciated by Saunders in 1953 and it is still used today because it presents a series of patterns which can help explaining energy expenditure during the gait cycle. The theory consists in six determinants that correspond to specific gait patterns that can help to minimize the horizontal and vertical displacements from the center of mass (COM), demonstrating a sinusoidal path. The determinants are denominated as: 1st – Pelvic Rotation; 2nd – Side Pelvic Tilt; 3rd – Knee Flexion during Stance Phase; 4th and 5th – Foot, Ankle and Knee Mechanisms, and finally, 6th – Lateral Displacement (Saunders, Inman, & Eberhart, 1953). In 2009, Herr introduced three new determinants of gait: 7th – Feet Inversion-Eversion-Inversion; 8th – Lateral Flexion of the trunk; and 9th – Anteroposterior Trunk Flexion (Herr, 2009).

In this work, the most relevant determinants are the 3rd, 4th, 5th and 7th as they refer to the mechanisms of the lower limb. Basically, in normal walking the 3rd is related to the knee mechanisms such as the flexion and extension movement. In figure 3.6 it is possible visualize the mechanisms associated to the knee (extension and flexion). The first movement (extension) occurs in the stance phase on the range 0% to 10% of the gait cycle and the maximum value is approximately 10º. The second one (flexion) occurs in the swing phase on 60% to 100% of gait cycle and maximum value is 60º to 70º. In the left side of figure it is possible visualize the movement that the knee made in the gait.

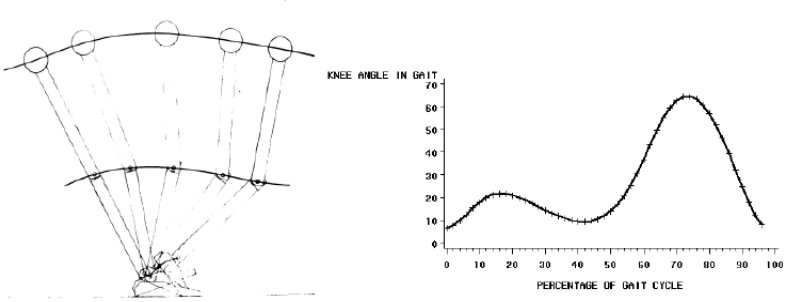

Figure 3.6 – 3rd Gait Determinant – Knee Flexion during Stance Phase (Saunders et al., 1953)**.**

In the 4th and 5th gait determinant refer to the rotation of the ankle during controlled (weight acceptance) and powered (propulsion). These determinants can be viewed schematically in Figure 3.7. In (a) it is possible to analyze the controlled plantar flexion which occurs to regulate the angular momentum in medio-lateral and also as shock absorption mechanism. In (b) it is possible to analyze the powered plantar flexion, where propulsion occurs, to regulate also of the angular momentum in medio-lateral direction and also avoids the abrupt variation of the COM in the vertical direction (associated with the initiation of the knee flexion).

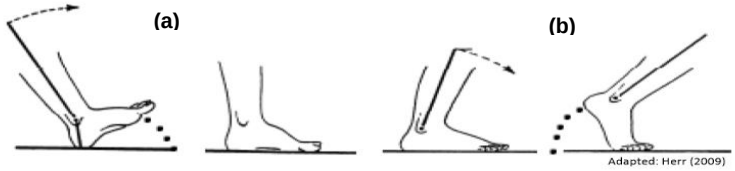

Figure 3.7 – 4th and 5th Foot, Ankle and Knee Mechanisms (Herr, 2009)**.**

The 7th gait determinant considers the inversion and eversion of the foot (rotation of calcaneus on talus) throughout the gait cycle. In Figure 3.8 it is possible to observe the typical values of the rotation of the calcaneus on the talus. In the first 20% of gait cycle occurs the internal rotation or inversion, in range of 20% to 40% the angle is neutral (approximately 0º), and at the remaining 60% occurs the external rotation or eversion (Silva, 2012).

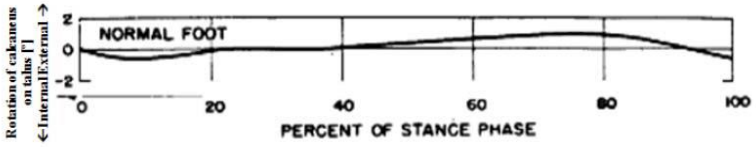

Figure 3.8 – 7th Gait Determinant (Herr, 2009)**.**

3.4 Plantar Pressure

3.4.1 Foot alignment vs. arch type of foot and Centre of Pressure

Plantar pressures and Center of Pressure vary from person to person and can explain various characteristics associated with one's feet. The first one focuses on the type of arch the foot assumes and that directly influences the alignment of the foot. Essentially there are three types of plantar arch: the normal arched, the high arched and the flatfoot.

In the first case the alignment of the foot is normal and it bases around the base of support on the ground. The second case promotes a lateral alignment of the foot and thereby on the midfoot exist support or pressure on its lateral side. Finally, in the last case the alignment of the foot is medial and is fully supported by the planting area. These types of foot alignment also influence the progression of the curve of the foot. In neutral alignment the curve of the foot progresses from the Lateral Heel, passing by the side of the midfoot and ends at Toe 1. On the supinated foot (high arched foot) the same happens with the difference that the end of its progression it occurs slightly on the medial Toes, therefore the end

of the centre-of-pressure, COP curve is shifted to the area of Toes 2-3. Finally, in the pronated foot, the center of pressure curve passes in the medial part of the foot, almost like with a nearly straight line and ends at Toes 1. In the Figure 3.9 it is possible visualize the foot alignment vs type of foot (a) and the progression of the centre-of-pressure curve, for normal subjects (b) (Hutton & Dhanendran, 1979).

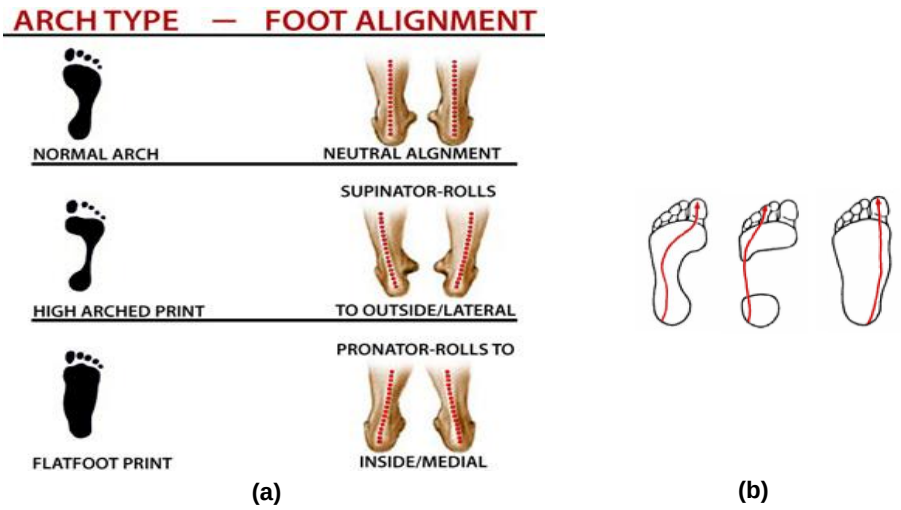

Figure 3.9 – Foot alignment (a) vs. Arch type and Different Centre of Pressure (b) (Podiatry, 2014)**.**

3.4.2 Pressure Distribution

The standing alignment type described above can influence the distribution of plantar pressures throughout the gait cycle, but in a normal population there is almost always the same pattern of distribution.

In the following figure, Figure 3.10, it is possible show the progression of plantar pressure curve in gait and the movement phases of gait can be associated to the contact area of the foot with the ground. In the figure 3.10 it can be seen that in the IC there is only pressure at heel zone (a); in loading response and midstance (foot-flat) occurs one pressure across the plantar area (b); during the TO pressure exists only in the metatarsophalangeal area (c). Note that not all people land their toes, (fact recorded during the analysis of plantar pressures).

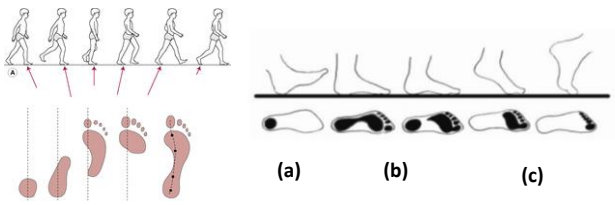

Figure 3.10 – Pressure Distribution on Gait Cycle (Farlex, 2014)**.**

3.5 Gait Cycle and Achilles tendon

3.5.1 Motion of limbs and articulations

In order to verify the results of the kinetics, the kinematics and the muscle activations of the Achilles tendon it was necessary to understand what are the movements associated with body segments that comprise the lower limb. In the Table 3.1, given below, the motions of the leg, the ankle joint, the subtalar joint and the tarsal joint can be analyzed. However, the joint to get more attention will be the ankle joint, as it is on this one that the Achilles tendon is inserted. The Achilles tendon promotes the movements of dorsiflexion and plantar flexion in both phases but, according to the literature, the most significant phase is the stance phase that comprising both movements (Rodgers, 1988). Up to approximately 15%, it takes the plantar flexion motion, then the dorsiflexion until about 40% to 50% of the cycle and on the last 10% of the stance phase occurs plantar flexion again. In the last 40% of the gait cycle (swing phase) is present only the dorsiflexion.

Table 3.1 – Summary of phases of gait cycle and accompanying motions of lower limb joints (Rodgers, 1988)**.**

	Stance Phase (%)			**Swing Phase (%)**	
	0 20	20 40	40 60	60 80	80 100
Events	Heel-Strike	Foot Flat Mid-Stance Heel Rise	Toe-Off		Heel-Strike
Lower Limb	Medial Rotation	Lateral Rotation		Medial Rotation	
Ankle Joint	Plantar Flexion	Dorsiflexion	Plantar Flexion	Dorsiflexion	
Subtalar Joint	Pronation	Supination		Pronation	
Transverse Tarsal Joint	Free Motion	Increasingly Restricted		Free Motion	

3.5.2 Gait Cycle and muscles related to the Achilles tendon

During the gait cycle, several muscles of the lower limb that are activated in the phases describe this cycle. According to the literature the muscles responsible for the motion of the ankle joint are five: the *Soleus*, the *Gastrocnemius*, the *Posterior Tibialis*, *Anterior Tibialis*, the *Longus Flexors* and lastly the *Dorsiflexors*. As can be seen in the following table, (see Table 3.2), it is possible to visualize that the most required muscles in the gait cycle are the first four and they are present throughout the stance phase. In the case of the *Soleus*, it starts its activation approximately at half of the loading response and ends at the terminal stance and the same happens with the *Gastrocnemius*. The *Posterior Tibialis* starts its activation early in the stance phase and only ends at the end of it. As can be seen the *Longus Flexors* and the *Dorsiflexors* are the muscles less requested for the motion of this joint. In the case of *Longus Flexors,* they only act in the midstance and in the terminal stance and in the case of the *Dorsiflexors* they act only in terminal stance placing greater emphasis on the performance of the swing phase (Completo & Fonseca, 2011).

Table 3.2 – Muscle Activations of Ankle Joint in gait cycle (Completo & Fonseca, 2011) - adapted.

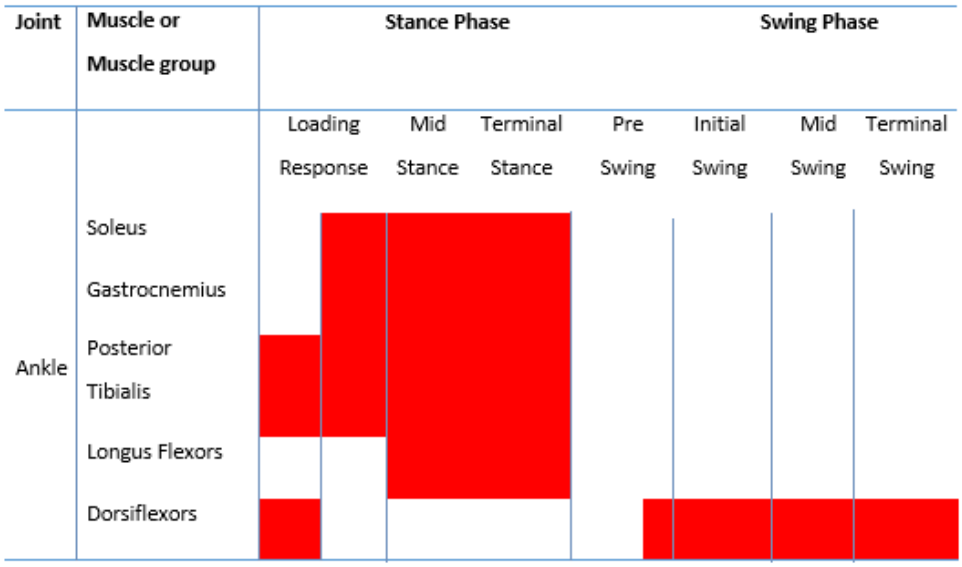

To better understand the patterns associated with the muscles it is necessary to understand the concepts of Mechanical Power and Muscle Force.

Mechanical Power, $\boldsymbol{P_J}$, is the work performed per unit time. It can be calculated as expressed in equation (1):

$$\boldsymbol{P_J = M_J . \omega_j} \tag{1}$$

where, $\boldsymbol{M_J}$ is the flexion-extension moment and $\boldsymbol{\omega_j}$ is the joint angular velocity. The mechanical power is used to quantify the rate of generated or absorbed energy by the muscles (positive: generating a concentric contraction and negative: generating an eccentric contraction) and it is measured in Watts (W).

The Muscle Force it is the force on the muscle in order to perform certain movement and it is measured in N (Winter, 1991). The equation of Muscle Force, $\boldsymbol{F_{max}}$, depends on the type of fibers of the muscle and on the pennation angle. In case of the muscle fibers are aligned with line of action of the muscle, the expression is:

$$\boldsymbol{F_{max} = CSAM \times K} \tag{2}$$

In case of the muscle fibers not being aligned with line of action of the muscle the expression is:

$$\boldsymbol{F_{max} = CSAM \times K \times \cos\theta} \tag{3}$$

Where **CSAM** is the cross-sectional area of the muscle, **k** is the muscular tension and $\boldsymbol{\theta}$ is the pennation angle (Completo & Fonseca, 2011).

In the next table, presenting by Silver et al, in 1985, we can check the force values for each muscle involved in the movement of plantar flexion and dorsiflexion and it is possible view that the

Soleus is the muscle that takes more force and the *Tibialis Posterior* is the one that takes less force in plantar flexion motion. These values are due to the balance of the force between dorsiflexors and plantar flexors of the foot and ankle (Coughlim et al., 2007).

Table 3.3 – Relative Force of Muscles (Coughlim et al., 2007)**.**

Muscle	Force (Units)
PLANTAR FLEXION	
Soleus	29.9
Medial Gastrocnemius	13.7
Lateral Gastrocnemius	5.5
Posterior Tibialis	5.5
Flexor Hallucis Longus	3.6
Flexor Digitorum Longus	1.8
DORSIFLEXION	
Anterior Tibialis	5.6

Chapter IV

4. Multibody Dynamic Systems

The human body assumes an enormous number of components that can undertake relative displacements and rotations when moving, which makes these movements difficult to study. To carry out a movement analysis, it is necessary develop a proper computational model. In this way, it is now necessary to 'convert' the human body into a multibody system that can be used to obtain the values of the targeted biomechanical variables. In order to analyze these type of systems it is necessary to understand several concepts related with multibody dynamics presented below (Silva, 2003).

4.1 Multibody Systems

A multibody system comprises two or more rigid bodies that are connected by kinematic joints. The motion of the system can occur due to the application of external forces or due to the action of mechanical actuators, as shown in Figure 4.1.

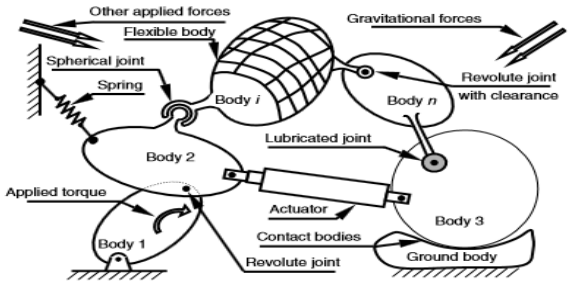

Figure 4.1 – Schematic representation of a generic multibody system (Flores et al., 2008)**.**

A rigid body can be defined as a non-deformable body with a fixed length, keeping any two points of this rigid body at the same distance. In Biomechanics, the rigid bodies are usually applied to model

body segments or bones, while the actuators are used to model muscles. Other mechanical elements, such as springs or dampers can be used to model tendons and ligaments.

This type of mechanical systems are essentially subjected to two distinct types of analyses: forward and inverse dynamic analysis. For these type of analyses the type of coordinates, which describe the position and orientation of the multibody system, needs to be defined. Several formulations, such as natural coordinates, Cartesian coordinates, relative coordinates, etc., can be used to model the system. It is important to note that OpenSim, the software used in this work in the simulation of the experimental motion, uses in its formulation relative coordinates. In this type of coordinates, the position of each segment is defined in relation to the previous segment.

In figure 4.2, the relationship between the global reference frame and a rigid body is shown. As it can be seen, the position of the upper body is related to the origin of the global reference frame through the vector $\underset{r_4}{\rightarrow}$. On the other hand the position of the lower body is defined considering its relation with the previous segment, i.e. the upper body (Silva & Ambrósio, 2003; Silva, 2012).

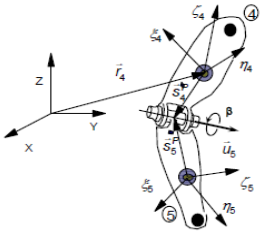

Figure 4.2 – Relative coordinates (Silva, 2012)**.**

Generally the coordinates of a multibody system are defined through generalized coordinates and are represented by vector **q**,

$$\mathbf{q} = \{q_1, q_2, \dots, q_n\}^T \tag{4}$$

where **n** represents the total number of coordinates that describe the model.

When the coordinates used to describe a mechanical system are dependent, it means that they are related by algebraic expressions which define the topology of the system. These expressions are referred as kinematic constraints (**Φ**) and define the properties of joints, rigid bodies and driver actuators. Two types of constraints exist: the scleronomics and the rheonomics. The first ones are usually applied to define properties of joints and rigid bodies and do not present an explicit dependency with the time, while the second ones present an explicit dependency on time and for that reason are usually applied in the modelling of driver actuators. The equation 5 expresses this relation:

$$\mathbf{\Phi}_{(q,t)} = \begin{Bmatrix} \mathbf{\Phi}_1(\mathbf{q}) \\ \vdots \\ \mathbf{\Phi}_{\mathrm{ns}}(\mathbf{q}) \\ \mathbf{\Phi}_{\mathrm{ns}+1}(\mathbf{q}, t) \\ \vdots \\ \mathbf{\Phi}_{ns+nr}(\mathbf{q}, t) \end{Bmatrix} = \mathbf{0} \tag{5}$$

where, $\boldsymbol{\Phi_i}$, is the **ith** kinematic constraints, n_s and n_r are respectively the total number of scleronomic and rheonomic constraints.

4.1.1 Kinematic Analysis of Multibody Systems

Kinematic analysis, also called initial position problem, focuses on the study of the movement of the bodies without considering the forces that generate it. This type of simulation enables the study of the trajectories of the system (positions), their velocities and accelerations as well as the analysis of the joint angular displacements and joint angular velocities.

The solution of the kinematic problem is obtained by finding the consistent points that satisfy the equation of kinematic constraints, i.e. to solve the equation 5. However due to the non-linearity of this equation, its solution can be obtained by applying numerical methods, such as the iterative Newton-Raphson Method. The results obtained by this method present a quadratic convergence in the neighborhood of the solution, which means that the error in each iteration is proportional the quadratic error of the previous iteration. This method involves the linearization of equation (5) which results from its replacement by the first two terms of its expansion in a Taylor series, evaluated around an initial approximation of the solution**.** Given this, for a given time *t,* equation (5) is rewritten as:

$$\boldsymbol{\Phi}(\mathbf{q}, t) \approx \boldsymbol{\Phi}(\mathbf{q_i}, t) + \boldsymbol{\Phi_q}(\mathbf{q} - \mathbf{q_i}) = \mathbf{0} \tag{6}$$

The iterative process of Newton-Raphson is defined by the system in the equation (7) and requires the evaluation of the Jacobian matrix of the system, equation (8).

$$\begin{cases} \boldsymbol{\Phi}(\mathbf{q}, t) \approx \boldsymbol{\Phi}(\mathbf{q_i}) + \dfrac{\boldsymbol{\partial \Phi}(\mathbf{q_i}, t)}{\partial q} \Delta \mathbf{q_i} = 0 \\ \Delta \mathbf{q_i} = \mathbf{q_{i+1}} - \mathbf{q_i} \; and \; t = cte \end{cases} \tag{7}$$

where $\frac{\boldsymbol{\partial \Phi}(\mathbf{q_i}, t)}{\boldsymbol{\partial q}}$ is the Jacobian matrix of constraints evaluated at the proximal solution, $\mathbf{q_i}$.

The Jacobian matrix of the constraints is defined as the matrix that contains the partial derivatives of each kinematic constraint with respect to the vector of generalized coordinates. Mathematically, this matrix is expressed as:

$$\boldsymbol{\Phi_q}(\mathbf{q_i}) = \begin{bmatrix} \dfrac{\boldsymbol{\partial \Phi_1}}{\boldsymbol{\partial q_1}} & \cdots & \dfrac{\boldsymbol{\partial \Phi_1}}{\boldsymbol{\partial q}_{nc}} \\ \vdots & \ddots & \vdots \\ \dfrac{\boldsymbol{\partial \Phi}_{\mathrm{nh}}}{\boldsymbol{\partial q_1}} & \cdots & \dfrac{\boldsymbol{\partial \Phi}_{nh}}{\boldsymbol{\partial q}_{nc}} \end{bmatrix} \tag{8}$$

Velocities and accelerations of all the elements that describe the mechanical system are calculated by applying the velocity and acceleration constraint equations. To obtain these equations, the equation (5) is differentiated with respect to time, yielding:

$$\boldsymbol{\Phi}(\mathbf{q},t)=\mathbf{0}\Rightarrow\dot{\boldsymbol{\Phi}}(\mathbf{q},\dot{\mathbf{q}},t)=\mathbf{0}\Rightarrow\ddot{\boldsymbol{\Phi}}(\mathbf{q},\dot{\mathbf{q}},\ddot{\mathbf{q}},t)=\mathbf{0} \tag{9}$$

where,

$$\begin{cases}\ddot{\boldsymbol{\Phi}}(\mathbf{q},\dot{\mathbf{q}},t)=\mathbf{0}\ \Leftrightarrow\ \boldsymbol{\Phi}_{\mathbf{q}}\dot{\mathbf{q}}=\boldsymbol{\nu}\\ \boldsymbol{\nu}=-\dfrac{\partial\boldsymbol{\Phi}}{\partial t}\end{cases} \tag{10}$$

$$\begin{cases}\ddot{\boldsymbol{\Phi}}(\mathbf{q},\dot{\mathbf{q}},\ddot{\mathbf{q}},t)=\mathbf{0}\Leftrightarrow\ \boldsymbol{\Phi}_{\mathbf{q}}\ddot{\mathbf{q}}=\boldsymbol{\gamma}\\ \boldsymbol{\gamma}=\ \mathbf{v}_{\mathbf{i}}-(\boldsymbol{\Phi}_{\mathbf{q}}\dot{\mathbf{q}})\dot{\mathbf{q}}\end{cases} \tag{11}$$

where $\boldsymbol{\nu}$ represents the vector of the right-hand side of the velocity constraint equation and $\boldsymbol{\gamma}$ the vector of the right-hand side of the acceleration constraint equation.

4.1.2 Dynamic Analysis of Multibody Systems

The concept of dynamics reflects a relationship between force and acceleration. Their result can be obtained through the solution of the Newton-Euler equations. Dynamic analysis can be defined as the study of the movement considering the forces and torques that generated it. In this type of analysis it is possible to obtain the internal forces (e.g. joint reactions) that act in the system and consequently to estimate the torques that originated the movement. This type of analysis is based on solving the equations of motion presented in equation 12:

$$\begin{cases}\mathbf{M}\ddot{\mathbf{q}}+\ \boldsymbol{\Phi}_{\mathbf{Q}}^{\mathbf{T}}\boldsymbol{\lambda}=\mathbf{g}\\ \boldsymbol{\Phi}_{\mathbf{q}}\ddot{\mathbf{q}}=\ \boldsymbol{\gamma}\end{cases} \tag{12}$$

where, **M** is the system mass matrix, $\ddot{\mathbf{q}}$ is the vector that contains the system generalized accelerations, $\boldsymbol{\lambda}$ is the vector of Lagrange multipliers, $\boldsymbol{g}$ is the generalized force vector, which contains all external forces and moments (Flores, Ambrósio, Claro, & Lankarini, 2008; Silva, 2012).

4.2 OpenSim Software

OpenSim is an open source software that allows the forward and inverse dynamic analysis and simulation of biomechanical models. Developed in the Stanford University, this software has been widely used by the biomechanics community, since it presents a set of features, models and packages, which enable a quick and easy analysis of the human motion. In addition, this software enables also the definition of new models, providing also a low-level computational tool, where users can develop or improve the current methodologies and algorithms implemented in the software.

Through this software, the motion acquired at the laboratory can be reproduced, obtaining relevant results such as angles, moments, muscle forces and muscle activations.

The analysis of motion in OpenSim app is based on a template provided by the community responsible for it. Every type of analysis requires a set of input files, implemented in xml language, which can be called by a Graphical User Interface (GUI). In this platform is also possible to code scripts to process data, analyze the results, and visualize the motion, among other options.

The process for obtaining the results depends on what the user wants to analyze. However, there is a common step of scaling in which the anthropometric parameters of the biomechanical model are adjusted to fit the subject in analysis. The software will adapt the virtual markers of the model in order to be coincident with the ones obtained experimentally in the laboratory.

After scaling, OpenSim allows the execution of a set of analyses/simulations that provide different outputs: Inverse Kinematics (IK) – calculation of joint angles/velocities/accelerations for the motion in study; Inverse Dynamics (ID) – computation of the joint torques; Reduce Residual Forces (RRA) – adjustment of the joint torques to be dynamically consistent with the GRFs data ; Static Optimization (SO) – optimization step in which the individual muscle forces are estimated for the net joint moments computed in ID (several physiological performance criteria can be defined to allow the solution of the muscle redundancy problem); Computed Muscle Control (CMC) – estimation of the excitations and forces of the muscles, through a control-optimization strategy associated with a forward dynamics simulation; and Forward Dynamics (FD) – integration of the differential equations in order to simulate movements (OpenSim, 2012). For this work, we considered the IK, ID and CMC analysis. The first two analyses are applied to obtain the kinetic and kinematic results and the CMC is used to obtain muscle activations/forces (Delp et al., 2014; Seth, Sherman, Reinbolt, & Delp, 2011).

4.2.1 Multibody Dynamic Systems in OpenSim

To create a multibody system in OpenSim it is necessary to take into account anthropometric data, such as the mass and length of the segments, and the location of the rigid bodies with respect to the parent body.

This software uses relative coordinates, where the position of the base body is given by a vector of Cartesian coordinates, as presented below:

$$\mathbf{q_0} = [\mathbf{r}^T\ \mathbf{p}^T]^T = [\mathrm{x\ y\ z\ e_0\ e_1\ e_2\ e_3}]^T \tag{13}$$

where **x**, **y** and **z** represent the Cartesian coordinates of the base segment and $\mathbf{e_0}$ $\mathbf{e_1}$ $\mathbf{e_2}$ $\mathbf{e_3}$ are the respective Euler parameters.

The system coordinates vector, **q**, includes the location of all the other segments in relation to the previous segment in the kinematic chain that define the model:

$$\mathbf{q} = [\boldsymbol{q_1}^T \beta_1 \ldots\ qnb\ \beta_{nb}\ ] \tag{14}$$

where $\boldsymbol{\beta_i}$ is the angle of the joint that connects the segment ***i-1*** and ***i***, and $\boldsymbol{n_b}$ is the number of segments. It is important to note that in this formulation, the kinematic constraints are implicitly defined.

The use of relative coordinates has as advantage the small number of coordinates and equations required to define the mechanical system. Moreover, the equations in this system are only differential equations. However, this last fact implies that the problem is highly nonlinear, requiring a complex computational implementation to solve the problem (Silva, 2012).

4.2.1.1 Inverse Kinematics in OpenSim

As defined previously, the study of kinematics is based on the study of motion without considering the forces acting on it. In a simple form, the IK tool provided by OpenSim is based on kinematic concepts. This tool allows the optimal adjustment of the position of the markers acquired in the laboratory with the biomechanical model. Essentially, the software will solve a weighted least squares problem, to minimize the distance between the experimental marker and the correspondent marker on the model. It is important to note that each marker on the model has a weight associated, which defines how strongly the marker's error must be minimized. The objective function used to solve the weighted least squares problem presents also a component related with the coordinate errors (difference between the experimental coordinates and the values obtained by computing the IK). This way, in IK analysis OpenSim finds the best solution that minimizes both the marker and coordinate errors:

$$\min_{q} = [\sum_{i \,\epsilon\, markers} wi \|{x_i}^{exp} - x_i(q)\|^2 + \sum_{j \,\epsilon\, unprescribed\ coord} \omega_j ({q_j}^{exp} - q_j)^2] \quad (15)$$

where $\boldsymbol{{x_i}^{exp}}$ is the experimental position of marker $\boldsymbol{i}$, $\boldsymbol{x_i(q)}$ is the position of the corresponding marker on the model (which depends on the coordinate value), and $\boldsymbol{{q_j}^{exp}}$ is the experimental value for coordinate $\boldsymbol{j}$. The marker weights, wi, and coordinates, ω_j, are specified by the user in one of the xml files. This least squares problem is solved using a general quadratic programming solver, with a convergence criterion of 0.0001 and a limit of 1000 iterations (OpenSim, 2012).

In order to perform an IK analysis, several files have to be given as inputs: the original biomechanical model (*.osim), the kinematic data file (*.trc), which contains the experimental marker trajectories for each frame, the scaled model (*.osim) provided by Scale Tool and the .xml file that contains the weights for each markers and coordinates. The output of this analysis is a motion file (*.mot), containing the generalized coordinate trajectories. A schematic representation of the inputs and outputs of the IK tool is presented in Figure 4.3.

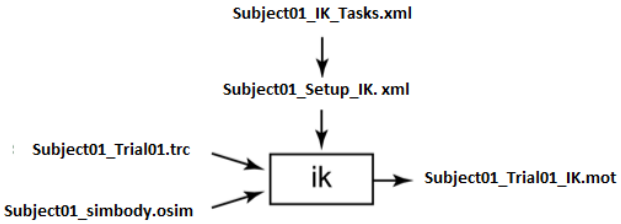

Figure 4.3 – Inputs and outputs of IK in OpenSim.

4.2.1.2 Inverse Dynamics in OpenSim

The ID analysis is a method that allows the assessment of the internal and external forces applied on the system, taking into account the kinematic constraints defined in the model and the acquired motion and external forces. This tool allows the computation of the generalized forces in all the joints of the model (e.g. internal reactions, torques, etc.) for a given movement through the solution of the equations of motion (equation 11) (Silva, 2003).

In order to perform an Inverse Dynamics analysis in this software, a set of input files should be given as inputs: the generic model (*.osim), the Inverse Kinematics motion file (*.mot) containing the generalized coordinates computed during IK and a file with the external forces that act in the system (in this study, this file will include the GRF for each trial) (*.mot). The obtained output is a file (*.sto) containing the joint moments, as shown in Figure 4.4.

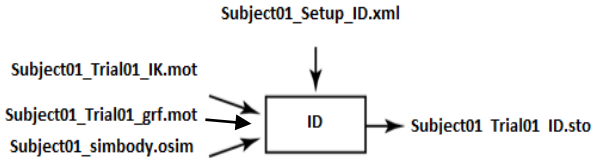

Figure 4.4 – Inputs and outputs files of ID in OpenSim.

4.2.1.3 Computed Muscle Control

The CMC aims to obtain computationally the muscle excitations/forces taking into account the acquired movement (OpenSim, 2012). According to the literature the CMC is a new approach for generating forward dynamic simulations that offers substantial performance benefits over conventional dynamic optimizations techniques (Thelen & Anderson, 2006).

In CMC, the muscles/actuators are described using Hill-Type muscle models, widely used in biomechanics. This model tries to reproduce simultaneously the contractile (CE) and passive behavior (PE) of the muscles. Essentially, it considers that two mechanical elements, one contractile and another elastic, act in parallel as represented in the Figure 4.5 (Silva, 2003).

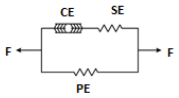

Figure 4.5 – Generic Hill-Type muscle model.

The algorithm of CMC uses a static optimization (with slow or fast target) criterion to distribute forces across synergistic muscles and a proportional-derivative, PD, control to generate a forward dynamic simulation that closely tracks the kinematics (Delp et al., 2007). The PD is based on the control law presented in equation (16):

$$\ddot{\mathbf{q}}^{*}(t+T) = \ddot{\mathbf{q}}_{\exp}(t+T) + \mathbf{k_v} \cdot \left[\dot{\mathbf{q}}_{\mathbf{exp}}(t) - \dot{\boldsymbol{q}}(t)\right] + \mathbf{k_p} \cdot \left[\dot{\mathbf{q}}_{\mathbf{exp}}(t) - \dot{\mathbf{q}}(t)\right] \quad (16)$$

where $\ddot{\mathbf{q}}^*$ is a set of desired accelerations which when achieved will drive the coordinates of the model, $\vec{q}$, toward the experimentally-derived coordinates, $\mathbf{q_{exp}}$, $\mathbf{k_v}$ is the feedback gain on the velocity error and $\mathbf{k_p}$ is the feedback gains on the position error. Because the forces that muscles apply to the body cannot change instantaneously, the desired accelerations are computed for some small time, T and it is typically chosen to be about 0.010 seconds. The next step is to compute the actuators controls, $\boldsymbol{x}$, that will achieve the desired accelerations $\ddot{\mathbf{q}}^*(t+T)$ and performed one static optimization.

The CMC considers one of four algorithms: Interior Point OPTimizer (Ipopt), CFSQP, IMDIF, and LAPACK. In this work the algorithm used was Ipopt that find the local solutions of mathematical optimization problems. The choice of this algorithm was based on the opinion of other OpenSim users. It was referred that Ipopt tends to present less convergence problems during the CMC simulation when compared with the other algorithms. The final step of CMC consists in use the computed controls to conduct a standard forward dynamic simulation.

As can be examined in Figure 4.6, the inputs are the generic model (*.osim), the IK motion file (*.mot), which contains the generalized coordinates over time, the external forces file (GRFs) (*.mot) and three xml files (*.xml) containing information related with the actuators (contains the residual and reserve actuators), the constraints (contains the limits on model actuators and specifies the maximum and minimum control signal or excitation for each actuator) and the tasks (file that specifies which coordinates to track and the corresponding weight). The output file contains the activation, force and power of the muscles considered in the model (OpenSim, 2012).

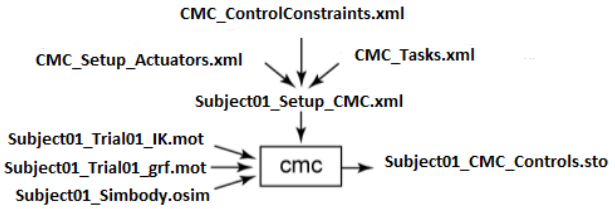

Figure 4.6 – Inputs and outputs files of Control Muscle Control in OpenSim.

Chapter V

5. Model and Protocol Definition

In this chapter, an acquisition protocol is introduced to study the differences in the walking patterns, force and pressure distribution of a population of individuals that were submitted to a surgical procedure to repair from an Achilles tendon rupture the proposed protocol. It is based on a set of previous studies also performed in the *LBL* (Gonçalves, 2010; Menezes, 2011).

The presented methodology includes a set of protocols defined to analyze the joint's articular limits, the static and dynamic distribution of force and pressure between both legs/feet and the kinematic and dynamic walking patterns. A set of health standard questionnaires were included to evaluate the recovering of the surgical procedure.

The biomechanical model applied in the analysis of the subjects' kinematics and dynamics, as well as the marker set protocol required to define it, is also addressed in this chapter.

5.1 Questionnaires

Three different questionnaires, which are directly or indirectly interconnected, were performed to acquire the subjects' medical history and to evaluate the post-operatory recovering. The first one aims to obtain clinical data relevant to the analysis. It is the most personalized, presenting a greater clinical accuracy. The other two AOFAS score and SF-36v2® Health Survey were performed to understand the performance of the patients after the surgical procedure in the four weeks prior to the review. These questionnaires were chosen by taking statistics of their daily routines.

The first questionnaire is a medical grade and was designed in association with orthopedic surgeons. Besides some personal information, this questionnaire includes questions related with the

surgery and the recovering (e.g. rupture and surgery data, type and duration of the physical rehabilitation performed during the recovering and the limitations in daily tasks).

The second questionnaire, AOFAS, is provided by the American Orthopedic Foot and Ankle Society and defines a score to quantify the degree of injury of the ankle-foot complex. The AOFAS score takes in consideration the pain, limitations, alignment and allowed movements in this joint (EORIF.com, 2008).

Lastly, the third protocol SF-36v2® Health Survey (provided by Quality Metric), is used to quantify the subjects' functional health and well-being from their point of view. It is considered by the medical community as a practical, reliable and valid physical and mental health questionnaire, which can be completed in 5 to 10 minutes (Metric, 2014).

5.2 Model Definition

Prior to the analysis and experimental acquisitions, a biomechanical model had to be defined. The one used in this work was a whole-body model with 18 segments and 37 degrees-of-freedom, provided in OpenSim's Neuromuscular Models Library (Delp et al., 2014). The models choice of considered essentially three issues: the movements in study, the segments in study and its complexity. For that reason several models were considered, as for example one model that comprises a torso and lower limb, a whole-body and a lower-body. However, after some research, the model that seemed most appropriate was the whole body since any changes that may occur on the feet can influence the entire body and vice-versa. The fact that the model contains arms is explained by the fact that several authors such as Thelen et al, in 2006, consider that their absence may cause changes (even minimal) in the swing phase, particularly in the first and second gait determinant (Seth et al., 2011; Thelen & Anderson, 2006). Therefore, the model applied in this work is the 3D Gait Model by Hamner (2012). Contains legs, trunk and arm segments and can be seen in Figure 5.1. It also contains 92 musculotendon actuators that are used to represent 76 muscles (represented by red lines) which simulate the muscle apparatus of the lower body. No actuators are used to simulate the upper body, avoiding the increase of the complexity and consequently an increase of the computational processing time required to solve the kinematic and dynamic problems.

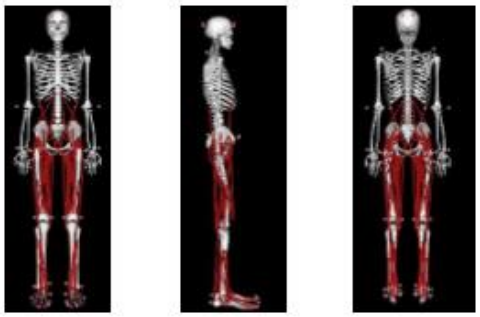

Figure 5.1 – Musculoskeletal model defined in OpenSim (Frontal View, Lateral View and Posterior View) used in the analyses.

The foot in this model is composed by three rigid bodies: 1) talus – rigid body; 2) calcaneus or hindfoot and 3) toes, as shown in Figure 5.2. The three most important joints for this case are the ankle

joint (that connects the leg to the talus – segment 1), the subtalar joint (which makes the connection between the segment 1 and 2) and metatarsophalangeal (which connects the segment 2 and 3) (Delp et al., 2014; Hamner, Seth, & Delp, 2010).

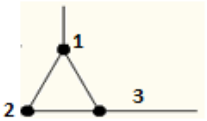

Figure 5.2 Schematic Representation of the foot segments.

The model is defined by 18 anatomical segments that are defined as rigid bodies, as can be seen in the table 5.1.

Table 5.1 – Anatomical segments of the model defined, and corresponding rigid bodies.

Number	Anatomical Segment	Rigid Body
1	Torso	Head and Neck and Thorax
2	Right Upper Arm	Right Humerus
3	Right Lower Arm	Radius and Ulna
4	Right Hand	Right Hand
5	Left Upper Arm	Left Humerus
6	Left Lower Arm	Left Radius and Ulna
7	Left Hand	Left Hand
8	Pelvis	Pelvis
9	Right Upper Leg	Right Femur
10	Right Lower Leg	Right Tibia
11	Right Foot	Heel
12	Right Foot	Talus
13	Right Foot	Toes
14	Left Upper Leg	Left Femur
15	Left Lower Leg	Left Tibia
16	Left Foot	Heel
17	Left Foot	Talus
18	Left Foot	Toes

5.3 Acquisition Protocol

The present work has been developed at the LBL. The kinematic data were acquired by fourteen infra-red (IR) cameras – Qualysis ProReflex MCU 1000 with sampling frequency of 100Hz and two video cameras Sony HC3E HD, with sampling frequency of 25Hz. Their arrangement can be seen in Figure 5.3. The spatial arrangement of the cameras was done this way to allow for better data collection (i.e. better visualization of markers).

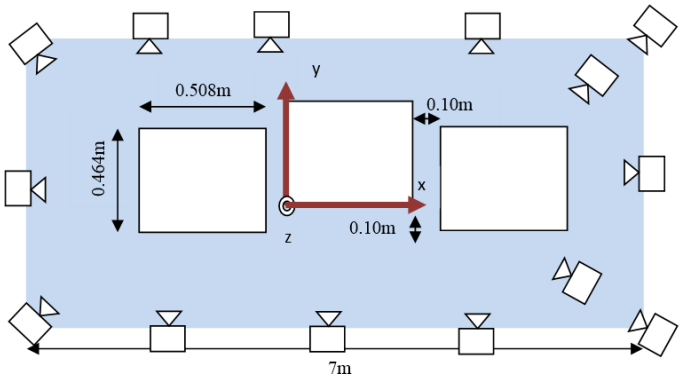

Figure 5.3 – Spatial arrangement of cameras in LBL.

In order to acquire the ground reaction forces, LBL is equipped with three AMTI-OR6-7 force platforms (508mm x 464mm). Their distribution can also be consulted in Figure 5.3. The acquisition of the GRFs in this work considered a sampling frequency of 1000Hz.

For the acquisition of plantar pressure data, LBL is equipped with a pressure platform footscan® 3D Gait (1m x 0.4m x 0.008m). For the time-distance parameters, the LBL is equipped with a GAITRite Electronic Walkway (CIR, 2011).

All systems are synchronized, so that the force plate could be simultaneously acquired with the IR and video camera. The software used for the motion acquisition was Qualysis Track Manager (QTM) version 2.9. The protocol use passive markers with flat base with 12 and 19mm of diameter. The lightweight markers are made of polystyrene hemispheres covered in special retro-reflective tape (Qualysis, 2014).

Since a whole-body model was defined, the required marker set protocol should cover all the anatomical segments considered in it, and therefore 47 markers were used. It should be noted that the correct definition of an object/body in space requires that at least three points are needed. Thus, all rigid bodies described in this work are described with at least three markers (e.g. the left thigh is outlined by marker of trochanter – Hip_Joint_L – and the markers of the medial and lateral knee – Knee_Lateral_L and Knee_Medial_L). Each joint is outlined by two markers (e.g. the left ankle joint is delineated by the markers of the lateral and medial malleolus – Malleolus_Medial_L and Malleolus_Lateral_L).

The location of the markers in the subject's body can be seen in the Figure 5.4 and the respective anatomical landmarks consulted in Table 5.2.

This protocol can be considered very extensive because it has many markers, making the whole process of placing markers very time consuming, however, and to more rigorously verify the results it was necessary to consider all of these. The whole process of putting the markers requires the following a protocol: a) preparing the markers (which are taped to the subjects' skin with duct tape), cleaning the subjects' skin using alcohol, identification of the anatomical landmarks (because they are used for computing the movements) and finally the placement of markers. Static and dynamic tests were performed. In the first case, two tests were performed, one the beginning and the other at the end of the acquisition). In the dynamic tests an average of ten valid trials were acquired to enable the stastical treatment of the data. The subjects were asked to walk with their natural cadence. No information was provided regarding the need of hitting correctly the force plates. A trial was considered valid when

subject walked with their natural cadence and the feet contacts the force plates within their boundaries. The trials started to be measured after a short period of adaptation to the laboratorial environment.

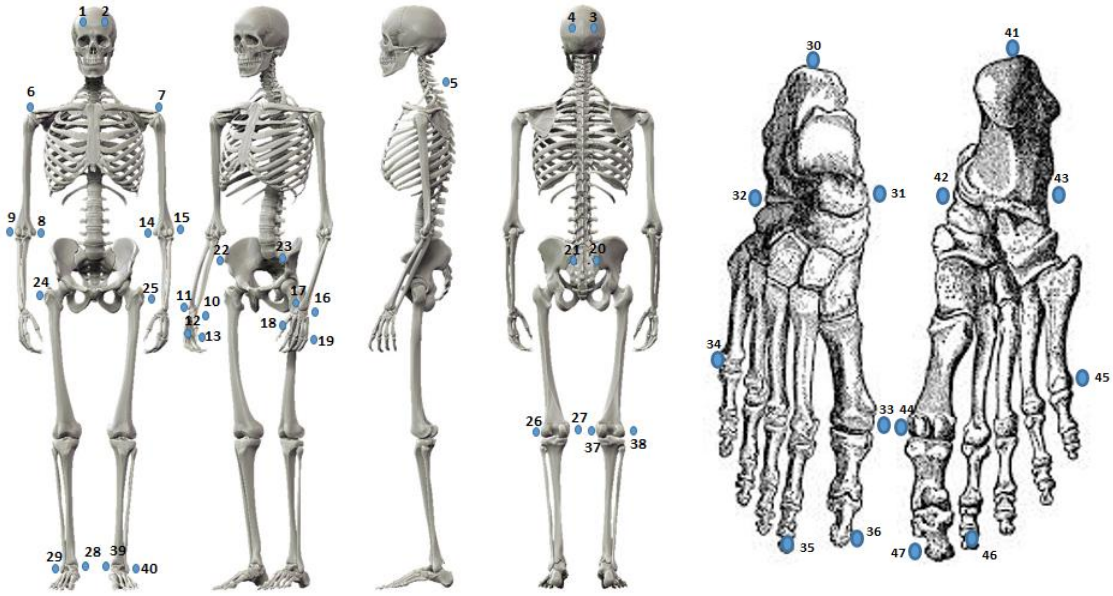

Figure 5.4 – Location of the markers in subject's body.

Table 5.2 – Markers List.

Number	Name	Anatomical Location	Rigid Body
1	Frontal_Bone_R	Temporal Line of Frontal Bone	Thorax
2	Frontal_Bone_L	Temporal Line of Frontal Bone	Thorax
3	Occipital_Bone_R	Occipital Protuberance	Thorax
4	Occipital_Bone_L	Occipital Protuberance	Thorax
5	C7	Spinous Process of C7	Thorax
6	Shoulder_R	Clavicle – Acromium	Thorax
7	Shoulder_L	Clavicle – Acromium	Thorax
8	Elbow_Medial_R	Most Prominent Point of Medial Epicondyle of Humerus	Right Humerus
9	Elbow_Lateral_R	Most Prominent Point of Lateral Epicondyle of Humerus	Right Humerus
10	Wrist_Medial_R	Most Prominent Point of Styloid Process of Ulna	Right Ulna
11	Wrist_Lateral_R	Most Prominent Point of Styloid Process of Radius	Right Radius
12	Metacarpus_II_R	Distal Head of II Metacarpus	Right II Metacarpus
13	Metacarpus_V_R	Distal Head of V Metacarpus	Right V Metacarpus
14	Elbow_Medial_L	Most Prominent Point of Medial Epicondyle of Humerus	Left Humerus
15	Elbow_Lateral_L	Most Prominent Point of Lateral Epicondyle of Humerus	Left Humerus
16	Wrist_Medial_L	Most Prominent Point of Styloid Process of Ulna	Left Ulna
17	Wrist_Lateral_L	Most Prominent Point of Styloid Process of Radius	Left Radius
18	Metacarpus_II_L	Distal Head of II Metacarpus	Left II Metacarpus
19	Metacarpus_V_L	Distal Head of V Metacarpus	Left V Metacarpus
20	PSIS_R	Posterior Superior Iliac Spine	Pelvis
21	PSIS_L	Posterior Superior Iliac Spine	Pelvis
22	ASIS_R	Anterior Superior Iliac Spine	Pelvis
23	ASIS_L	Anterior Superior Iliac Spine	Pelvis
24	Hip_Joint_R	Center of Acetabulum	Right Femur
25	Hip_Joint_L	Center of Acetabulum	Left Femur
26	Knee_Medial_R	Most Prominent Point of Lateral Femoral Epicondyle	Right Femur
27	Knee_Lateral_R	Most Prominent Point of Medial Femoral Epicondyle	Right Femur
28	Malleolus_Medial_R	Most Prominent Point of Medial Malleolus	Right Tibia
29	Malleolus_Lateral_R	Most Prominent Point of Lateral Malleolus	Right Tibia
30	Calcaneous_R	Upper Ridge of the Calcaneus Posterior Surface	Right Calcaneous
31	Navicular_R	Medial apex of the tuberosity of the navicular	Right Calcaneous
32	Cuboid_R	Lateral apex of the tuberosity of the cuboid	Right Calcaneous
33	Metatarsal_I_R	Medial aspect of the head of Metatarsal I	Right Calcaneous
34	Metatarsal_V_R	Lateral aspect of the head of Metatarsal V	Right Calcaneous
35	Phalange_II_R	Top head of the Phalange II	Right Toes
36	Hallux_R	Medial aspect of the Hallux	Right Toes

37	Knee_Medial_L	Most Prominent Point of Lateral Femoral Epicondyle	Right Femur
38	Knee_Lateral_L	Most Prominent Point of Medial Femoral Epicondyle	Right Femur
39	Malleolus_Medial_L	Most Prominent Point of Medial Malleolus	Right Tibia
40	Malleolus_Lateral_L	Most Prominent Point of Lateral Malleolus	Right Tibia
41	Calcaneous_L	Upper Ridge of the Calcaneus Posterior Surface	Right Calcaneous
42	Navicular_L	Medial apex of the tuberosity of the navicular	Right Calcaneous
43	Cuboid_L	Lateral apex of the tuberosity of the cuboid	Right Calcaneous
44	Metatarsal_I_L	Medial aspect of the head of Metatarsal I	Right Calcaneous
45	Metatarsal_V_L	Lateral aspect of the head of Metatarsal V	Right Calcaneous
46	Phalange_II_L	Top head of the Phalange II	Right Toes
47	Hallux_L	Medial aspect of the Hallux	Left Toes

5.4 Data Treatment Protocol

For the treatment of the kinematic and kinetic data, two software, OpenSim and Matlab® were be used. Matlab® is a high-level coding software with an interactive environment for numerical computation and visualization, in which one can easily analyze data, develop algorithms and create models and applications (MathWorks, 2014a). In this work, a script developed in this program was used to convert the files obtained from the QTM software into OpenSim files. Figure 5.5 presents the steps required to acquire and process the data until it is ready to be analyzed in OpenSim.

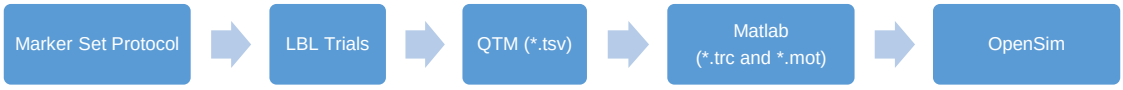

Figure 5.5 – Flow-Chart summarizing the data treatment.

5.4.1 Data Treatment using QTM

In order to perform a kinetic and kinematic analysis, it was crucial to previously treat the data obtained in LBL. The acquisition of the markers trajectory and their treatment was performed using the QTM software. An Automatic Identification of Markers (AIM) model with 47 reflective markers was defined for an efficient assignment of the trajectories. The acquisitions were divided by gait cycles, defining the IC of one of the feet with the second force plate as the 0% of the GC. The next IC of the same foot was defined as 100% of the GC. At least 10 frames should be considered respectively before and after the first and last event to ensure the correct smoothing of the data. The kinematic and kinetic data obtained using the QTM was exported to *.tsv files (table-separated value) in order to be processed in Matlab® software, in which the input files of the OpenSim software will be created.

5.4.2 Preparing the OpenSim input files

The initial step for the use of data obtained from the LBL is the optimization of the musculoskeletal model obtained from the OpenSim database. The *.xml files (biomechanical model and job files) provided by the developers of the OpenSim were updated to be in accordance with the marker set protocol presented in section 5.3.

The second step included the design of the scripts required to convert the *.tsv files from the QTM to the OpenSim input files (kinematic – *.trc and GRFs – *.mot). As already referred, this step made use of the Matlab software. To obtain the *.trc file, a first step of data filtering was performed with the purpose of eliminating noise. A third order low pass digital Butterworth filter with a cut frequency of 6Hz was used. This frequency was chosen to enable the attenuation of the impact components and electrical noise (Winter, 1991). Since the global coordinate systems of the QTM, force plates and OpenSim are different (see Fig 5.6), a coordinate transformation had to be also coded.

The same steps were also coded to create the *.mot file. However, in this case the cutoff frequency was defined in the 20Hz. An additional step in which the location of the COP is calculated, was also included.

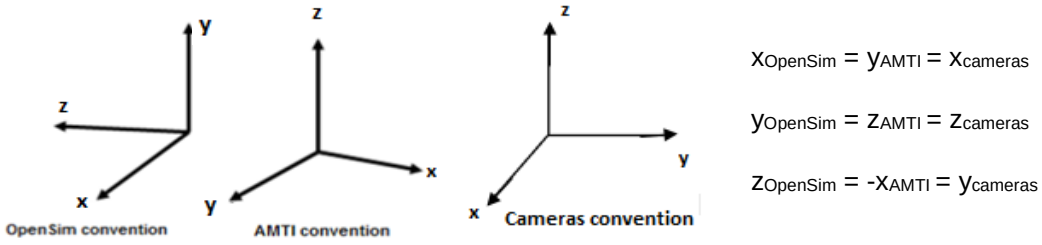

Figure 5.6 – Axes Convention (a) OpenSim, (b) AMTI and (c) Cameras.

Another important feature in the script (*.tsv to *.mot) is the division of the forces obtained by AMTI force plates into the several rigid bodies of the foot, particularly in the calcaneus and toes. The Figure 5.7 presents the progression of the vertical and antero-posterior components of the GRFs in the two foot segments during the stance phase. The COP is applied in the calcaneus approximately in the first 50% of the GC, which corresponds to the weight acceptance and midstance phases. With the evolution of the COP to an anterior position, these forces start to be applied in the toes segment. This event occurs usually during the beginning of the push-off phase (Malaquias, 2013).

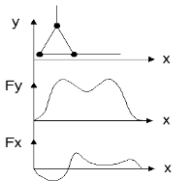

Figure 5.7 – Force progression in the two foot segments.

5.4.3 Data Treatment using OpenSim

As already referred, OpenSim software enable different types of analyses. In this case, only the ones with relevance for this work were explored (IK, ID, CMC). The intents and the implementation of each one were already discussed in Chapter IV. Since the analyses are not independent between them, a sequence of steps should be performed in order to achieve the desired results. In the figure 5.8, the correct sequence of steps is presented. The first steps include the scaling of the model, which is crucial to all the analyses, since it is through this step that the virtual model (position of markers) coded by the

OpenSim developers is adjusted to the experimental model obtained in laboratory. After this step, it is possible to perform the IK, ID and CMC simulations, considering the anthropometric properties of the subject in analysis.

In order to carry out the referred analyses a set of files coded in xml language, which have configuration values for the simulations, needs to be provided to the OpenSim. These files were also available in OpenSim database. In this work, the ones that are available in the model gait2392 package were used as suggested by Delp (Delp et al., 2014). The input and output files for each analysis were already reported in Chapter IV.

Figure 5.8 – Flow-Chart summarizing the data treatment in OpenSim.

5.4.4 Data Treatment using Footscan

The footscan software and pressure plate allows the fast evaluation of the plantar pressure distribution in non-pathologic and pathologic subjects. The data obtained by this software can be statically and dynamically evaluated, providing information related with temporal and spatial parameters, location of the areas with higher and lower pressures and forces, foot length and width, foot axis angle, subtalar joint angle, maximum peak of force/pressure and center of pressure (International, 2009). In the following figure (see Figure 5.9), the steps required to obtain the plantar pressure data were presented.

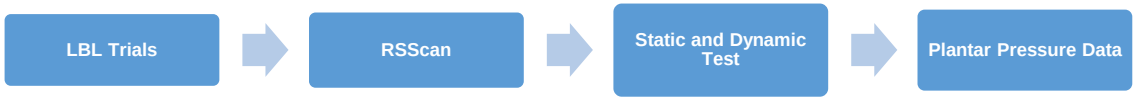

Figure 5.9 – Flow-Chart summarizing the data treatment in Footscan.

In this analysis, the obtained data does not require a special treatment, since the software already presents all the relevant results. However, some routines had to be developed to enable the statistical analysis of the data. Once more, these scripts were coded in Matlab®. Dynamical and static tests were performed for each subject. This software divides the foot into 10 different regions, enabling to assess the locations where the values of the forces and pressure are higher. Region 1 encompasses the 1st Toe (T1); Region 2 includes the 2nd to 5th Toes (T2-5); Region 3 encompasses the I Metatarsus (M1); Region 4 II Metatarsus (M2); region 5 the III Metatarsus (M3); region 6 the IV Metatarsus (M4); region 7 the IV Metatarsus (M5); region 8 the Midfoot (M8), region 9 the Medial Heel (MH), and finally the region 10 the Lateral Heel (LH). Figure 5.10 presents a schematic representation of the regions previously described.

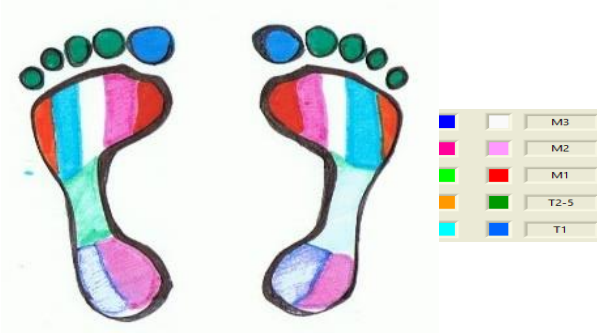

Figure 5.10 – Regions Division of the left foot and the right foot by footscan.

5.4.5 Data Treatment using GAITRite

The GAITRite software provides a valid and reliable measurement of the time-distance parameters in real-time. Moreover, this software enables also the statistical analysis of all the measured parameters. The information provided by this software is extensive and for that reason the data presented in this work will focus on the relevant time-distance parameters: cadence, step time, velocity and duration of each phase of the gait cycle (CIR, 2011).

Since the subjects can walk freely in a walkway without the restriction of the markers and the force plates, the obtained results will be more realistic. In order to perform a statistical analysis, at least ten trials should be performed. Figure 5.11 presents the steps required to obtain the information for each subject.

Figure 5.11 – Flow-Chart summarizing the data treatment in GAITRite.

5.4.6 Data Treatment using ANOVA

Several statistical tests can be applied to assess the existence of variation between different groups/populations. ANOVA is probably one of the statistical models most used in the study of significant differences between different groups and for that reason was the one applied in the analyses performed in this work.

Essentially, there are three types of ANOVA tests: Single factor; Two-Factor with Replication; Two-Factor without Replication. In the first type the difference between different groups is analyzed (simplest version of the ANOVA). The second type is used when we have a single group on which we have measured something a few times (verify the performance in the test). Lastly, the third test should be used in repeated measures, including an interaction effect.

The p-value tests the null hypothesis that data from groups are drawn from populations with identical means. If $p_{value} < 0.05$ the results are statically relevant. If $p_{value} > 0.05$ the results are not statically relevant. On the other hand, the variable F indicates how the data vary between groups. If the

F value is high means that the variations between groups are also high. If the variance is relatively low the variation is minimal (Daniel & Cross, 2013).

This type of analysis was also used in other works mainly to verify the significance level of parameters such as velocity and loading (Raja, Neptune, & Kautz, 2012). In this work, the single factor ANOVA was also used to verify the significance level of the time-distance parameters, and force and pressure distribution acquired for all the injured subjects against the control group.

Chapter VI

6 Results

6.1 Presentation of Results

Tests conducted at both the control group and the group of patients were listed and explained in the earlier chapters. In the case of patients, the questionnaires AOFAS and SF-36v2 (see appendix I and II) used in medicine were performed to check the scores on the state of health and fitness level of the ankle joint. The first one was conducted in paper format and the second was carried out online and results were processed automatically (EORIF.com, 2008; Metric, 2014).

The kinematic and dynamic gait patterns were acquired for a population of ten subjects (5 male and 5 female subjects) with no history of gait disorders were acquired in order to create a control group. Table 6.1 presents the characteristics (age, weight, height and job) of the control group acquired in this work.

Table 6.1 – Data of Control Group.

Subject (n=10)	Gender	Age (years)	Weight (kg)	Height (m)	Job
1	F	24	63	1.65	Student
2	F	47	115.2	1.63	Housewifely
3	F	28	59.6	1.59	Student
4	F	22	60.7	1.70	Student
5	F	26	77.6	1.67	Administrative
6	M	49	85	1.80	Carpenter
7	M	29	109.3	1.96	PhD Student
8	M	24	86	1.82	Research Fellow
9	M	24	78.2	1.76	Student
10	M	29	70.5	1.76	PhD Student
$\bar{x}$	-	**30.1**	**80.5**	**1.73**	-
σ	-	**9.23**	**18.26**	**0.11**	-

In Table 6.2 the information concerning 7 patients evaluated at LBL, 6 male elements and 1 female element can be checked. The average age is 46.8years, the weight 85.32kg and the height 1.73m. When comparing the ages of the control group and patients, the age range is slightly different, but the average age of the control group is practically coincident with the majority of patients' ages at the occurrence of Achilles tendon rupture, which situated between the years 2004 and 2008 and the latest in 2013. The most common cause for this injury was sports, especially playing football (predominantly in males).

Table 6.2 – Data of Patients.

Subject (n=7)	Gender	Age (years)	Weight (kg)	Height (m)	Job	Rupture Type	Year of Rupture	Cause of Rupture	Dominant Hand
1	M	43	109	1.80	Insurance Professional	Unilateral Left Leg	2008	Playing football	Right-Handed
2	M	45	73.7	1.83	Pharmaceutical	Unilateral Rigth Leg	2004	Playing football	Right-handed
3	M	49	96.4	1.73	Computer Engineer	Unilateral Right Leg	2007	Playing football	Right-Handed
4	M	49	80.5	1.70	Computer Engineer	Unilateral Right Leg	2007	Playing football	Right-Handed
5	M	47	91.5	1.84	Civil Engineer	Unilateral Right Leg	2004	Playing football	Left-Handed
6	F	48	60.8	1.68	Lawyer	Bilateral	2004	Walking	Right-Handed
7	M	40	71	1.78	Brisa employee	Unilateral Right Leg	2013	Playing football	Right-Handed
$\bar{x}$	-	46.8	85.32	1.73	-	-	-	-	-
σ	-	3.14	15.38	0.06	-	-	-	-	-

In the Graph 6.1 is presented below, it can be seen that most injuries occurred in the right lower limb. Since only one patient was right-handed, contrary to the assertion laid down in Chapter II that states that the injury occurs predominantly in the contralateral limb. The statement that the predominant sex is male is corroborated, since the majority of patients are male and the databases of the hospital also evidence the same.

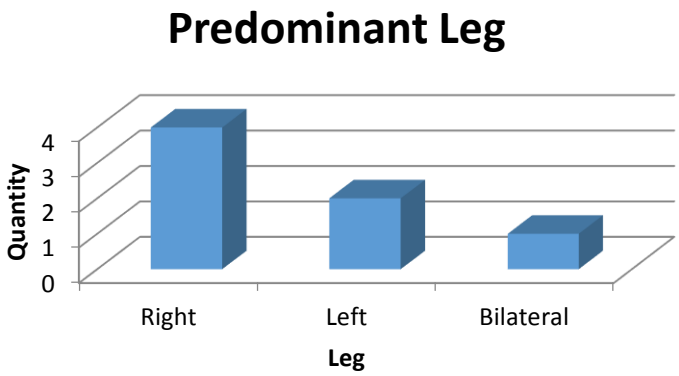

Graph 6.1 – Predominant Leg vs. Quantity of patient with rupture in the limb.

6.2 Discussion of Results

6.2.1 Questionnaires

All patients, after surgery, were treated for physical rehabilitation, including physiotherapy with different time durations. According to the results of the questionnaires (view table 6.3), when compared to the literature, it was found that these lie within the average – AOFAS Score: 100 points and SF-v36: 50 points. There were several patients who reported some changes in terms of gait after suffering the injury and that still persists. The highlights were the lack of balance and some difficulty walking on uneven surfaces (e.g. walking in the beach). In the case of a female patient, it can also be said that she cannot use any type of high heel shoes due to the instability and lack of balance. It should be noted that not all patients resumed physical activities, not by medical advice, but by personal choice.

Table 6.3 – Results of questionnaire – AOFAS score and SF-36v2.

Subject (n=7)	AOFAS Score (points)	SF-36v2 Physical Health – Mental Health (points)	
1	100	55	59
2	98	54	57
3	90	54	60
4	100	54	60
5	100	57	56
6	78	52	59
7	85	52	60
$\bar{x}$	**93**	**54**	**58.7**
σ	**8.19**	**1.60**	**1.48**

6.2.2 Measured Results

The results measured in the lab were the range of motion of the ankle joint, i.e. its dorsiflexion and plantar flexion, and the perimeter of *Gastrocnemius*. Relatively to the *Gastrocnemius* perimeter, a slight difference was found between the injured and healthy member, and the smallest perimeter occurs in all cases in the operated leg. The difference in circumference varies between 0.5cm and 2cm, as shown in the table 6.4 then presented results individually. The overall mean difference of the perimeters of the two legs is 1.36cm.

Table 6.4 – Perimeter of Leg.

Subject (n=7)	Perimeter of Injured Leg (cm)	Perimeter of Healthy Leg (cm)	Difference (cm)	% Reduction
1	38	39	1	2.5
2	30.5	33	2.5	7.6
3	37	39	2	5.1
4	34	35	1	2.8
5	37.5	38	0.5	1.3
6	33	35	2	5.7
7	36.5	37	0.5	1.3
$\bar{x}$	-	-	**1.36**	**3.76**
σ	-	-	**0.74**	**2.23**

From the average results of the movements of plantar flexion and dorsiflexion (view table 6.5), it was found that the plantar flexion and dorsiflexion are within the range of values reported in the literature (Nordin & Victor, 2001). Only two patients, 2 and 6, show values of plantar flexion slightly below of values referenced. Regarding dorsiflexion, values for both limbs are similar and only the patient 6 takes a smaller amplitude difference between the limbs. Analyzing the results it was also found that in general the amplitude of the plantar flexion is different between the injured and healthy limb. In general, it can be concluded that the injured limb has a smaller amplitude.

Table 6.5 – Articular Movements – Dorsiflexion and Plantar flexion.

Subjects (n=7)	Plantar flexion (40º to 55º) Injured – Healthy		Dorsiflexion (10º to 20º) Injured – Healthy	
1	50	55	10	10
2	30	30	10	10
3	50	50	10	10
4	40	45	20	20
5	50	50	15	15
6	10	30	5	10
7	40	50	10	10
$\bar{x}$	**38.57**	**44.29**	**11.43**	**12.14**
σ	**13.55**	**9.42**	**4.40**	**3.64**

6.2.3 Time-Distance Parameters

The most relevant data to be taken into account in the time-distance parameters is cadence, speed, step time, and percentage of stance and swing phase. These data were compared between patients, subjects of control group, control group vs patients, and lastly with data referenced by several authors in the literature.

Relatively on the data of control group (view table 6.6) it can be seen that the cadence (107.68 steps/min) is within the average normal values, which according to Winter, are between 101 to 122 steps/min (Winter, 1991). The speed of 1.14m/s lies slightly below the parameters considered normal (1.5m/s) (Murray, Drought, & Ross, 1964). With respect to the percentage of Stance Phase and Swing Phase it also checks that the group control takes almost 60% and 40% of the gait characteristic.

Table 6.6 – Time-Distance Parameters of Control Group.

Control Group (n =10)	Cadence (steps/min)	Velocity (cm/s)	Step Time (s) Left – Right		% Stance Left – Right		% Swing Left – Right	
1	109.6	113.1	0.55	0.55	60.6	60.5	39.4	39.5
2	110	111.7	0.55	0.54	62.7	62.2	37.3	37.8
3	119.3	115.7	0.51	0.50	56.7	59.7	43.3	40.2
4	110.3	114.2	0.55	0.54	58.8	60.2	41.3	39.8
5	117.7	119.4	0.51	0.51	58.8	59.5	41.1	40.5
6	94.6	99.3	0.64	0.63	59.6	60.9	40.4	39.1
7	104.5	129.1	0.57	0.58	60.9	60.3	39.2	39.8
8	106.7	118.7	0.57	0.56	61.2	62.4	38.8	37.7
9	106.2	122.7	0.56	0.57	57.9	57.9	42.1	42.1
10	97.9	103.3	0.62	0.60	61.2	62.4	38.8	37.7
$\bar{x}$	**107.68**	**114.72**	**0.56**	**0.56**	**59.84**	**60.6**	**40.25**	**39.41**
σ	**2.43**	**2.77**	**0.01**	**0.01**	**1.71**	**1.37**	**1.71**	**1.34**

In the group of analyzed patients, it was found that the mean values of the patients in relation to the cadence and speed are within normal parameters (cadence = 106.5steps/min and speed = 112.56cm/s). However, when compared with the control group they were slightly lower values. Regarding step time (0.57s) it was found that this is slightly above the control group (0.56s) but when compared healthy and injured leg the step time is the same. Finally, the percentages of the phases of the gait cycle also differ. In the case of stance phase it increased by about 1 to 2% while the swing phase decreased by 1.5 to 2%. The increase in the stance phase can be explained by the fact that the muscle group which is attached to the Achilles tendon acts in a dominant way in this stage. In Table 6.7, given below, the results for individual patients can be viewed.

Table 6.7 – Time-Distance Parameters of Patients.

Subjects	Cadence (steps/min)	Velocity (cm/s)	Step Time (s) Healthy – Injured		% Stance Healthy – Injured		% Swing Healthy – Injured	
1	95.4	102.8	0.62	0.63	61.4	61.2	38.6	38.9
2	105.7	113.6	0.56	0.58	62.5	61.4	37.5	38.5
3	103.8	106.6	0.57	0.59	62.3	62.4	37.7	37.6
4	121.3	136.8	0.50	0.49	58.4	59.6	41.5	40.4
5	108.2	108.2	0.58	0.59	61.4	61.2	38.5	38.9
6	102	109.5	0.59	0.59	61.8	61.7	38.2	38.3
7	109.2	110.4	0.55	0.55	60.1	62.1	39.9	37.9
$\bar{x}$	**106.51**	**112.56**	**0.57**	**0.57**	**61.13**	**61.37**	**38.84**	**38.64**
σ	**7.37**	**10.37**	**0.03**	**0.04**	**1.33**	**0.84**	**1.30**	**0.84**

6.2.3.1 ANOVA Results

For results obtained in the time-distance parameters a statistical analysis of variations (ANOVA) was performed for velocity. In this case, ANOVA: Single factor for speed (view table 6.8) was conducted.

Table 6.8 – ANOVA: single factor of velocity.

F	P-value	F crit
0.20389527	0.660804	4.543077165

It was found that the groups (patients vs control group) assume a low variability in speed. As F (≈ 0.2) is small and the P-value is greater than 0.05, that indicates that the differences between groups are not significant as value at Fcritic is higher than the variation between.

6.2.4 Plantar Pressure Results

Regarding the data of plantar pressures there are many variables to take into account, including the characteristics of foot pronation and supination, the subtalar angle, the foot axis angle and the plantar pressure and force.

In table 6.9, given below, it can be visualized standing type parameters assessed by viewing in static images of the plantar pressures (view Appendix III). It is noted that the type of foot generally is neutral and there is no variation between both feet, except in patients 1 and 6.

Table 6.9 – Foot characteristics.

Subjects	Type Foot
1	Flat Foot
2	Normal Foot
3	Normal Foot
4	Normal Foot
5	Normal Foot
6	High Arched Foot (Right) and Normal Foot (Left)
7	Normal Foot

In table 6.10, given below, the subtalar angle can be visualized, which indicates the amount of pronation in the rear foot during impact. The higher values indicate more pronation. In general, it appears that the average values differ in both feet and the maximum value is shown on the injured foot. Through these values it can be stated that subjects 1, 2, 5 and 7 assume greater pronation on the injured foot and the others on their healthy foot. With respect to the foot axis angle a positive angle indicates the lateral rotation of the foot, while a negative angle indicates medial rotation. In this case, the mean value of all patients shows above average which is 6º for males and 7º for females. Just two patients assume internal rotation. Patient 2 medially rotates the injured foot and patient 6 medially rotates both feet. For the rest of all patients, the lateral rotation is displayed in both feet (Murray, Drought, & Ross, 1964).

Table 6.10 – Subtalar Angle and Foot Axis Angle.

Subjects	Subtalar Angle (º) Healthy – Injured (Max)		Subtalar Angle (º) Healthy – Injured (Min)		Foot Axis Angle (º) Healthy – Injured	
1	11.69	8.35	1.53	-0.05	14.62	8.30
2	7.68	21.95	-0.72	5.25	22.24	-2.19
3	10.68	1.62	9.09	-2.77	20.67	0.031
4	8.36	5.94	-4.78	0.11	10.59	10.46
5	7.87	11.69	-3.37	-2.7	10.16	11.11
6	9.21	5.38	-3.49	-2.36	-0.006	-0.21
7	3.31	7.26	-3.09	-1.48	13.09	23.46
$\bar{x}$	**8.40**	**8.88**	**-0.69**	**-0.57**	**13.05**	**7.28**
σ	**2.49**	**6.04**	**4.44**	**2.62**	**6.86**	**8.33**

Regarding normalized plantar forces it was found that in the control group, forces are similar in all subjects and the locations of high and low force are also the same, as shown in Table 6.11. These values refer to values collected by the local sensors of the pressure plate. The location of the foot that takes greater force is generally the heel, especially the medial heel. The area where it makes less force is in Toes 2-5. These sites are similar in both feet. The force values presented were normalized according to the body weight of the subject. The average of force value is higher in the left foot than the right foot, 2.83N/kg against 2.70N/kg. Male elements (6 to 10) present a very low values of plantar force compared to the female elements (1 to 5).

Table 6.11 – Minimum and Maximum Force Normalized of Control Group (N/kg).

Subjects	Force (Max) (N/kg) Left – Right		Location Left – Right		Force (Min) (N/kg) Left - Right		Location Left – Right	
1	3.04	2.73	Meta 4	Heel Medial	0.25	0.20	Toes 2-5	Toes 2-5
2	3.90	2.45	Heel Medial	Heel Medial	0.22	0.09	Toes 2-5	Toes 2-5
3	5.05	4.24	Heel Medial	Heel Medial	0.05	0.36	Toes 2-5	Toes 2-5
4	3.73	4.37	Heel Medial	Heel Medial	0.13	0.03	Toes 2-5	Toes 2-5
5	3.49	3.72	Heel Medial	Heel Medial	0.38	0.34	Toes 2-5	Toes 2-5
6	0.91	0.98	Meta 4	Meta 2	0.05	0.07	Midfoot	Toes 2-5
7	1.90	3.25	Toes 1	Midfoot	0.38	0.73	Toes 2-5	Toes 2-5
8	3.43	4.70	Heel Lateral	Heel Medial	0.41	0.38	Meta 4	Meta 4
9	0.75	0.90	Heel Medial	Heel Medial	0.06	0.08	Toes 2-5	Toes 2-5
10	0.82	0.99	Heel Lateral	Heel Medial	0.55	0.44	Toes 2-5	Midfoot
$\bar{x}$	**2.70**	**2.83**	-	-	**0.25**	**0.27**	-	-
σ	**1.43**	**1.40**	-	-	**0.17**	**0.21**	-	-

Similarly to what happened with the forces, also with the pressures (table 6.12), the values and locations of high and low pressure are similar between subjects. The lowest pressure is carried out on Toes 2-5, which makes sense because most people do not land the fingers, as it could be observed during the dynamic test in LBL. Again the medial heel takes usually the highest pressure values yet sometimes these occur in Meta 3 instead. The values shown in table 6.12 are also normalized weight. The average maximum pressure is 0.31 N/cm^2 on the left foot and 0.28 N/cm^2 on the right foot, with the difference of 0.03 N/cm^2.

Table 6.12 – Minimum and Maximum Plantar Pressure of Control Group (N/cm^2).

Subjects	Pressure (Max) (N/cm^2) Left – Right		Location Left – Right		Pressure (Min) (N/cm^2) Left – Right		Location Left – Right	
1	0.34	0.34	Meta 3	Meta 3	0.02	0.05	Toes 2-5	Midfoot
2	0.17	0.09	Heel Medial	Meta 4	0.01	0.01	Toes 2-5	Toes 2-5
3	0.32	0.32	Heel Medial	Meta 3	0	0.03	Toes 2-5	Toes 2-5
4	0.25	0.22	Meta 3	Heel Medial	0.01	0.02	Toes 2-5	Toes 2-5
5	0.29	0.03	Toes 2-5	Meta 3	0.03	0.02	Toes 2-5	Toes 2-5
6	0.63	0.62	Meta 3	Meta2	0.03	0.05	Midfoot	Toes 2-5
7	0.10	0.11	Meta 3	Meta 3	0.02	0.03	Toes 2-5	Toes 2-5
8	0.50	0.60	Heel Lateral	Heel Medial	0.04	0.05	Toes 2-5	Toes 2-5
9	0.27	0.32	Meta 2	Meta 2	0.03	0.03	Toes 2-5	Toes 2-5
10	0.20	0.19	Heel Lateral	Meta 3	0.02	0.02	Midfoot	Midfoot
$\bar{x}$	**0.31**	**0.28**	-	-	**0.02**	**0.03**	-	-
σ	**0.15**	**0.19**	-	-	**0.01**	**0.02**	-	-

The values of the plantar pressures for patients are also similar and the areas where they perform more and less force also. The area of higher pressure on the healthy leg occurs mostly in Meta 3 for all subjects, while on the injured foot it varies between the medial heel and Meta 2-3. The area of lower pressure occurs in the midfoot for almost all subjects. The values shown in the following table are

normalized to the body weight of each subject. The average maximum pressure (0.43 N/cm^2) occurs in the left leg and the difference for the right leg is of 0.04 N/cm^2.

Table 6.13 – Minimum and Maximum Pressure of patients (N/cm^2).

Subjects	Pressure (Max) (N/cm^2) Healthy – Injured		Location Healthy – Injured		Pressure (Min) (N/cm^2) Healthy - Injured		Location Healthy – Injured	
1	0.33	0.29	Meta 3	Heel Medial	0.02	0.02	Meta 1	Toes 2-5
2	0.54	0.4	Meta 3	Heel Medial	0.02	0.02	Midfoot	Midfoot
3	0.46	0.38	Meta 3	Heel Medial	0.04	0.06	Midfoot	Midfoot
4	0.52	0.55	Meta 3	Meta 2	0.04	0.03	Midfoot	Meta 5
5	0.38	0.41	Heel Lateral	Meta 3	0.03	0.03	Toes 2-5	Toes 2-5
6	0.43	0.42	Toes 1	Heel Medial	0.07	0.04	Meta 5	Midfoot
7	0.42	0.26	Meta 4	Meta 2	0	0	Meta 1	Toe 1
$\bar{x}$	**0.44**	**0.39**	-	-	**0.03**	**0.03**	-	-
σ	**0.06**	**0.08**	-	-	**0.02**	**0.02**	-	-

The area of greatest force lies, for the majority of the subjects, in the lateral heel for the healthy foot and medial heel in the case of the injured foot. The areas of lowest strength remain in the Midfoot and the in Toes 2-5. The maximum force differs from the healthy foot to the injured foot approximately 0.08N/kg, and the maximum force occurs on the injured leg as well as the minimum.

Table 6.14 – Minimum and Maximum Force of patients (N/kg).

Subjects	Force (Max) (N/kg) Healthy – Injured		Location Healthy – Injured		Force (Min) (N/kg) Healthy – Injured		Location Healthy – Injured	
1	0.49	0.45	Heel Lateral	Meta 3	0.03	0.02	Meta 1	Toes 2-5
2	0.82	0.61	Meta 3	Heel Medial	0.03	0.03	Midfoot	Midfoot
3	0.68	0.56	Meta 3	Heel Medial	0.05	0.9	Midfoot	Midfoot
4	0.07	0.81	Midfoot	Meta 2	0.07	0.07	Midfoot	Midfoot
5	0.58	0.62	Heel Lateral	Meta 3	0.04	0.06	Toes 1	Toes 2-5
6	0.79	0.87	Heel Lateral	Meta 3	0.04	0.06	Meta 1	Toes 2-5
7	0.07	0.51	Heel Medial	Heel Lateral	0.05	0.05	Toes 2-5	Toe 1
$\bar{x}$	**0.50**	**0.57**	-	-	**0.04**	**0.24**		
σ	**0.29**	**0.25**	-	-	**0.01**	**0.31**	-	-

Comparing the data related to the patients and the control group it was found that there are differences in the location of the application of the force and minimum/maximum pressure on the foot. Regarding to the force it is found that at the level of the IC, the force is applied at the same site (medial heel), but during the progression, in the patients group, it varies slightly in a more medial way in the foot shape. For the pressure it was found that patients produce higher pressure levels on the heel which does not happen on the control group. Looking at Table 6.14, it has been found that relative to patients, and on the level of plantar force the leg which takes the largest value is the contralateral to the lesion in most of the cases (exception for patient 4 and 5). These results can be explained by the tendency to "protect" the injured limb overloading the contralateral.

6.2.4.1 ANOVA results

For the results of plantar pressure analysis, a statistical analysis of variations (ANOVA) was performed on certain variables as plantar force and pressure. In this case, the Single Factor ANOVA were conducted: force and pressure levels presented by the patients (healthy and injured leg) and to the control group (left Leg only).

Table 6.15 – ANOVA: single factor of Maximum Force.

Leg	F	P-value	F crit
Healthy Leg vs Left Leg	14.28474	0.001818	4.543077
Injured Leg vs Left Leg	15.82218	0.001213	4.5430077

Table 6.16 – ANOVA: single factor of Minimum Force.

Leg	F	P-value	F crit
Healthy Leg vs Left Leg	9.2074	0.001818	4.543077
Injured Leg vs Left Leg	0.066594363	0.001213	4.5430077

In the case of maximum and minimum force (table 6.15 and 6.16) it was found that exists a high variability between groups (patients vs control group) with more significance in maximum force, since the greater will be the largest F variation among groups. However, the P-value to be less than 0.05 that indicates differences between groups exists. As the Fcritic is less than the variation between groups can be said that the results are significant. For the analysis of the variance at the plantar force it was found that only the data of the maximum force in the left leg are significant because it has a P-value of ≈0.07.

Table 6.17 – ANOVA: single factor of Maximum Pressure.

Leg	F	P-value	F crit
Healthy Leg vs Left Leg	3.79076	0.07051	4.543077
Injured Leg vs Left Leg	1.779132	0.2021567	4.54307

Table 6.18 – ANOVA: single factor of Minimum Pressure.

Leg	F	P-value	F crit
Healthy Leg vs Left Leg	1.608641	0.224015	4.543077
Injured Leg vs Left Leg	0.05532	0.941693	4.543077

In the case of maximum and minimum pressure (table 6.17 and 6.18) it was found that the groups (patients vs control group) concluded that there is greater variability in the healthy leg ($F_{Left} > F_{Right}$). However, considering the P-value of 0.05, it indicate that the difference between results are not significant because it is higher than 0.05.

6.3 Kinematic Results

6.3.1 Static GRF

Obtaining the values of static GRF was taken on force plates, with the subject in the anatomical reference position and with one foot on each plate (arrangement of plates described in Chapter V).

In table 6.19 and table 6.20, listed below, one can see the static GRF for both the control group (comparing the right with the left foot) and for patients (comparing the healthy foot with injured foot). There are two subjects (one from the control group and one patient) whose result could not be obtained.

Table 6.19 – Static GRF of Control Group (*could not get this value).

Subjects (n =10)	Static GRF (N/Kg) Right Foot – Left Foot		Difference
1	≈5.12	≈4.95	≈0.17
2	≈5.00	≈4.79	≈0.21
3	≈5.20	≈4.6	≈0.94
4	≈5.00	≈4.83	≈0.17
5	*	*	*
6	≈4.65	≈5.15	≈0.5
7	≈4.97	≈4.82	≈0.15
8	≈4.68	≈5.15	≈0.47
9	≈4.97	≈4.85	≈0.12
10	≈4.90	≈4.89	≈0.01
$\bar{x}$	4.94	4.89	0.30
σ	0.17	0.16	0.27

Table 6.20 – Static GRF of Patients (*could not get this value).

Subjects (n =7)	Static GRF (N/Kg) Normal Foot – Injured Foot		Difference
1	≈5.6	≈4.2	≈1.4
2	≈4.75	≈5.05	≈0.3
3	*	*	*
4	≈4.8	≈5	≈0.2
5	≈4.7	≈5.1	≈0.39
6	≈4.8	≈4.8	0
7	≈5.2	≈4.8	≈0.4
$\bar{x}$	4.98	4.83	0.45
σ	0.32	0.30	0.45

Analyzing data from the static GRF of the control group it was found that most subjects assumes greater force in right leg and this must be related to the fact that most of the subjects are right-handed, meaning that their dominant hand and with the greater force is the right one. It was also found that the difference in values between the legs ranges from 0.01 to 0.5N/kg and the mean value of the difference is 0.30N/kg. In the group of patients the range of difference values ranges from 0 to 1.4N/kg (higher than the control group) and the mean value is 0.45N/kg. There are only two patients (1 and 7) in which the limb that has the greatest force is the healthy one. The remaining ones show greater force in the injured limb. This may be due to the physical therapy sessions that were applied only in the injured limb. Patient 6 has equal force in both limbs as he does sports in a daily based.

6.3.2 Dynamic GRF

The graphs 6.1 to 6.4 show the dynamic GRF normalized during the movement of the 7 patients. It was possible observe that in almost all cases the force distribution is similar in both legs and varies between 10 to 12N/kg, presenting typical 'M' shape curve. Almost all the subjects present the weight acceptance in the 10% to 15% of gait cycle and both peaks shows 1.1 to the weight. Except the patient 3, all other patients show the higher variability in the injured foot. In general, the values of the forces have become almost equal, however patients 2, 3 and 6 show a difference between the injured foot and healthy foot. In the patient 6 there is a big difference between both feet, but this patient presented a bilateral rupture. Comparing the results with control group the forces are similar.

(a)

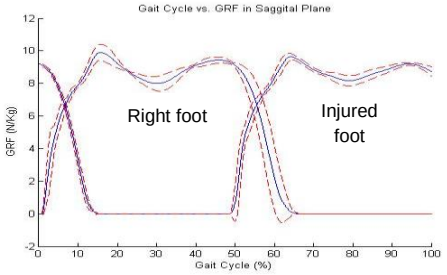

(b)

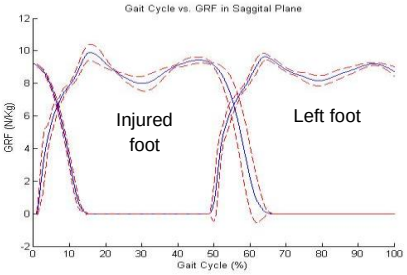

Graph 6.1 – GRF in sagittal plane of patient 1: Right Foot vs Injured Foot (a); GRF in sagittal plane of patient 2: Right Foot vs Injured Foot (b).

(a)

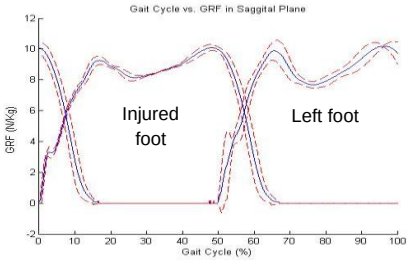

(b)

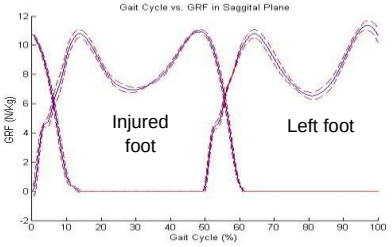

Graph 6.2 – GRF in sagittal plane of patient 3: Right Foot vs Injured Foot (a); GRF in sagittal plane of patient 4: Injured Foot vs Left Foot

(a)

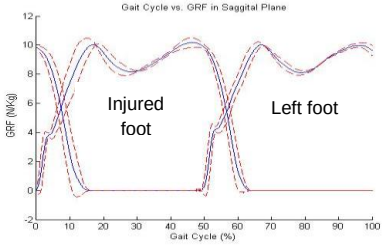

(b)

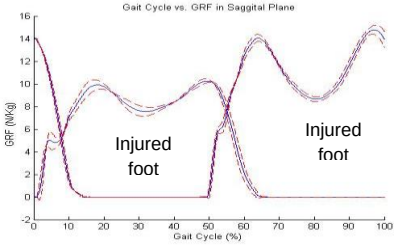

Graph 6.3 – GRF in sagittal plane of patient 5: Injured Foot vs Left Foot (a); GRF in sagittal plane of patient 6: Injured Foot vs Injured Foot.

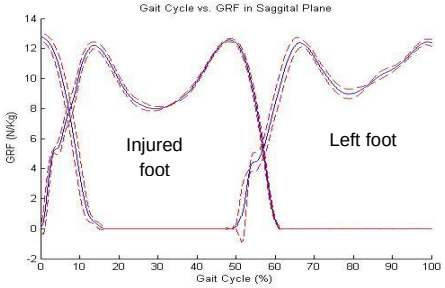

Graph 6.4 – GRF in sagittal plane of patient 7: Injured Foot vs Left Foot.

6.3.3 Kinematic Data

For this type of analysis, the most relevant angles such as the hip angle, the knee angle, the ankle angle, the subtalar angle and the metatarsophalangeal angle (MTP) were selected to be analyzed. The hip angle is the angle between the thigh and the trunk/pelvis – the positive value is flexion and the negative value is extension. The knee angle is the angle between the thigh and the knee and in this angle it is possible visualize the 3rd gait determinant. The ankle angle is angle between foot and leg, and positive value corresponds to dorsiflexion and negative value corresponds to plantar flexion. This angle is related to the 4th and 5th gait determinants. The subtalar angle allows one to check the value of the rear foot pronation during the impact with the ground. The metatarsophalangeal is the angle between metatarsus and phalanges of the foot.

To obtain the results, each leg individually and both legs simultaneously was evaluated. We also compared the values of each subject individually, between subjects of the same gender, opposite gender and with the control group.

6.3.3.1 Gait Cycle Analysis – one stride

In this analysis the stride patterns of patients were compared. The graphs, 6.5 to 6.11, presented below, compare the right limb and left limb of all patients during a gait cycle. In this case we can observe the different or contralateral movements corresponding to the events of the gait cycle time. Compared with the values reported in the literature it was found that these are in agreement therewith. Analyzing the graphs showed below was found that patients 3, 5 and 6 show values of standard deviation that are higher than the others that present a more preserved deviation.

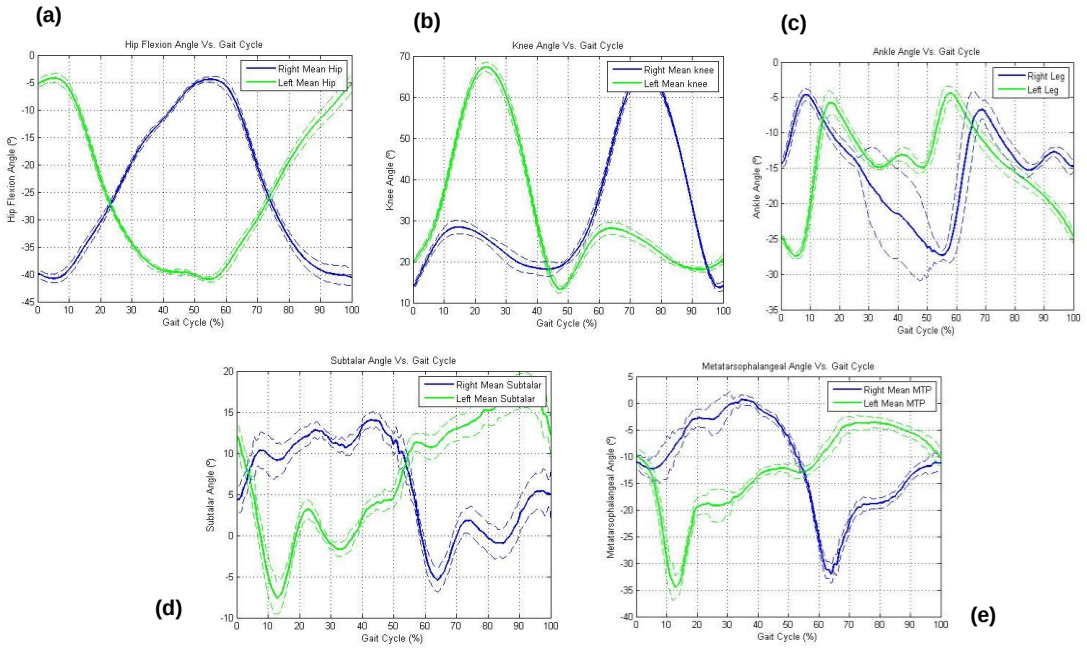

Graph 6.5 – Joint angles of patient 1: (a) Hip Flexion Angle, (b) Knee Angle, (c) Ankle Angle, (d) Subtalar Angle and (e) Metatarsophalangeal Angle for one stride.

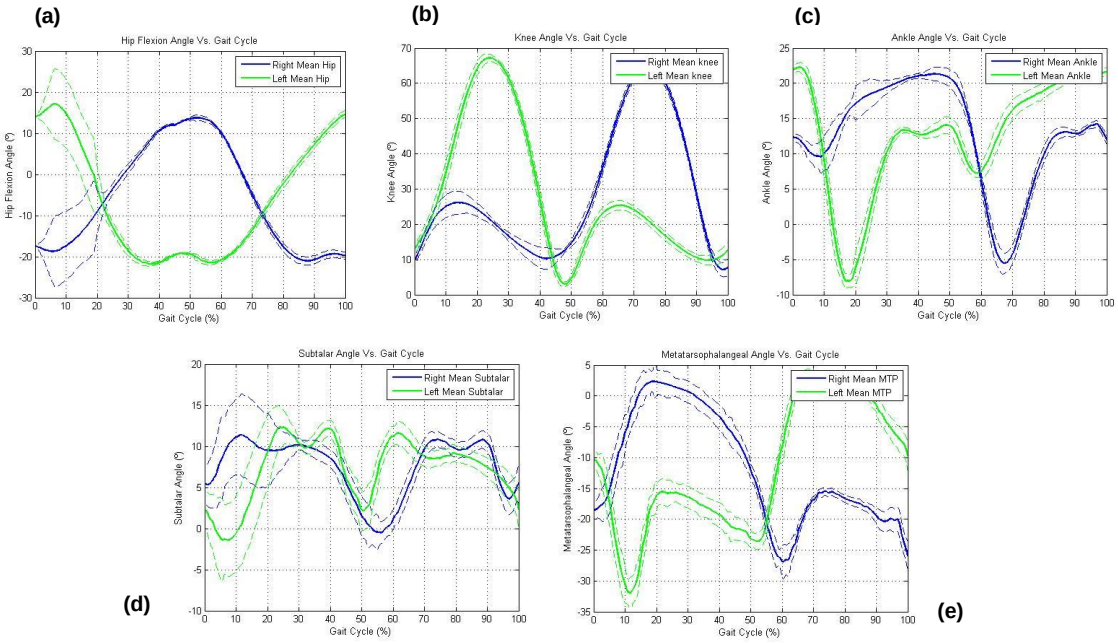

Graph 6.6 – Joint angles of patient 2: (a) Hip Flexion Angle, (b) Knee Angle, (c) Ankle Angle, (d) Subtalar Angle and (e) Metatarsophalangeal Angle for one stride.

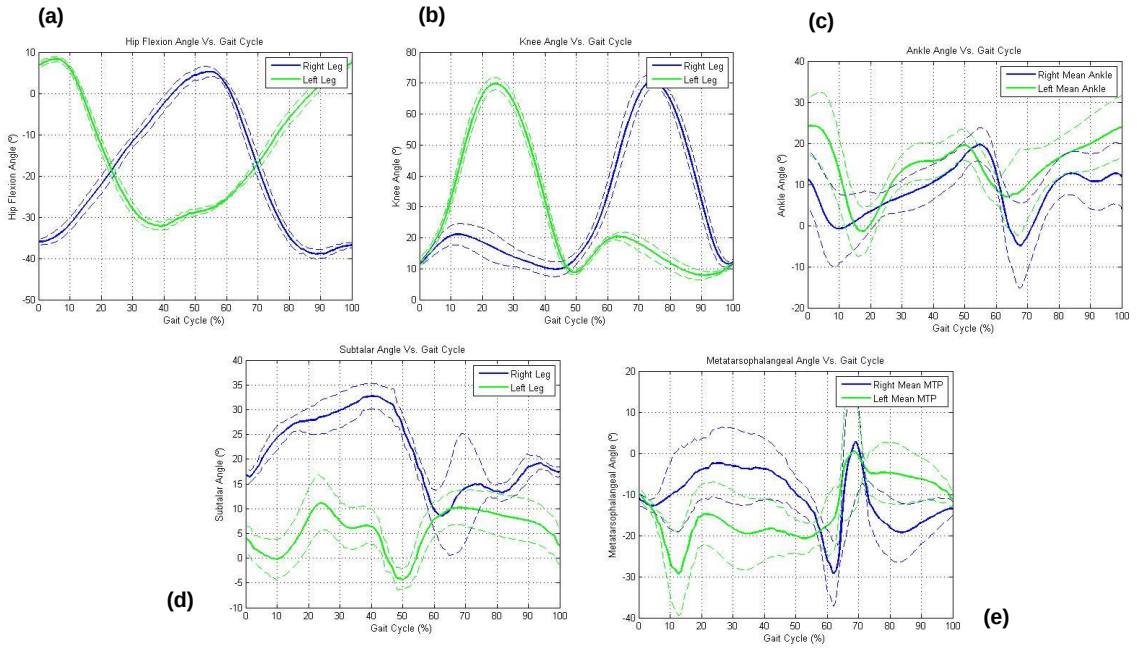

Graph 6.7 – Joint angles of patient 3: (a) Hip Flexion Angle, (b) Knee Angle, (c) Ankle Angle, (d) Subtalar Angle and (e) Metatarsophalangeal Angle for one stride.

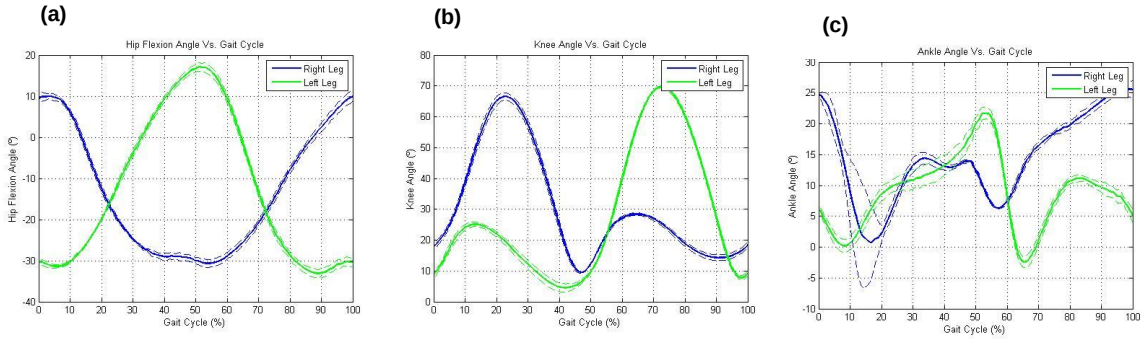

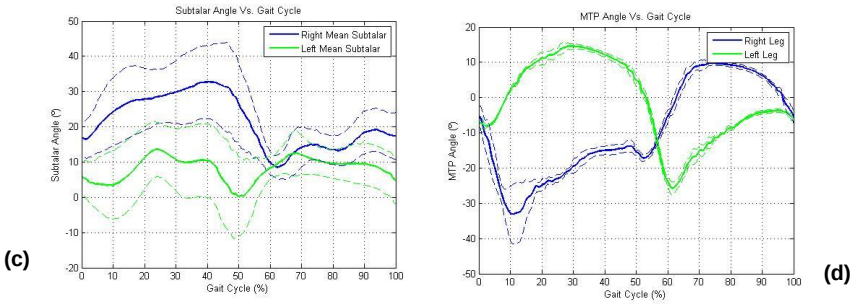

Graph 6.8 – Joint angles of patient 4: (a) Hip Flexion Angle, (b) Knee Angle, (c) Ankle Angle, (d) Subtalar Angle and (e) Metatarsophalangeal Angle for one stride.

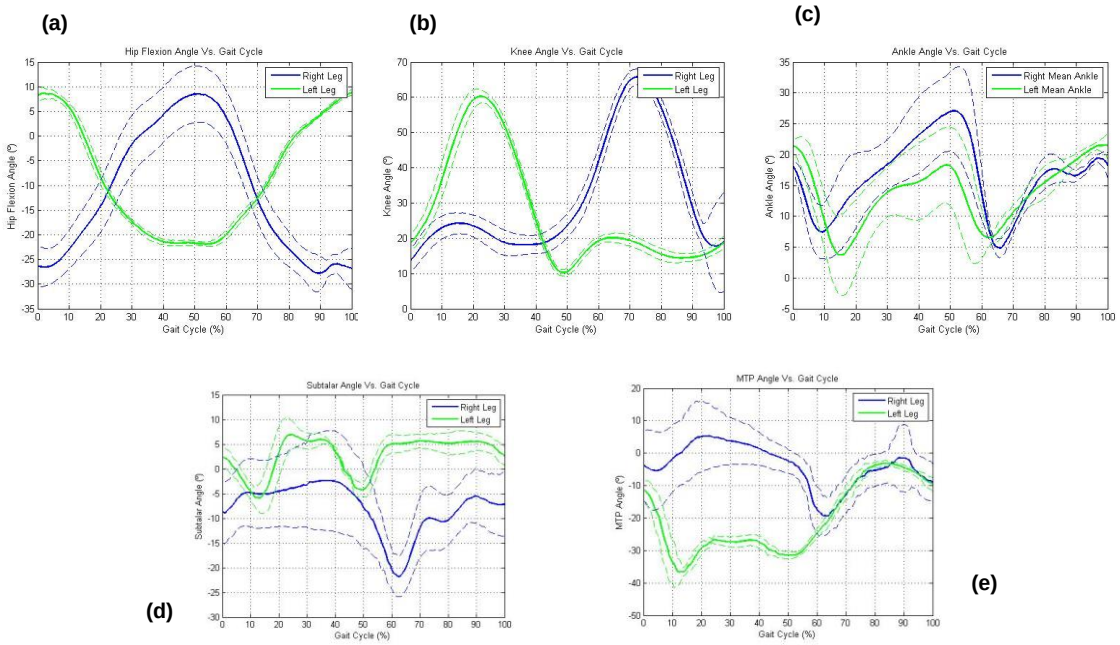

Graph 6.9 – Joint angles of patient 5: (a) Hip Flexion Angle, (b) Knee Angle, (c) Ankle Angle, (d) Subtalar Angle and (e) Metatarsophalangeal Angle for one stride.

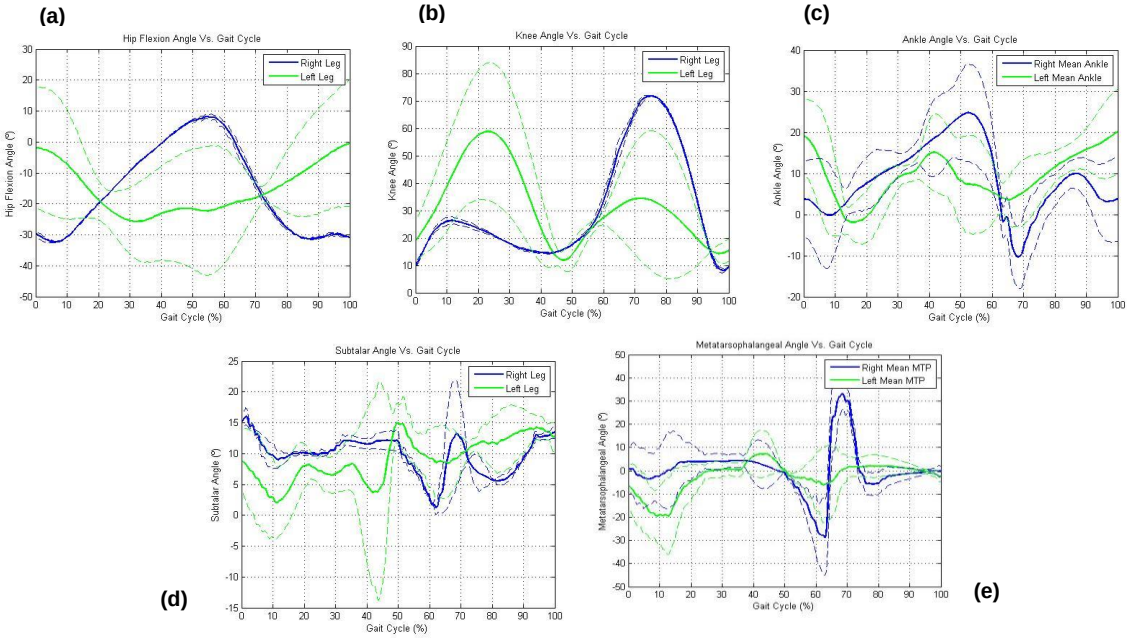

Graph 6.10 – Joint angles of patient 6: (a) Hip Flexion Angle, (b) Knee Angle, (c) Ankle Angle, (d) Subtalar Angle and (e) Metatarsophalangeal Angle for one stride.

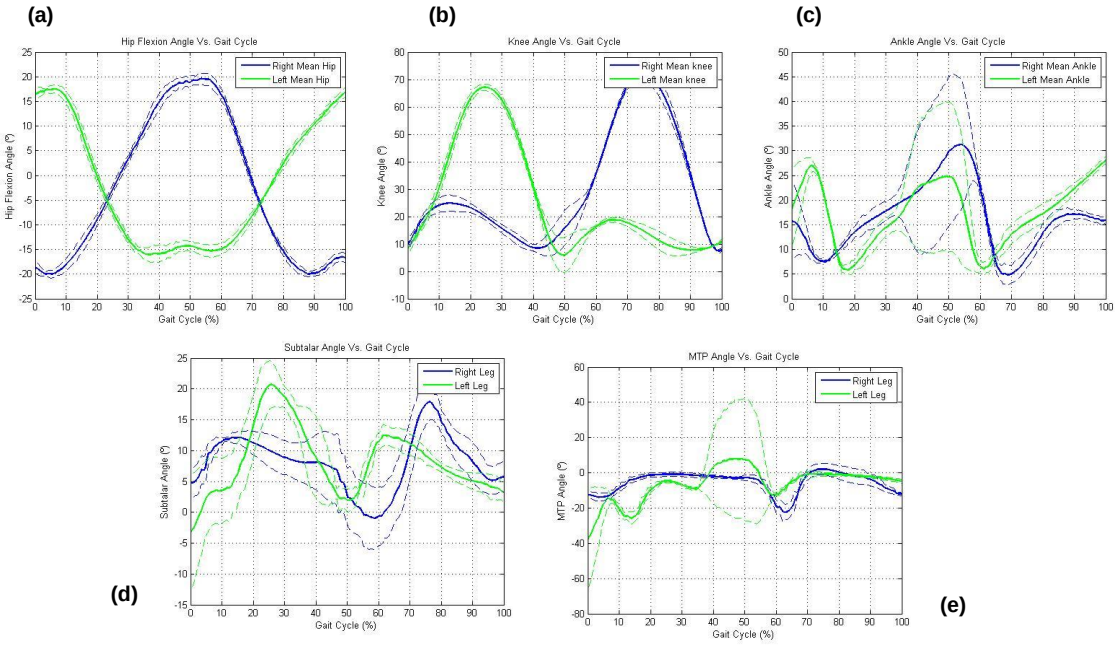

Graph 6.11 – Joint angles of patient 7: (a) Hip Flexion Angle, (b) Knee Angle, (c) Ankle Angle, (d) Subtalar Angle and (e) Metatarsophalangeal Angle for one stride.

6.3.3.2 IK Analysis – healthy foot vs injured foot

At this point of the study an analysis of intra-variability in the same subject (comparing healthy foot with the injured) was carried out. The graphs (view graphs 6.12 to 6.18) allow us to assess each patient individually, comparing the healthy foot and the injured foot. Through the analysis of all the graphs was possible to conclude that intra-variability occurs almost always in the same angles. The most critical variation, occurred in the knee angle, in the ankle angle, in the subtalar angle and MTP angle. It was also concluded that the injured limb showed a smaller amplitude on the plantar flexion and on the dorsiflexion and that this difference is more significant in the case of dorsiflexion (on patients).

Patient 1 had a rupture in the left leg that it is represented by the green curve. Analyzing the results, the hip flexion shows similar in both feet and takes the maximum angle (≈40º) in approximately 50% of gait cycle (terminal stance and preswing). In the knee angle, the data in the sagittal plane, are also similar in both limbs reaching a maximum value of flexion in the range of 60° to 70° at the swing phase. With regard to the flexion on the controlled plantar flexion it can be seen that the values are slightly different in both legs. The right leg assumes 30º while left leg assumes 20º. In this angle it is possible show the great difference that can demonstrate a shortening of the Achilles tendon. For the ankle angle, the values are similar for plantar flexion and dorsiflexion. The analysis of the subtalar joint angle assumes various oscillations (these oscillations may be due to the position of the markers during the experimental protocol, since this angle is sensitive to their location). It is possible show that the angle in right leg is shorter than the one in left leg. The difference between legs is approximately 10º in dorsiflexion motion. In the MTP angle occurs the same but the differences of value (≈10º) occurs in IC and loading response (plantar flexion motion) and in the midswing and terminal swing (dorsiflexion). In

conclusion, the results are according to the values reported in literature and the angles that demonstrate more variations comparing both feet are the knee, subtalar and MTP angle, namely during dorsiflexion movement.

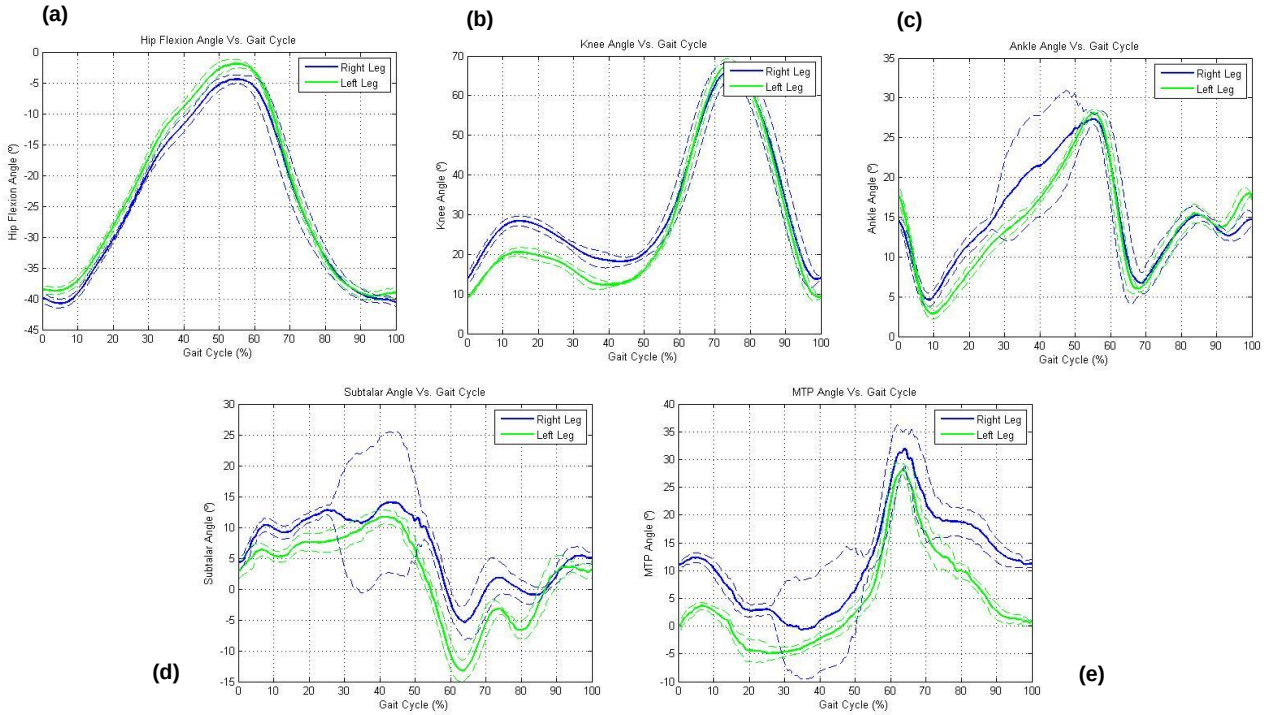

Graph 6.12 – Intra-variability joint angles of patient 1: (a) Hip Flexion Angle, (b) Knee Angle, (c) Ankle Angle, (d) Subtalar Angle and (e) Metatarsophalangeal Angle.

Patient 2 had a rupture in the right limb and it is represented by the blue curve. Analyzing the results, the hip flexion shows similar in both feet and takes the maximum angle (≈40º) in approximately 50% of gait cycle (terminal stance and preswing) but demonstrate a variability in both legs at the IC which may indicate that the foot does not always enter the same way in this event. For knee angle the values are also similar in both limbs reaching a maximum value of flexion in the range of 60° to 70°, in the swing phase. With regard to the flexion during controlled plantar flexion it can be seen that the values are similar (20º to 30º). For the ankle angle the values differ in both legs. In plantar flexion varies approximately 5º (in loading response event) and the same occurs in dorsiflexion. In this case the injured leg is the leg with smaller angular amplitude. In the subtalar angle the variation is similar to both legs but it is possible to observe that the injured leg is more constant in amplitude. In the MTP angle, the curves are similar but in the plantar flexion at the TO event is more pronounced in the healthy leg. In conclusion, the results are in according to the values reported in literature and the angles that demonstrate more variations comparing both feet are in the subtalar and MTP angle, namely in dorsiflexion moment.

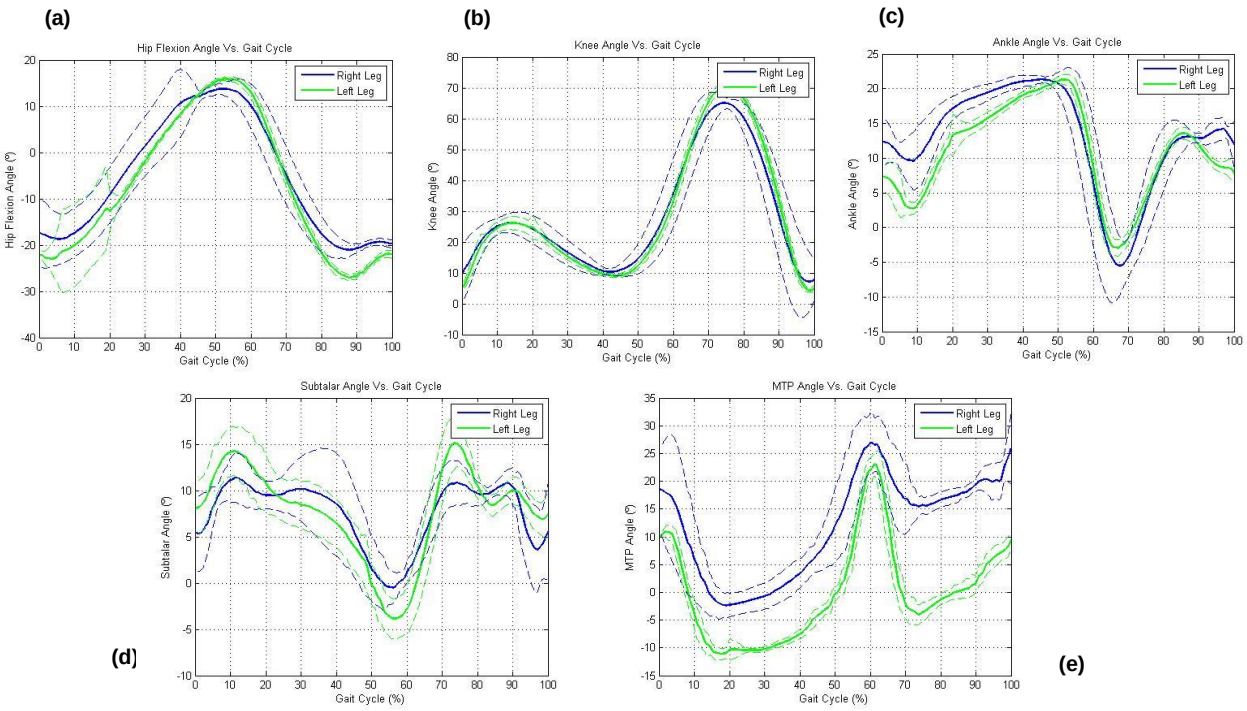

Graph 6.13 – Intra-variability joint angles of patient 2: (a) Hip Flexion Angle, (b) Knee Angle, (c) Ankle Angle, (d) Subtalar Angle and (e) Metatarsophalangeal Angle.

Patient 3 had a rupture in the right limb and it is represented by the blue curve. The hip flexion, presents values between -30° and 0° and it was found that both angular curves assumes approximately equal values, but a pronounced standard deviation exists much in both curves which may indicate that in this case the patient presents a gait with some degree of variability. In the knee angle, the data in the sagittal plane are similar for both legs with a maximum flexion at swing phase on range between of 60° and 70°. With respect to the flexion in controlled plantar flexion it can be seen that the values are also similar. However there is a slight difference between left and injured leg in the shape and amplitude of the curve. The injured leg assumes one amplitude of 20º and the left leg assumes one amplitude in range of 25º to 30º. For the ankle angle, it was found that this is in the range of referenced values and both curves are similar during swing but in stance phase during the plantar flexion (in firstly 10% of gait cycle) a difference of about 5º exists between legs (right ankle assume higher angles). In dorsiflexion occurs the same. In the subtalar angle exist one pronounced difference in both legs in the stance phase. The amplitude in the injured leg is superior to the left leg. Lastly, in MTP angle, the angular curves are different. The injured leg assumes one lower amplitude in stance phase but in the initial swing and midswing the dorsiflexion motion is more pronounced in the injured leg. In conclusion this patient presented significant variations in the knee, ankle, subtalar and MTP angles.

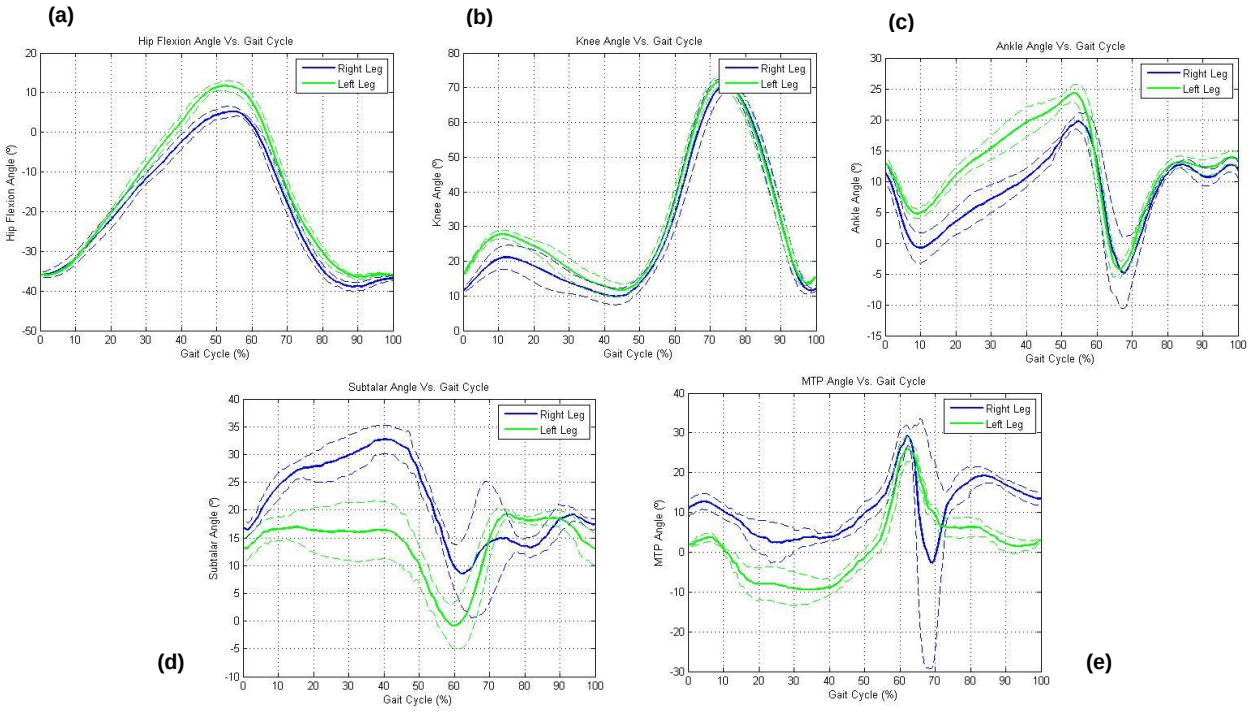

Graph 6.14 – Intra-variability joint angles of patient 3: (a) Hip Flexion Angle, (b) Knee Angle, (c) Ankle Angle, (d) Subtalar Angle and (e) Metatarsophalangeal Angle.

Patient 4 had a rupture in the right limb and it is represented by the blue curve. This patient present a huge variation in all angles and has also presented considerable differences between both feet. In the knee angle presents a lesser flexion in the controlled plantar flexion, the movement of the injured leg (≈20 against to ≈30 in the left leg). The ankle angle shows a decrease in dorsiflexion range of motion but the shape of curves is similar. In the subtalar angle there is a significant difference in plantar flexion in terminal stance. In the MTP angle the most significant difference occurs in the movement of the plantar flexion and dorsiflexion IC. The patient should be reevaluated again to confirm the results now presented.

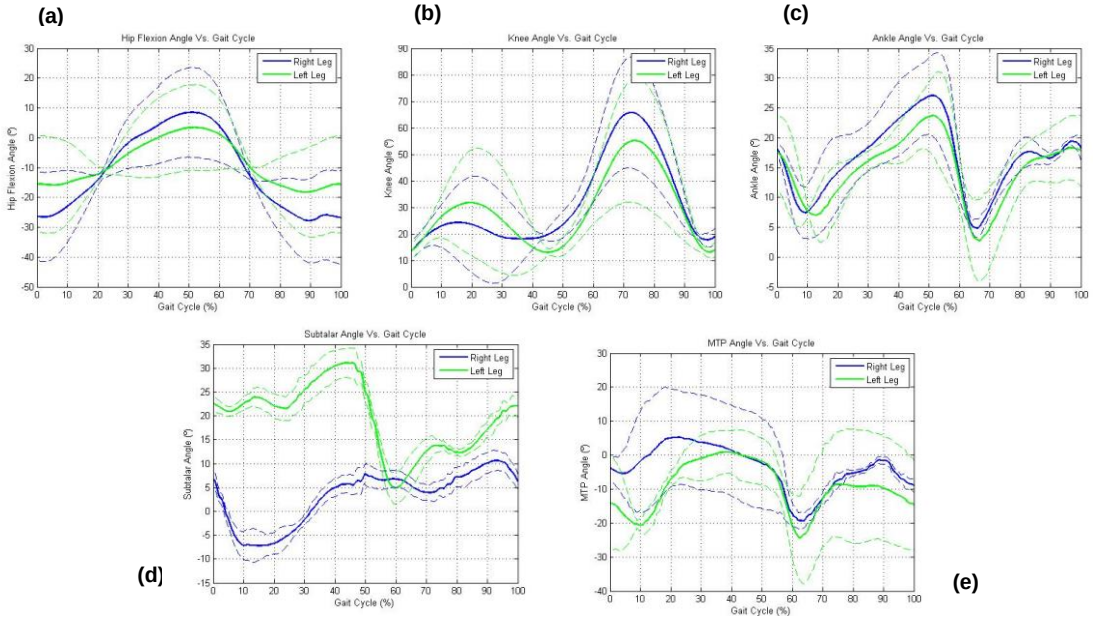

Graph 6.15 – Intra-variability joint angles of patient 4: (a) Hip Flexion Angle, (b) Knee Angle, (c) Ankle Angle, (d) Subtalar Angle and (e) Metatarsophalangeal Angle.

In the patient 5, the hip flexion has a high angular variability between -10° to 30° for extension and flexion, respetivelly. It was also found that both angle curves are similar. Regarding the knee angle, data are similar in both legs for flexion, 60° to 70°. With regard to the flexion (at IC) the values are different. In the injured leg, these range from 25° to 30° and in left leg values vary between 15° to 30°. For the ankle angle the angle varies between 0° and -25° and the curves are similar. For the subtalar angle, when compared with the reference values, it shows a higher amplitude. Due to the oscilation of curves it is not possible to say if the foot is more pronated or supinated. Finally, the MTP angle, has an angular range between 0° and -30°.

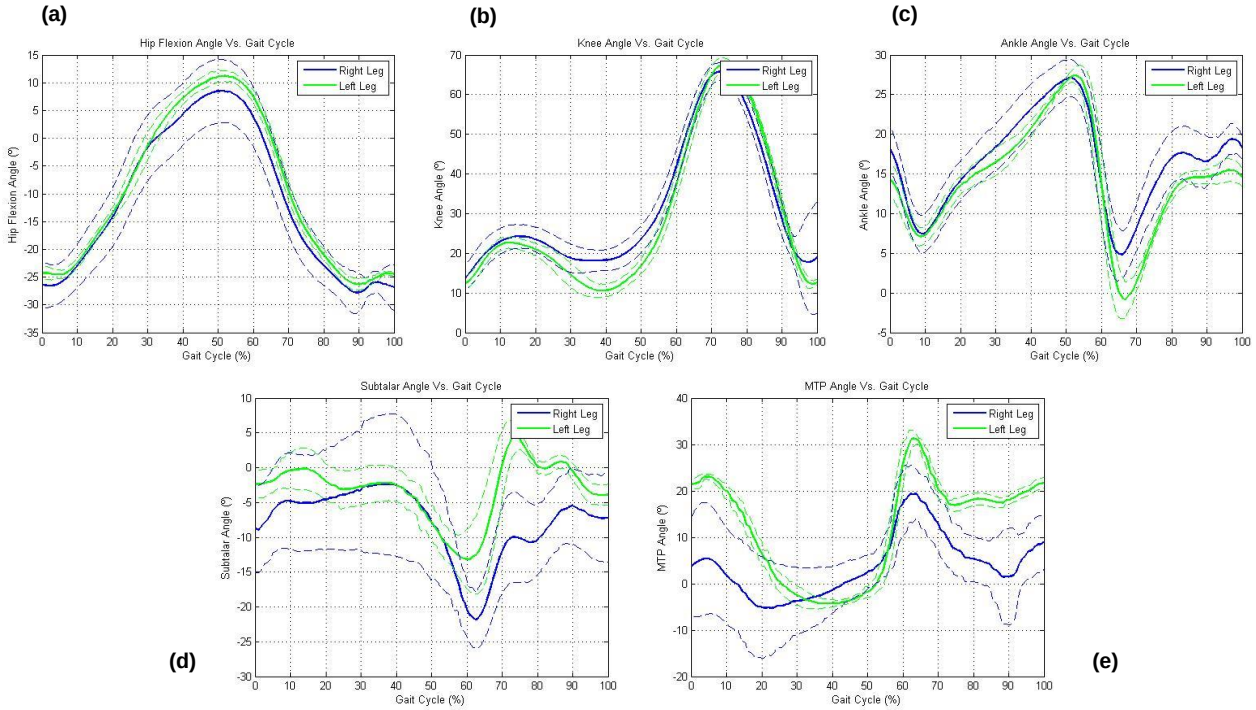

Graph 6.16 – Intra-variability joint angles of patient 5: (a) Hip Flexion Angle, (b) Knee Angle, (c) Ankle Angle, (d) Subtalar Angle and (e) Metatarsophalangeal Angle.

Patient 6 had a bilateral rupture. This patient exhibited a huge variation in all angles and has shown considerable differences between both feet. The standard deviation associated with all angles is high and therefore may suggests that there was a considerable degree of variability in gait events during data acquisition. This patient reported some problems with balance, which are supported by the variability in the results. The variability in ankle angle occurs in dorsiflexion during the stance phase and plantar flexion at the end of stance phase. In the case of MTP there is a peak dorsiflexion range of motion.

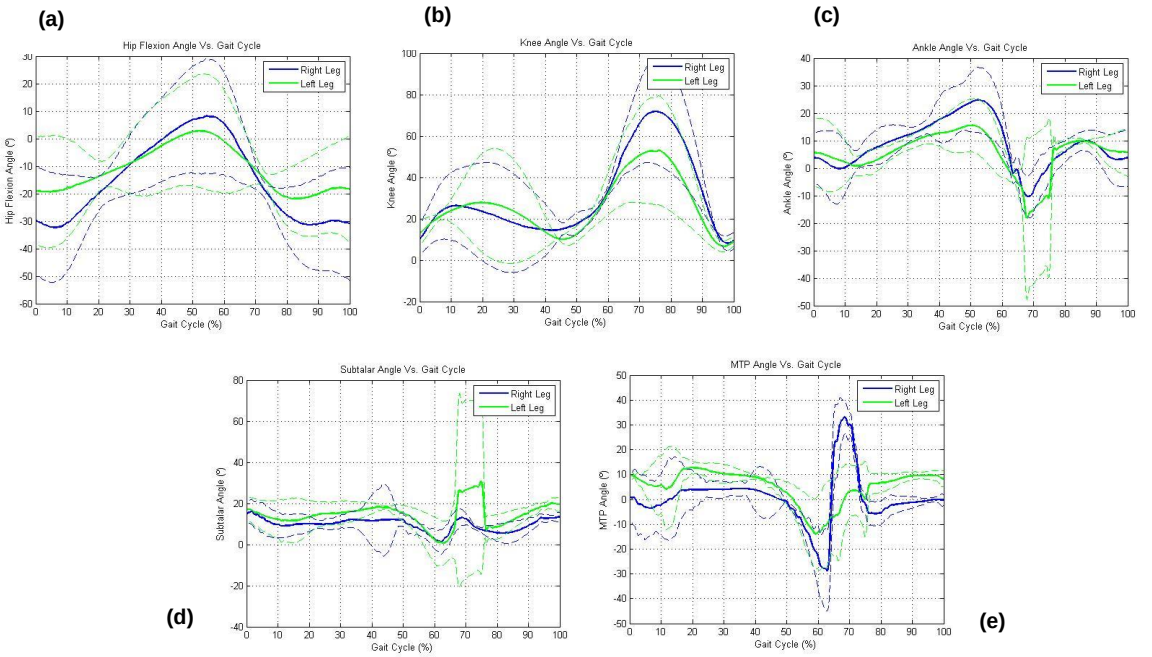

Graph 6.17 – Intra-variability joint angles of patient 6: (a) Hip Flexion Angle, (b) Knee Angle, (c) Ankle Angle, (d) Subtalar Angle and (e) Metatarsophalangeal Angle.

Patient 7 had a rupture in the right limb and it is represented by the blue curve. This patient shows a similar behavior for both feet. The most significant difference occurs in MTP angle where the right foot presents greater variability. In this case dorsiflexion, in swing phase assumes that once an abnormality occurs abruptly between 60% and 70% of gait occurs after a slight motion of plantar flexion.

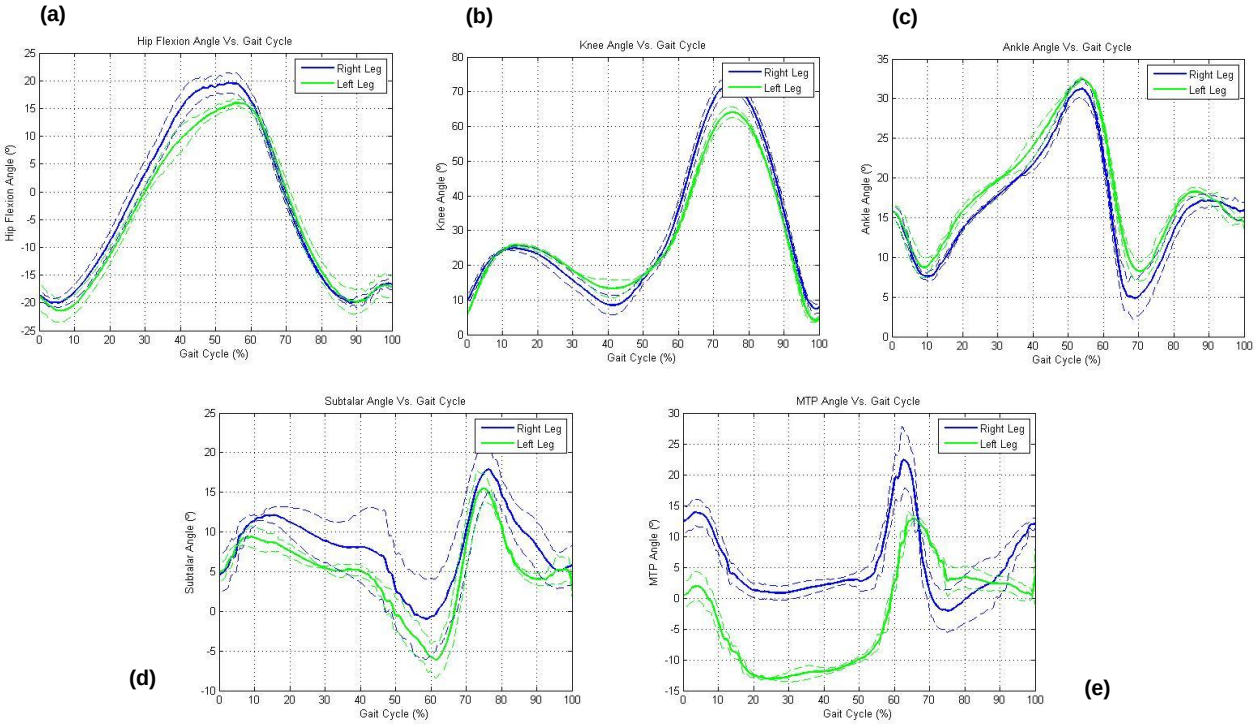

Graph 6.18 – Intra-variability joint angles of patient 7: (a) Hip Flexion Angle, (b) Knee Angle, (c) Ankle Angle, (d) Subtalar Angle and (e) Metatarsophalangeal Angle.

In the following tables (table 6.21 and 6.22), we can examine the maximum amplitude for each patient, in order to be easier to do an overall comparison. The values are taken from different stages of the gait cycle. In the hip, the extension value is taken from IC and final swing phase and the flexion is taken from the terminal stance and preswing events. Relatively to the knee angle, the minimum flexion is analyzed in loading response or midstance and the flexion is analyzed in initial swing/midswing. Lastly, the ankle angle, the subtalar angle and MTP angle are analyzed in IC, weighted acceptance and TO for plantar flexion and in the foot flat and midstance to the dorsiflexion respectively.

It was found that all values are within the same pattern. For the knee angle it was concluded that all patients have a decrease in flexion during controlled plantar flexion movement, except patient 2. In the MTP angle it was concluded that in the injured foot, dorsiflexion is always lower in all patients and that there is variability between subjects. In this variable we cannot assume that the lowest values are in the injured foot because only 3 cases confirmed this assumption. However, if this relationship exists, this can be explained by the surgery technique used that can cause a shortening/lengthening of the Achilles tendon, which explains the variability in feet. In the case of the ankle angle, there was a consistence in the data obtained. This variable obtained computationally cannot be compared with the amplitude obtained experimentally (view table 6.5) because it cannot estimate the maximum or minimum joint motion during gait because these motions depend on patient's position (static or dynamic) and the position of knee, as stated Susan Hall (Completo & Fonseca, 2011; Hall, 2003; Winter, 1991).

Table 6.21 – Hip flexion angle (a) and Knee Angle (b) of patients.

	HIP FLEXION (Maximum º)			
	Flexion		Extension	
	Injured Foot	Healthy Foot	Injured Foot	Healthy Foot
1	-2	-5	-38	-40
2	10 – 15	15 - 20	(-25) – (-30)	-20
3	0 – 10	0 – 20	-35	-30
4	-10	0 – 5	-28	-15
5	10	0 – 5	-25 – (-30)	-15 – (-20)
6	10	0 – 5	-30	-20
7	20	15	-20	-18

	Knee Angle (Maximumº)			
	Flexion		Flexion (SwP)	
	Injured Foot	Healthy Foot	Injured Foot	Healthy Foot
1	60 - 70	60 - 70	20	30
2	60 - 65	65 -70	20 -25	20 -25
3	65 - 70	60 - 65	20	20 -30
4	75	65	20 – 25	30
5	60 - 70	50 - 60	25 – 30	30
6	60 - 70	50 - 60	20 – 30	20 – 30
7	70 - 80	60 - 70	20 – 30	20 – 30

Table 6.22 – Ankle Angle (a) and MTP angle (b) of patients.

	ANKLE ANGLE (Maximum º)			
	Plantar Flexion		Dorsiflexion	
	Injured Foot	Healthy Foot	Injured Foot	Healthy Foot
1	0-5	5	25 -30	25 - 30
2	-5	-3	20	20
3	-5	-3	22	18
4	5 – 10	5 – 10	25 - 30	20 - 25
5	5	0 – 5	25 - 30	20 - 25
6	-10	-15	20 - 25	10 - 15
7	10	5	30	30 - 35

	MTP ANGLE (Maximum º)			
	Plantar Flexion		Dorsiflexion	
	Injured Foot	Healthy Foot	Injured Foot	Healthy Foot
1	-30 –(-35)	-25 – (-30)	5	0
2	-25	-23	10	3
3	-20 – (-25)	-30	5-10	-10 – (-5)
4	0 – (-10)	-10 - (-20)	0 – 10	0
5	-20	-20 – (-30)	0 – 10	0 -5
6	-30	-12	30	13
7	-20	0 - 10	-10	10 -20

6.3.3.3 IK Analysis – Patients vs Control Group

In this analysis the two legs of the patients were compared with the control group. The following graphs are relative to individual assessment for each patient. The red curve represents the control group, while healthy and injured limb are represented by the same colors as in the previous graphs.

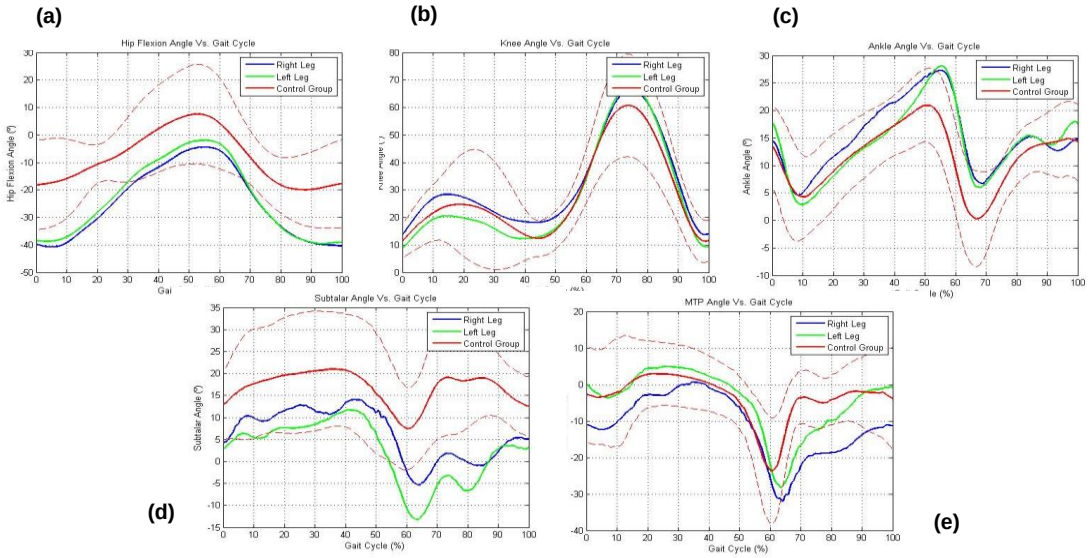

Graph 6.19 – Control Group vs patient 1: (a) Hip Flexion Angle, (b) Knee Angle, (c) Ankle Angle, (d) Subtalar Angle and (e) Metatarsophalangeal Angle.

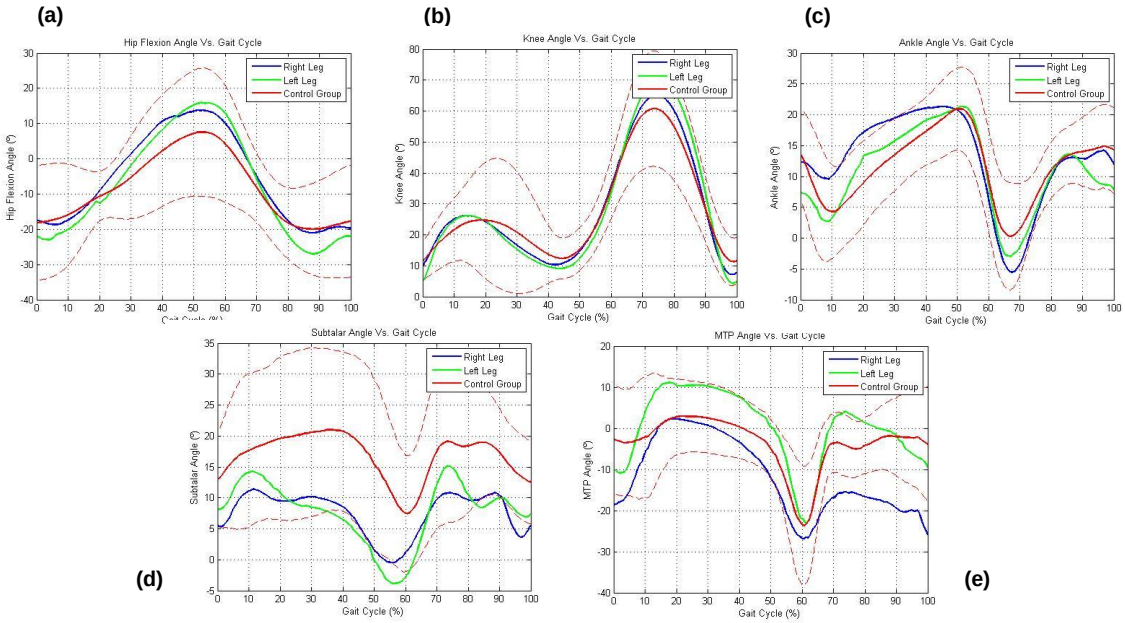

Graph 6.20 Control group vs. Patient 2: (a) Hip Flexion Angle, (b) Knee Angle, (c) Ankle Angle, (d) Subtalar Angle and (e) Metatarsophalangeal Angle.

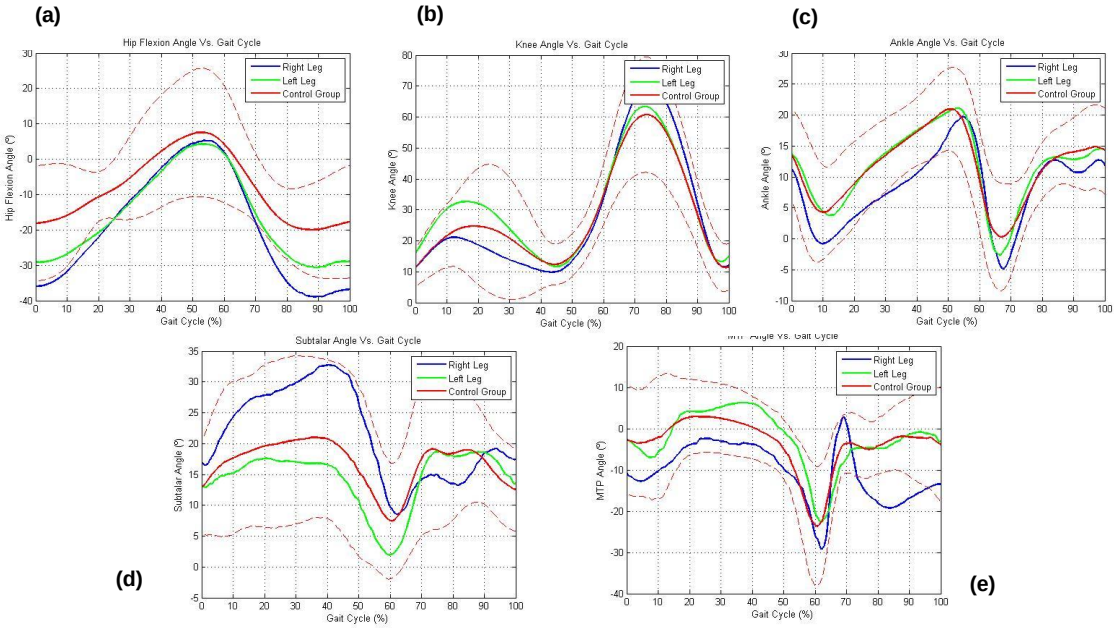

Graph 6.21 – Control group vs. Patient 3: (a) Hip Flexion Angle, (b) Knee Angle, (c) Ankle Angle, (d) Subtalar Angle and (e) Metatarsophalangeal Angle.

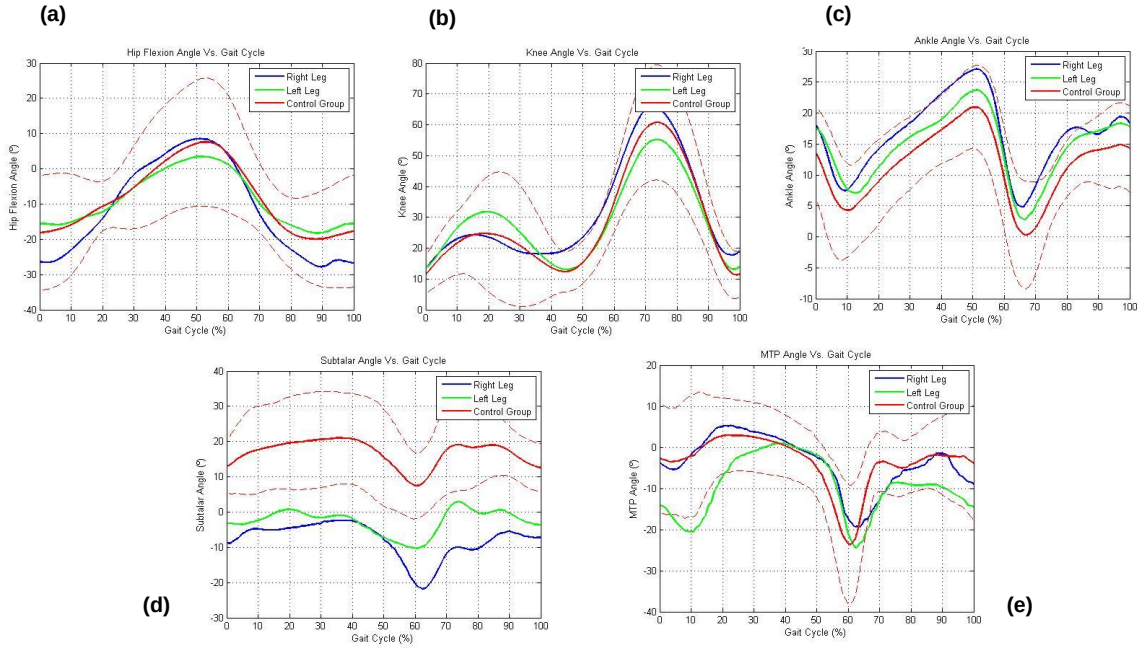

Graph 6.22 – Control group vs. Patient 5: (a) Hip Flexion Angle, (b) Knee Angle, (c) Ankle Angle, (d) Subtalar Angle and (e) Metatarsophalangeal Angle.

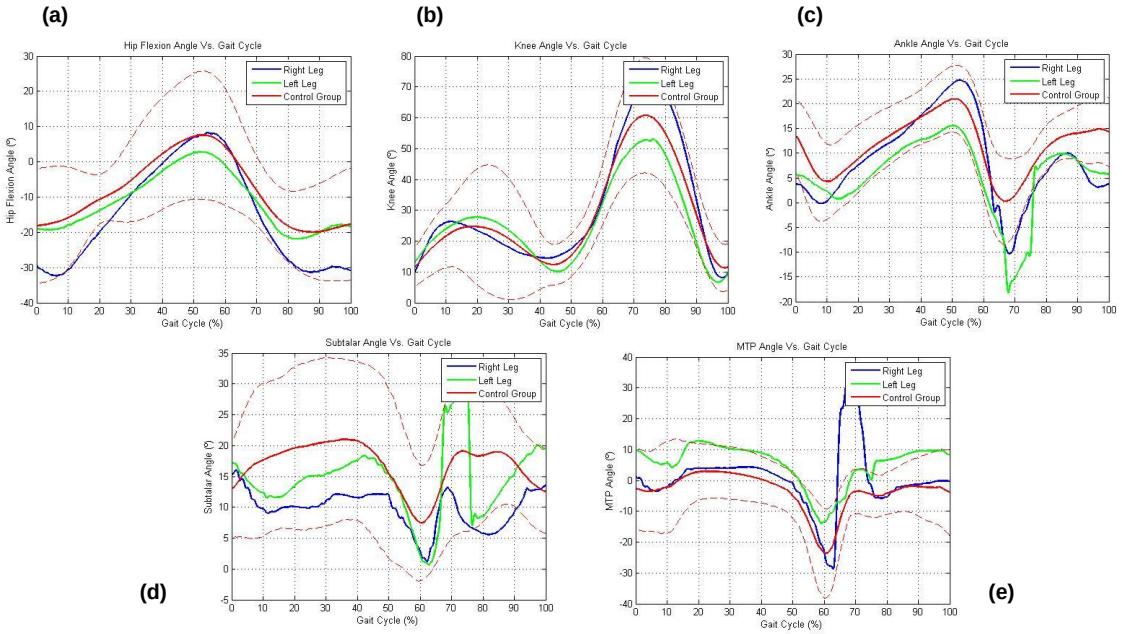

Graph 6.23 – Control group vs. Patient 6: (a) Hip Flexion Angle, (b) Knee Angle, (c) Ankle Angle, (d) Subtalar Angle and (e) Metatarsophalangeal Angle.

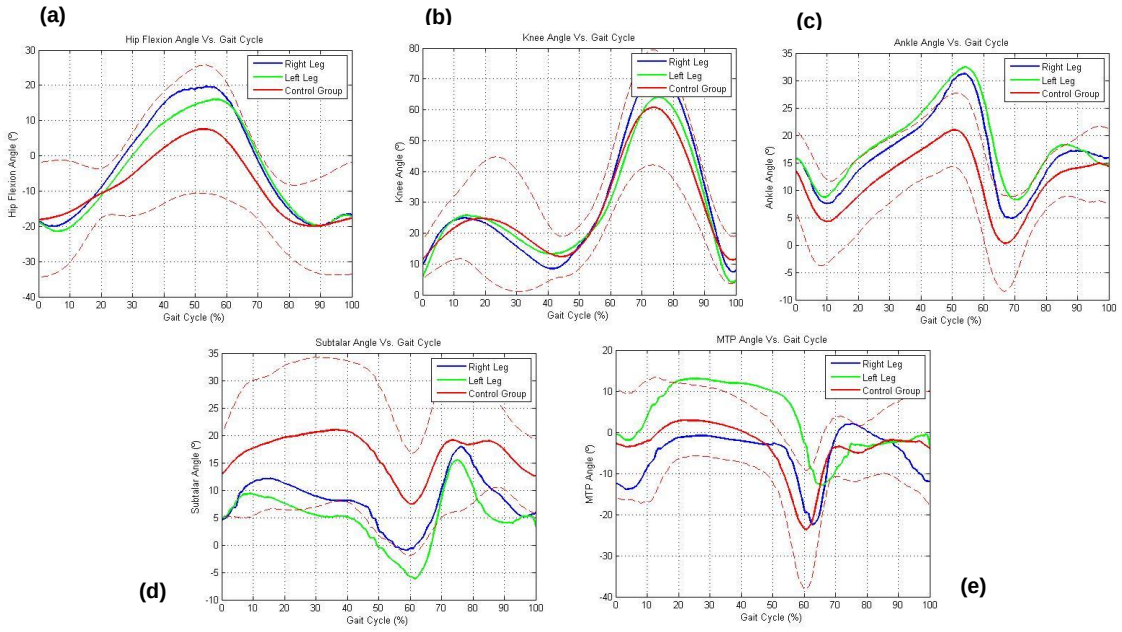

Graph 6.24 – Control group vs. Patient 7: (a) Hip Flexion Angle, (b) Knee Angle, (c) Ankle Angle, (d) Subtalar Angle and (e) Metatarsophalangeal Angle.

Through the analysis of all patients it was found that the results for most patients within one standard deviation of the control group and data reported in literature. There are two cases where it was found that the results obtained the ones from differ from control group: patient 5 and 7. In the case of

patient 5, the subtalar angle is not within the values obtained for the control group and in patient 7 the same is assumed also for the ankle angle.

It was also established that in almost all pathological subjects, the healthy leg, shows less variation when compared to the control group. Comparing the results of all patients with the control group, we found that the most variability occurs in the ankle, subtalar and MTP angle. In these cases, the patterns of the curves of the patients are slightly different ones of the control group. The most important difference lies in dorsiflexion that, in the case of the injured leg varies significantly. In case of MTP angle, in terminal swing, in some cases (3 and 7), a significant difference occurs, since in this phase of the gait cycle, dorsiflexion is occurring when in fact plantar flexion was expected. In the first case, the patient performs a plantar flexion (≈65% to 70% of gait cycle) and then performs a slight dorsiflexion, unlike the patient 7 that performs, until the end of the cycle, a plantar flexion. In the case of the subtalar joint angle, it has been found that the one observed in the plantar flexion is more pronounced (i.e. its maximum peak is higher) than the control group. It was also possible to observe that the rupture of the Achilles tendon, although interfering with the movement of knee flexion does not generate a significant variability in the magnitude of this angle.

6.3.4 Dynamic Analysis

6.3.4.1 ID Analysis – Healthy Foot vs. Injured Foot

In this analysis the same moments of force in joints presented in the previous sections were assessed. In all patients, in general, the curves and the values of moments are similar to the data reported by Winter (Winter, 1991). There is a generalized variability between both legs, except in patient 1. The hip flexion moment showed some variability between the legs of the same patient and between patients. According to the results it was observed that the injured limb assumed a greater irregularity in moment the curve. Relatively to the knee moment, an intra-variability is present in almost all subjects. Some differences were found between the curves presented in literature and these obtained experimentally. Patients 2 and 3 showed the peak of flexion at approximately 15% of the gait cycle, i.e. during the midstance. Patients 5, 6 and 7 show a peak at the interval 40% to 50% of the gait cycle, that corresponds to the terminal stance, being thus in disagreement with Winter (Winter, 1991). Regarding the ankle moment it was concluded that there is an intra-variability in the subjects. When compared, the subjects also assume some variability. In this case is ambiguous to say that the injured leg is the one that presents less moment. Patients 2 and 3 showed a decrease in the value of the controlled plantar flexion, unlike patient 5 who takes a value greater than the injured leg. However the values of the ankle moment in this phase are identical in all cases. The values of power plantar flexion are in all cases very closed and occurs around 50%. The moment in the MTP joint is similar to the ankle moment, however, assumes lower values and is very similar in all patients except in patient 7. The intra-variability in this moment occurs during the controlled plantar flexion in all cases. Regarding powered plantar flexion it was found that in all cases the injured limb has a smaller moment. At the level of the subtalar moment it was found that this is similar between patients except patient 7, and is less significant in the injured

limb. The following graphs depicts the moments at force for each patient. Only in patient 1 (graph 6.25) the injured limb is represented in blue (right leg), the in remaining (6.25 to 6.29) it is shown in green (left leg). In general, there was a decrease in the joint moment shown of the injured leg.

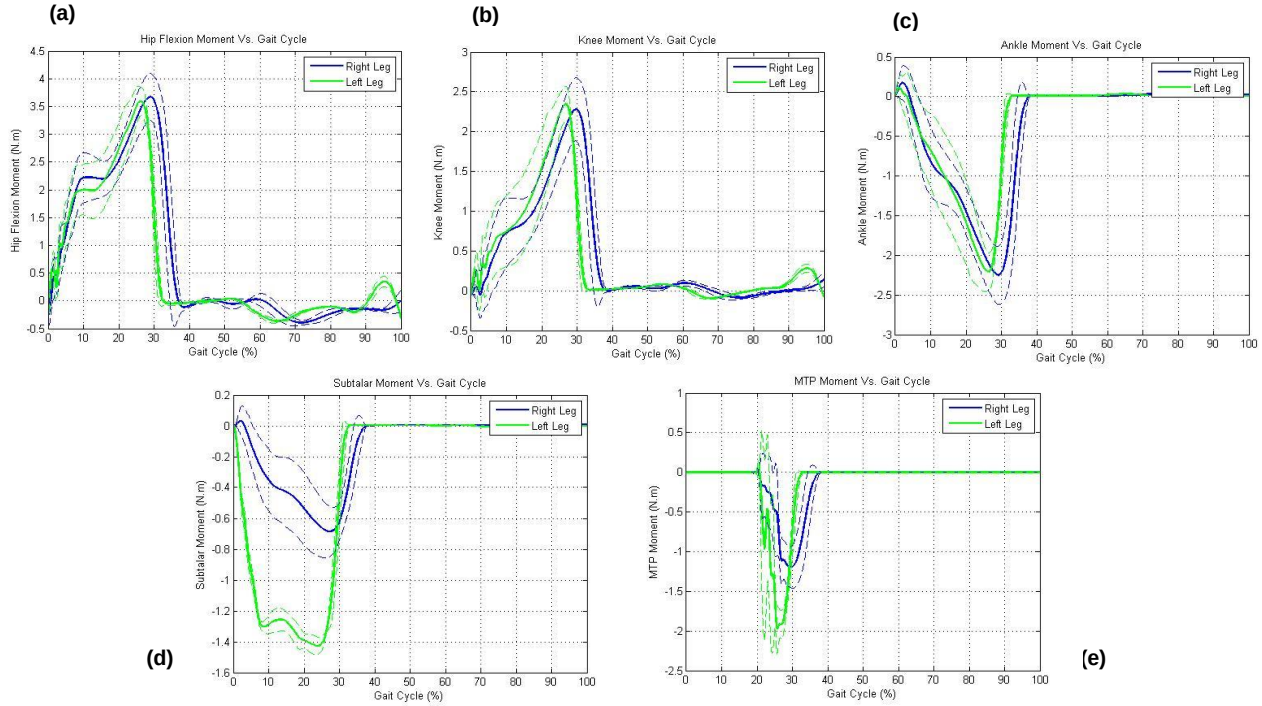

Graph 6.25 – Intra-variability moment of patient 1: (a) Hip Flexion Moment, (b) Knee Moment, (c) Ankle Moment, (d) Subtalar Moment and (e) Metatarsophalangeal Moment

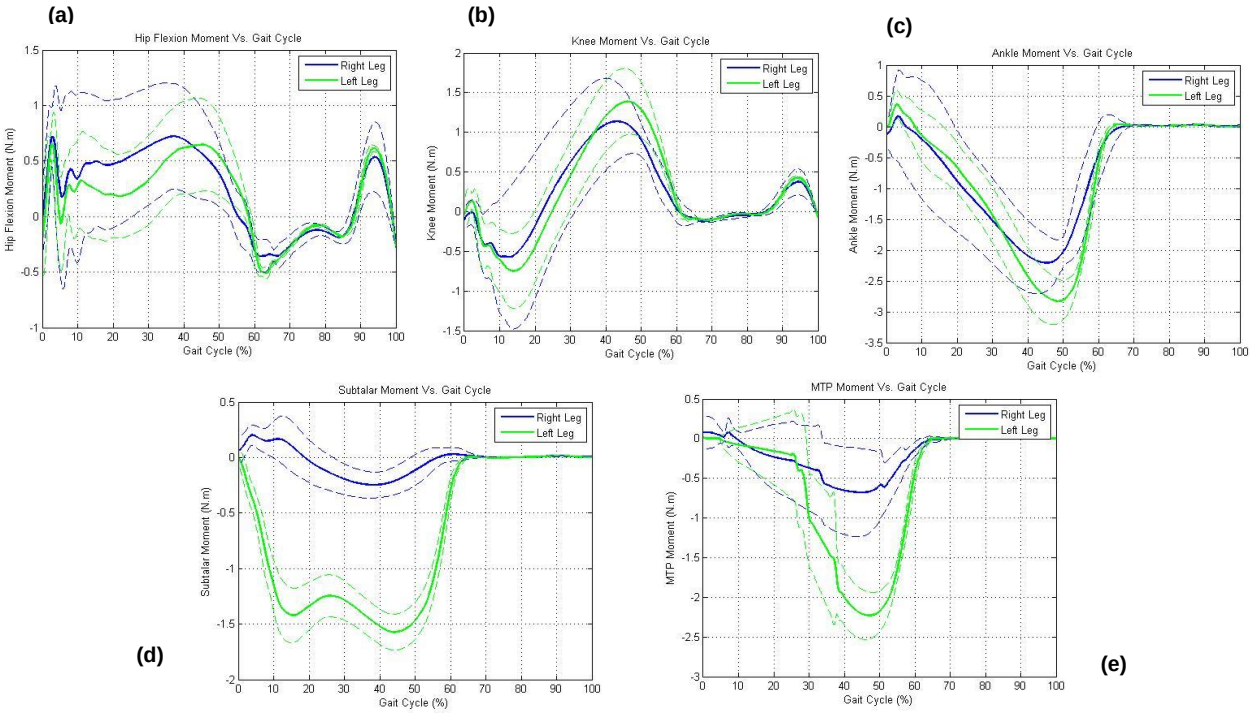

Graph 6.26 – Intra-variability moment of patient 2: (a) Hip Flexion Moment, (b) Knee Moment, (c) Ankle Moment, (d) Subtalar Moment and (e) Metatarsophalangeal Moment.

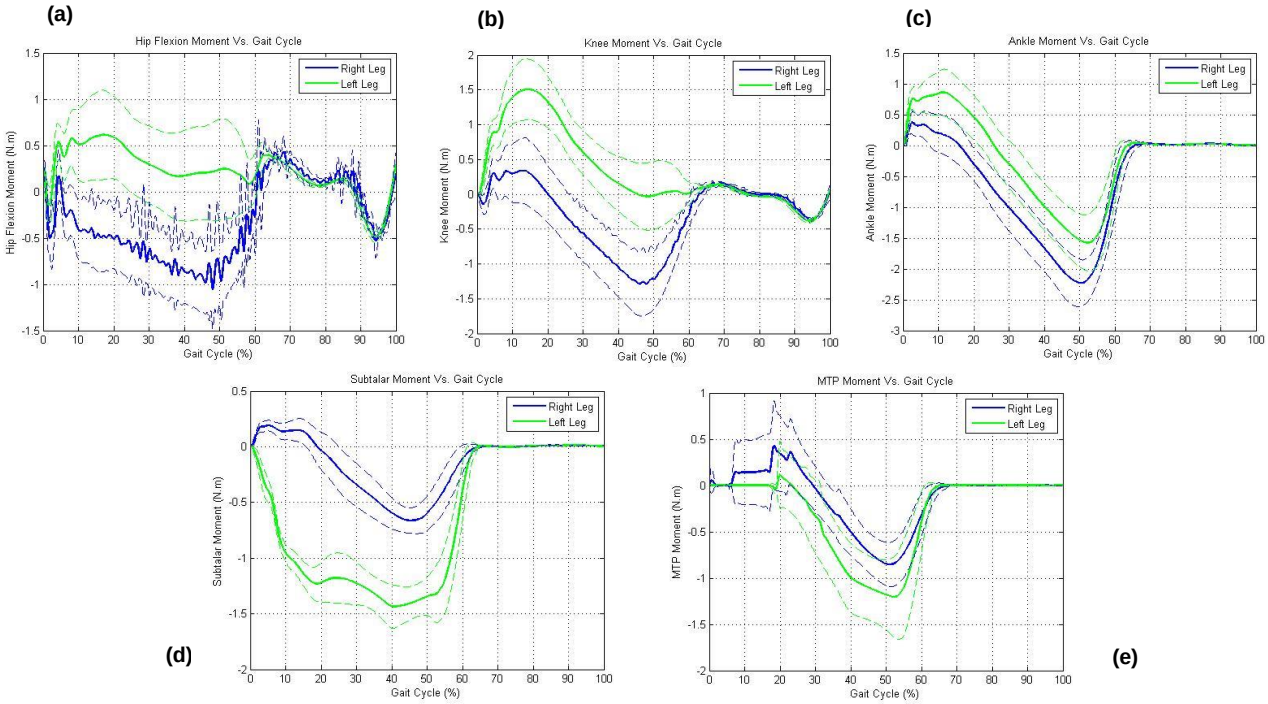

Graph 6.27 – Intra-variability moment of patient 3: (a) Hip Flexion Moment, (b) Knee Moment, (c) Ankle Moment, (d) Subtalar Moment and (e) Metatarsophalangeal Moment.

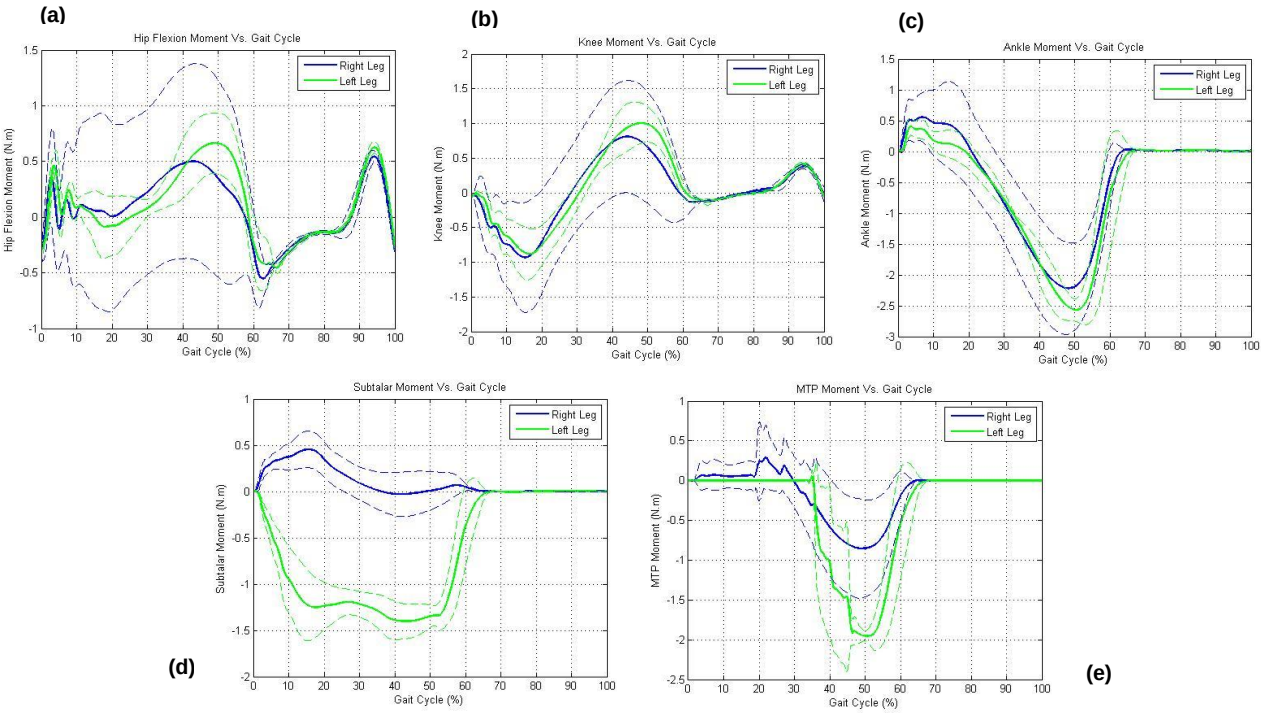

Graph 6.28 – Intra-variability moment of patient 5: (a) Hip Flexion Moment, (b) Knee Moment, (c) Ankle Moment, (d) Subtalar Moment and (e) Metatarsophalangeal Moment.

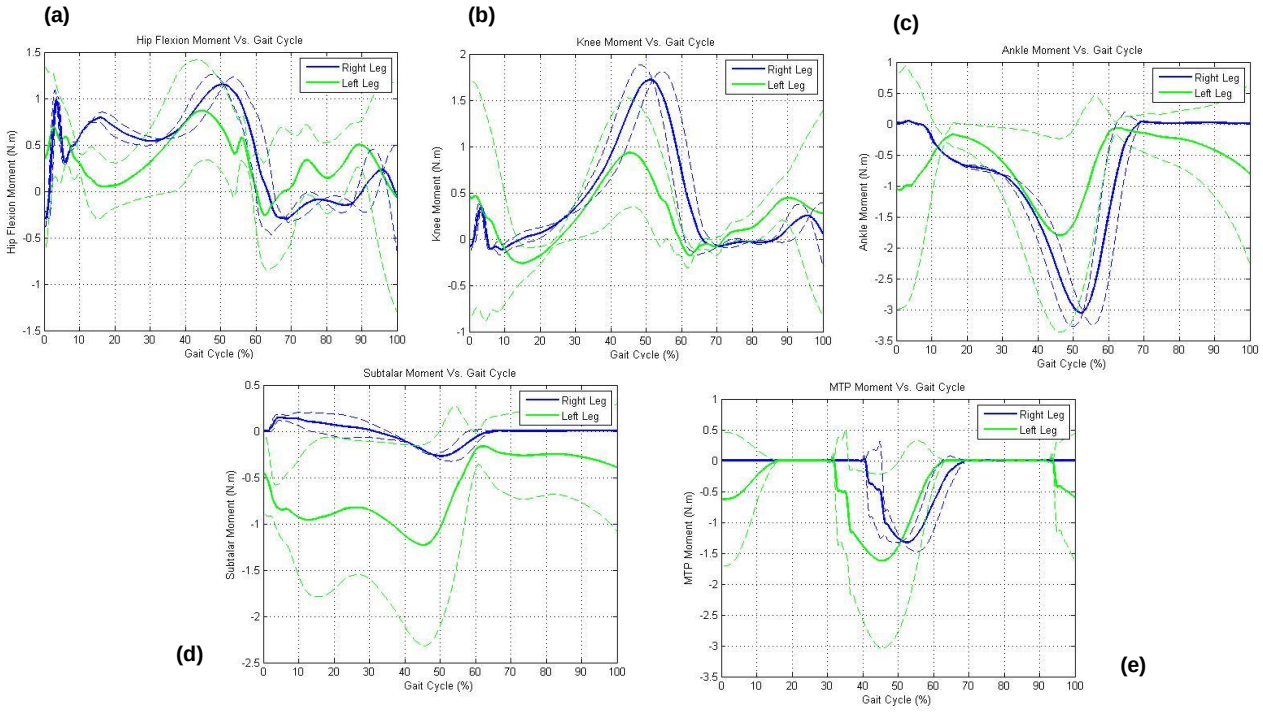

Graph 6.29 – Intra-variability moment of patient 6: (a) Hip Flexion Moment, (b) Knee Moment, (c) Ankle Moment, (d) Subtalar Moment and (e) Metatarsophalangeal Moment.

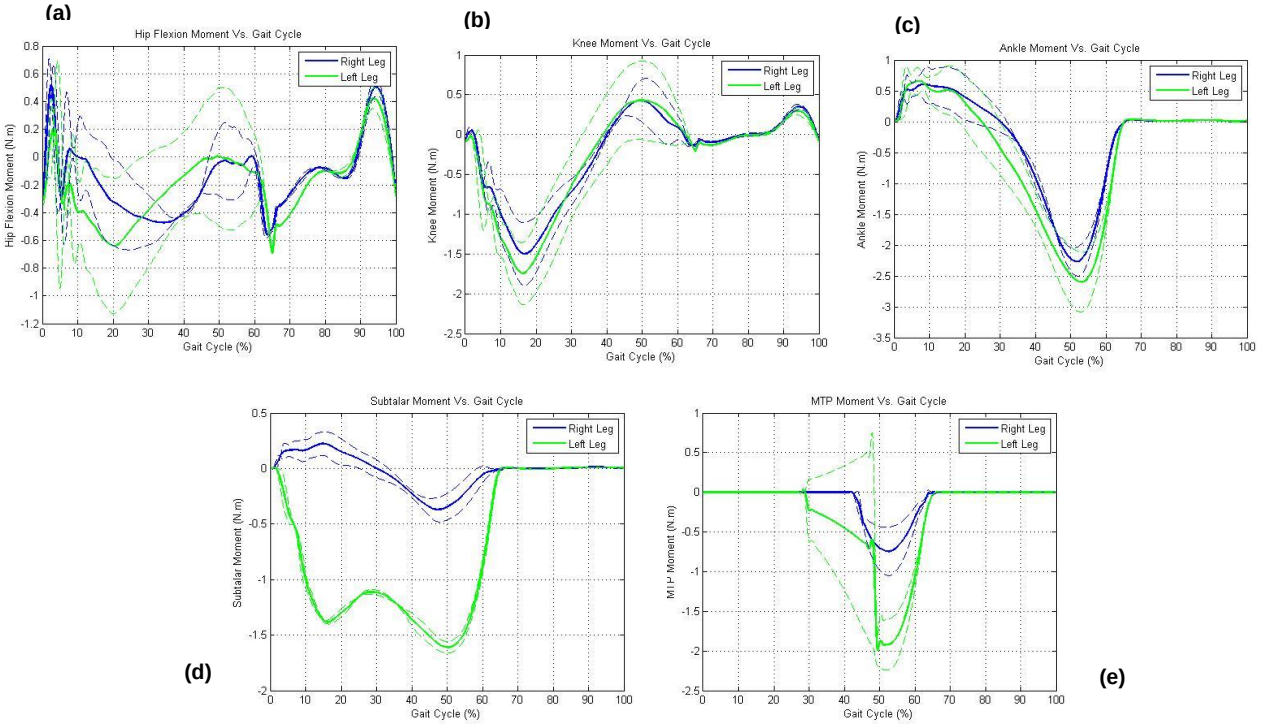

Graph 6.30 – Intra-variability moment of patient 7: (a) Hip Flexion Moment, (b) Knee Moment, (c) Ankle Moment, (d) Subtalar Moment and (e) Metatarsophalangeal Moment.

6.3.4.2 ID Analysis – Patients vs Control Group

The hip flexion moment assumes a marked variability in the injured limb compared with the control group. In patient 1 the variability was demonstrated in both legs and the values are slightly apart from the standard deviation of the control group and the values reported in the literature. The remaining patients showed a consistent variability in the control group and the reported values, and all patients, except 5, showed greater variability in the injured leg. At the level of the knee moment, it was found that there is variability between the studied group and the control population, but the values obtained are in range of one standard deviation. For all individuals, the maximum moment occurs in ≈45% of the gait cycle. The data of the control group and pathological subjects relative to the ankle moment assume similar curves. However, the value of the controlled plantar flexion moment of the control group is the upper and the lower in the powered plantar flexion. For the MTP moment, it was found that the moment obtained from the patient is much higher than that obtained by the control group. It was found that this moment is similar to the ankle moment, but in different phases of the gait. It was also found that the moment is presented in the end of stance phase. However, unlike the control group, which assumes a controlled plantar flexion (30% to 35%), some patients do not (1, 2, 6, and 7). At the level of the subtalar moment there was a marked variability between patients and the control group. In case of patients the variability was showed in the healthy leg.

After this analysis we concluded that the moments assume a greater variability are the ankle moment, subtalar moment and MTP moment in all cases.

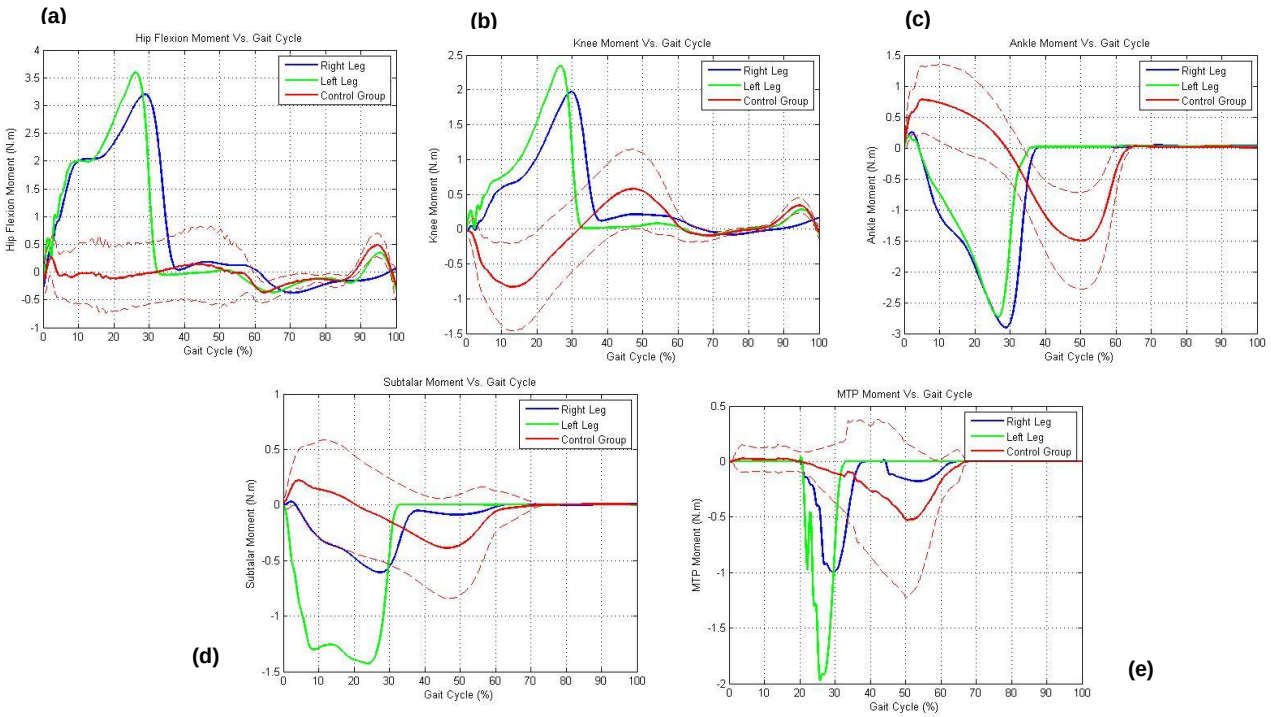

Graph 6.31 – Moment of patient 1 vs Control Group: (a) Hip Flexion Moment, (b) Knee Moment, (c) Ankle Moment, (d) Subtalar Moment and (e) Metatarsophalangeal Moment.

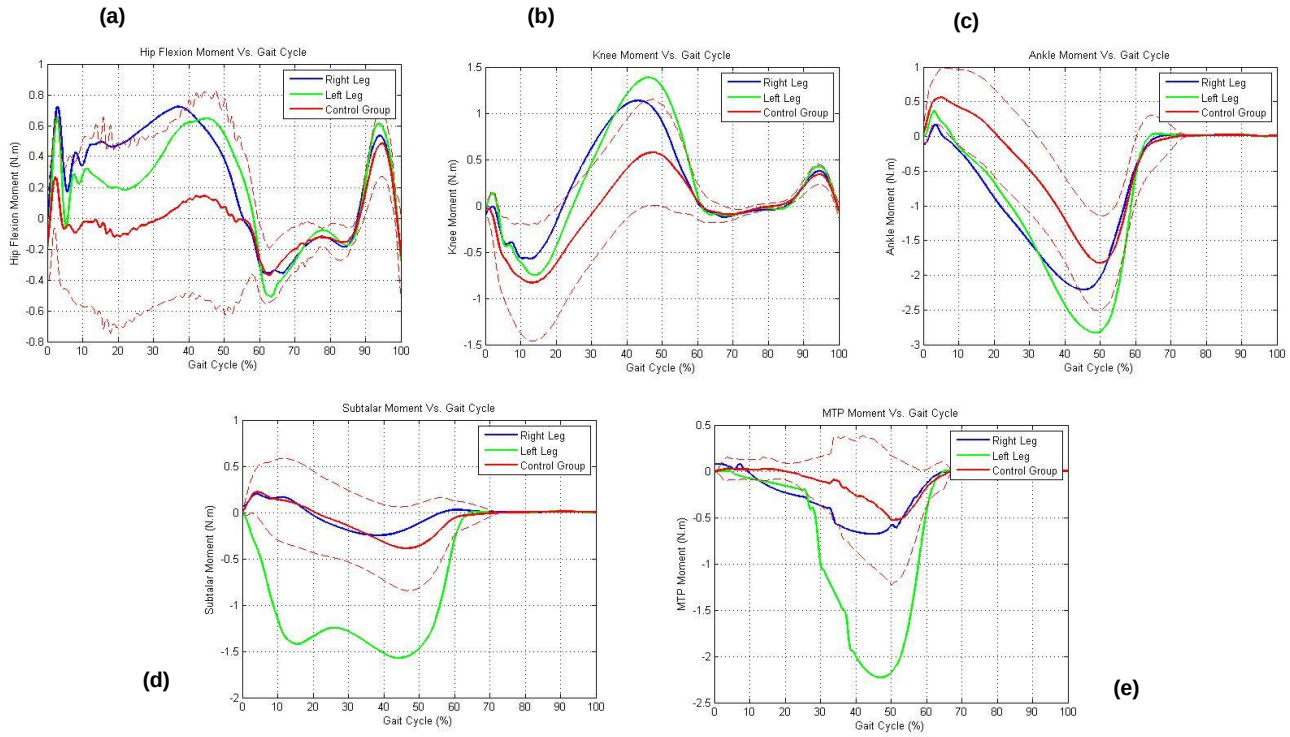

Graph 6.32 – Moment of patient 2 vs Control Group: (a) Hip Flexion Moment, (b) Knee Moment, (c) Ankle Moment, (d) Subtalar Moment and (e) Metatarsophalangeal Moment.

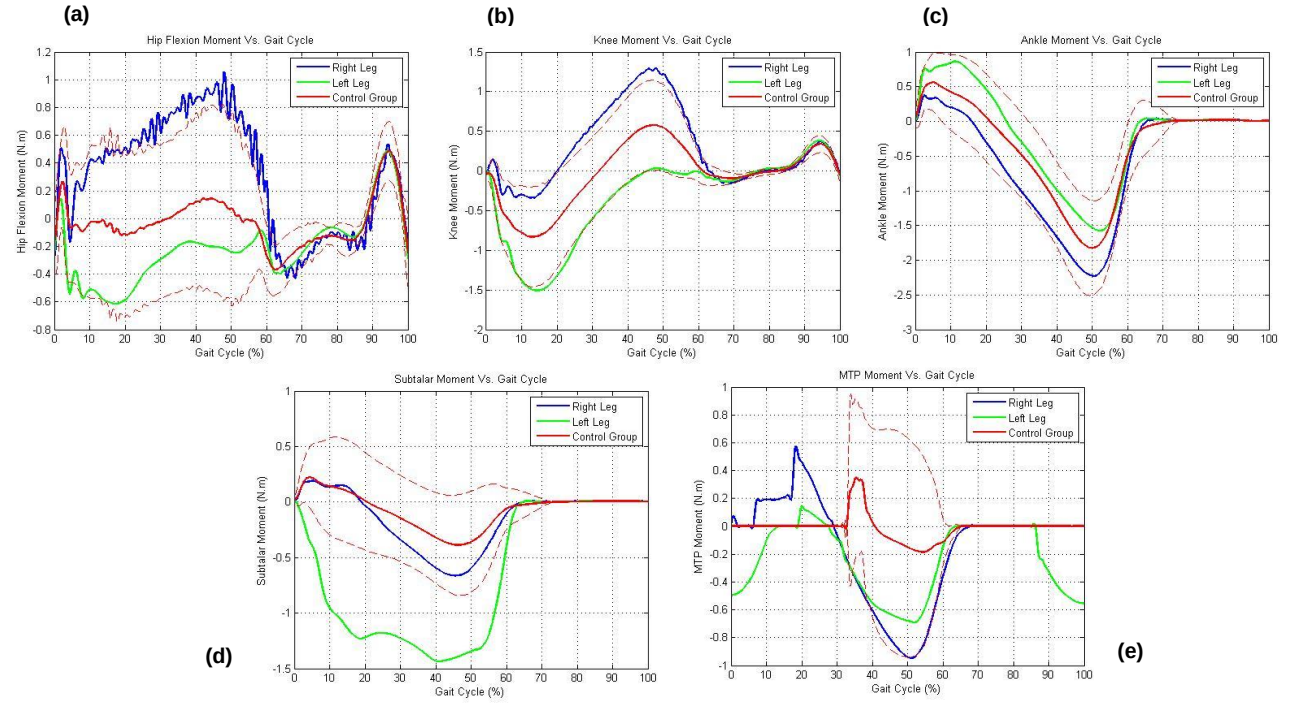

Graph 6.33 – Moment of patient 3 vs Control Group: (a) Hip Flexion Moment, (b) Knee Moment, (c) Ankle Moment, (d) Subtalar Moment and (e) Metatarsophalangeal Moment.

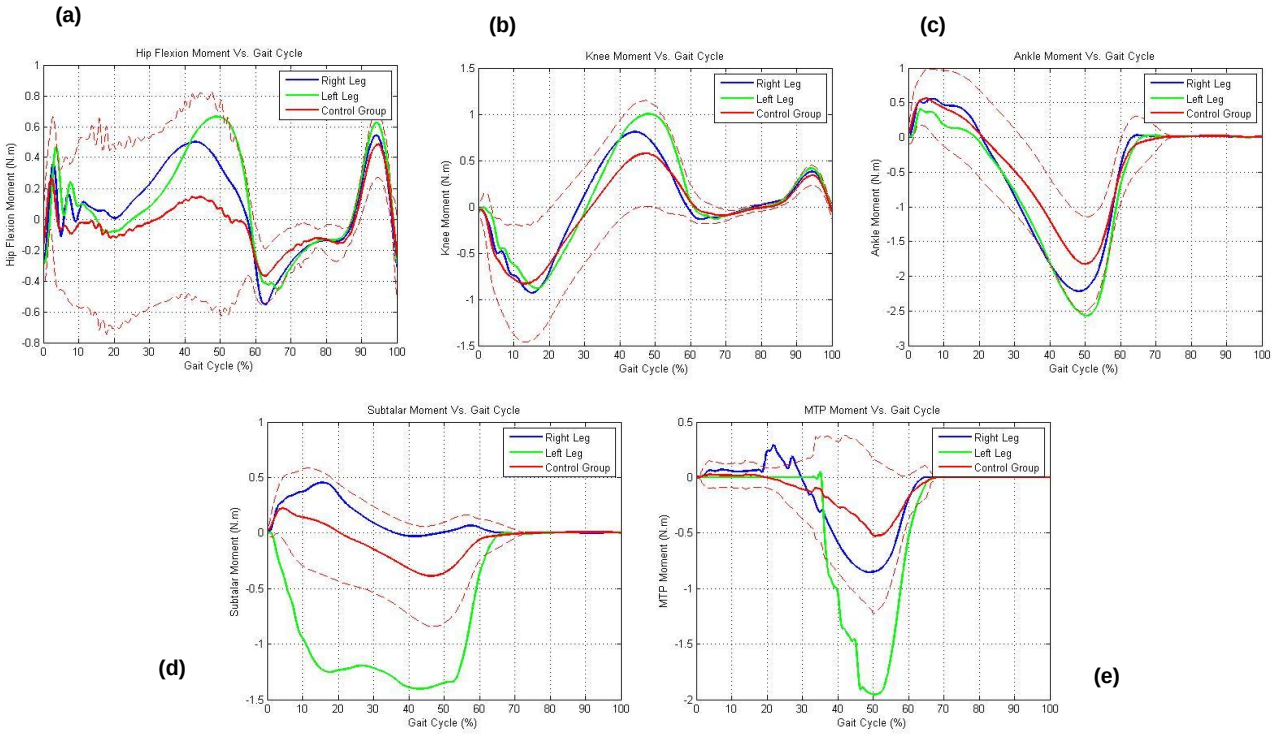

Graph 6.35 – Moment of patient 5 vs Control Group: (a) Hip Flexion Moment, (b) Knee Moment, (c) Ankle Moment, (d) Subtalar Moment and (e) Metatarsophalangeal Moment.

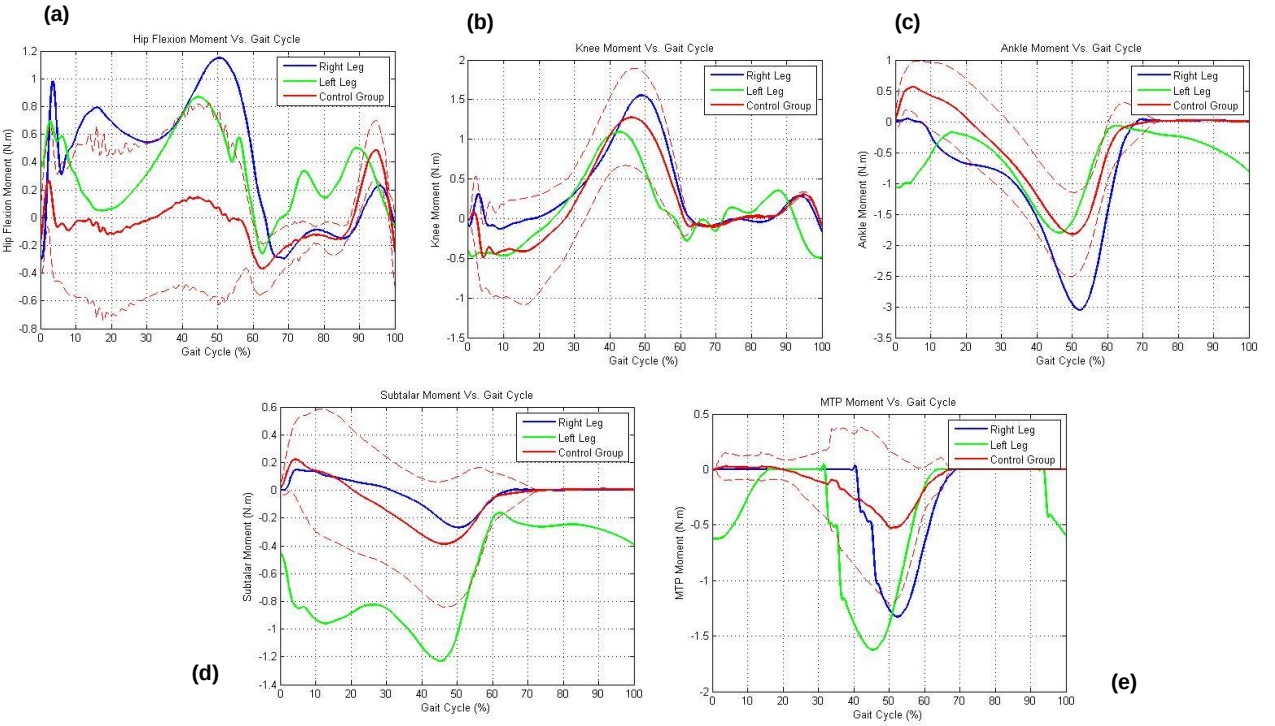

Graph 6.34 – Moment of patient 6 vs Control Group: (a) Hip Flexion Moment, (b) Knee Moment, (c) Ankle Moment, (d) Subtalar Moment and (e) Metatarsophalangeal Moment.

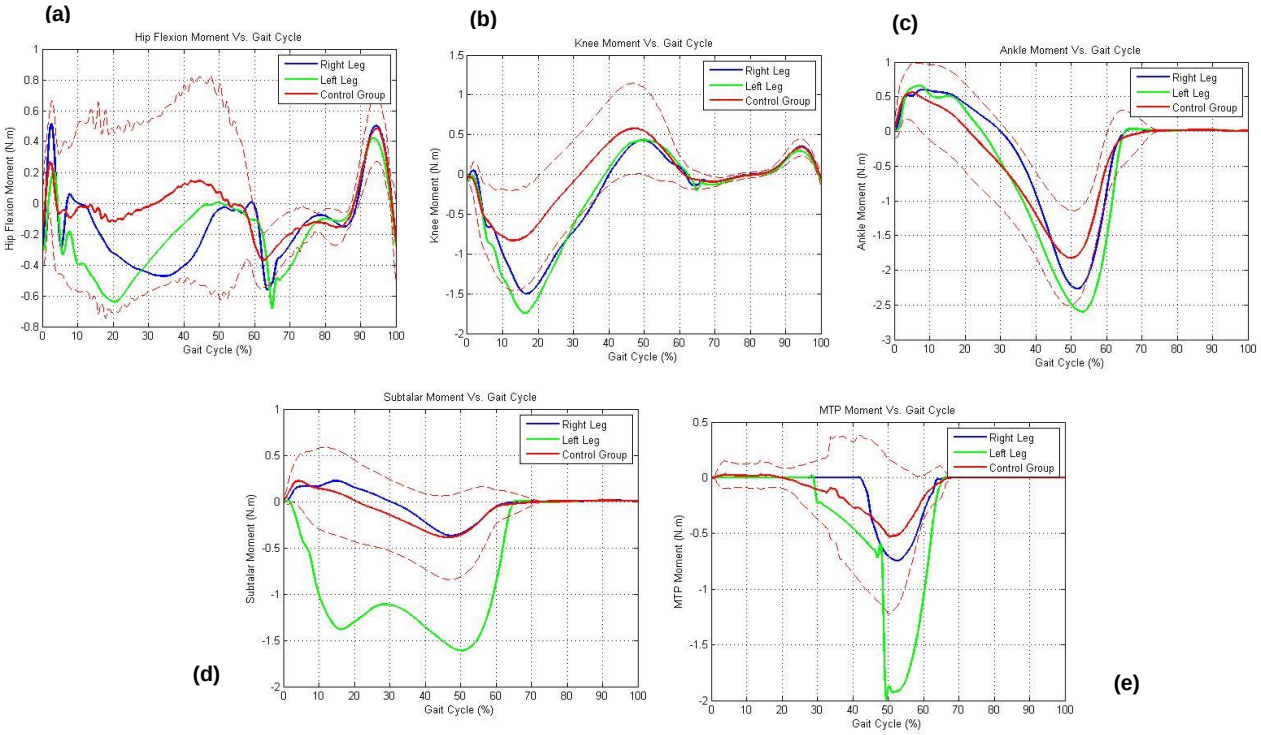

Graph 6.36 – Moment of patient 7 vs Control Group: (a) Hip Flexion Moment, (b) Knee Moment, (c) Ankle Moment, (d) Subtalar Moment and (e) Metatarsophalangeal Moment.

6.3.4.3 CMC – Patients

Relatively to an analysis of the CMC, the average values were calculated considering 4-5 trials per subject. It was also not considered the force applied in the three rigid bodies at the foot but only the force applied to the calcaneus. These analyses were performed to the injured leg when this leg was in contact with the second force plate (view figure 5.3). In the following graphs the injured leg is shown in blue in almost all patients, except for 1 (injured leg represented by red line) and 6 (bilateral rupture). In this graphs, one can see the mechanical power and force of muscles *Tibialis Anterior*, *Soleus*, *Medial* and *Lateral Gastrocnemius* individually during the gait cycle. In the summarizing tables, the mechanical power and force of these previous muscles and the *Flexor Digitorum Longus* (FDL), *Flexor Hallucis Longus* (FHL) are presented.

Comparing the muscle power of all muscles, in patient 1, it was found that the highest power occurs in the *Soleus* and the lower power occurs in *Flexor Hallucis* and *Digitorum Longus*. The patterns shown by all the muscles are in accordance with those reported by Neptune (Sasaki & Neptune, 2006). Regarding muscle force, the left Soleus has a normalized force of approximately 18.34N/kg and left *Lateral* and *Medial Gastrocnemius* of 11.09N/kg and 5.50N/kg respectively. With regard to the curves, these are in accordance with the curves obtained by electromyography Winter (Winter, 1991).

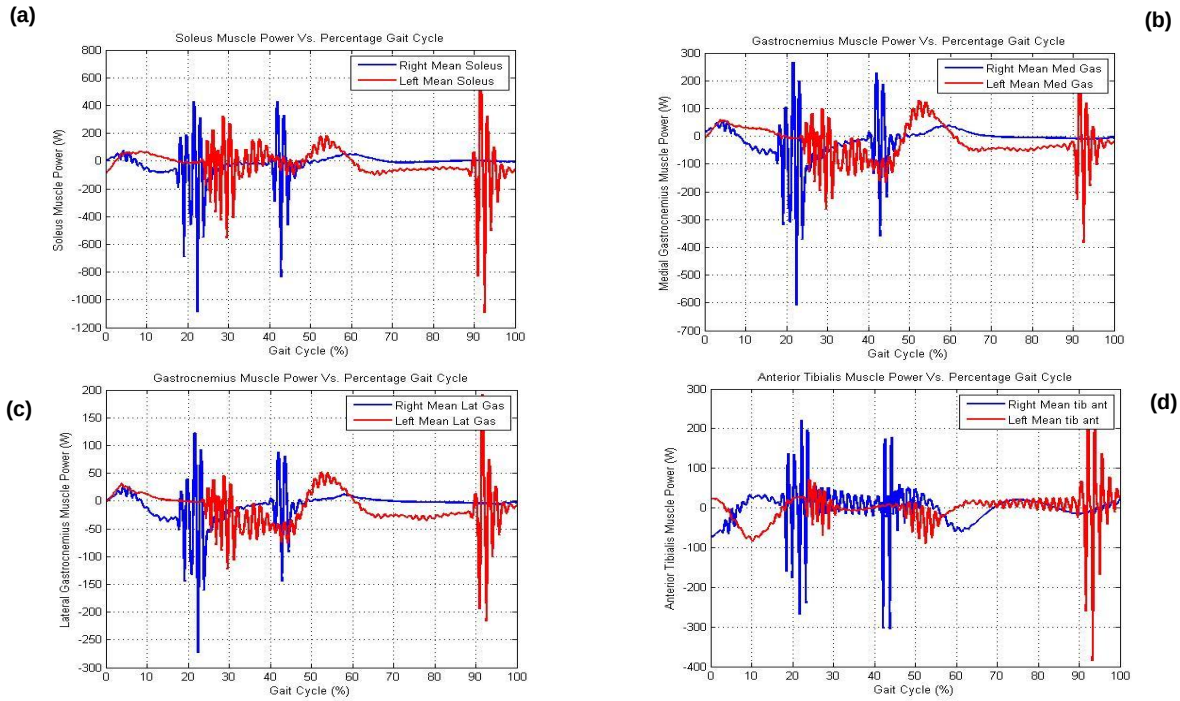

Graph 6.37 – Muscle Power of *Soleus* (a), *Medial Gastrocnemius* (b), *Lateral Gastrocnemius* (c), *Anterior Tibialis* (d) vs Gait Cycle of patient 1.

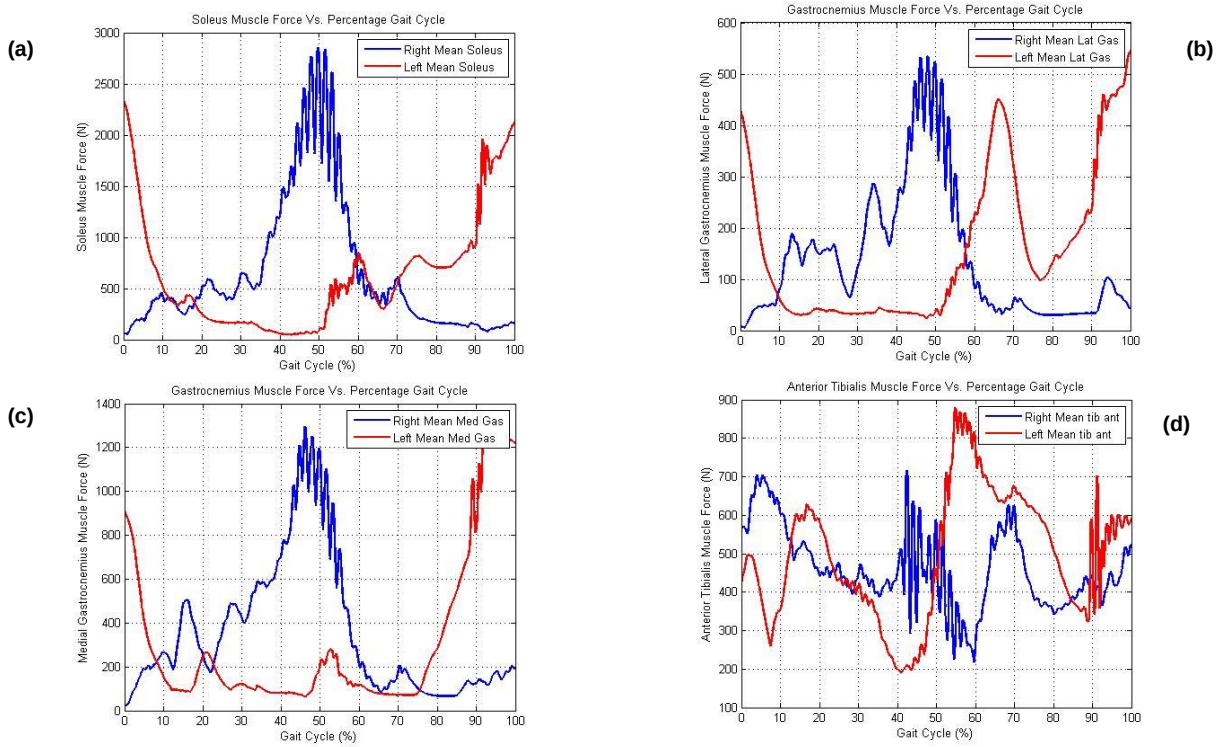

Graph 6.38 – Muscle Force of *Soleus* (a), *Medial Gastrocnemius* (b), *Lateral Gastrocnemius* (c), *Tibialis Anterior* (d) vs Gait Cycle of patient 1.

For patient 2, the muscles show similarities with the literature standards. However, the pattern shown by the *Tibialis Anterior* is slightly different, because this muscle must assume the maximum excitation after the 50% of gait cycle and in this case occurs about 10% earlier. In this case it was verified that the patient the injured leg in the right leg, because the power is superior.

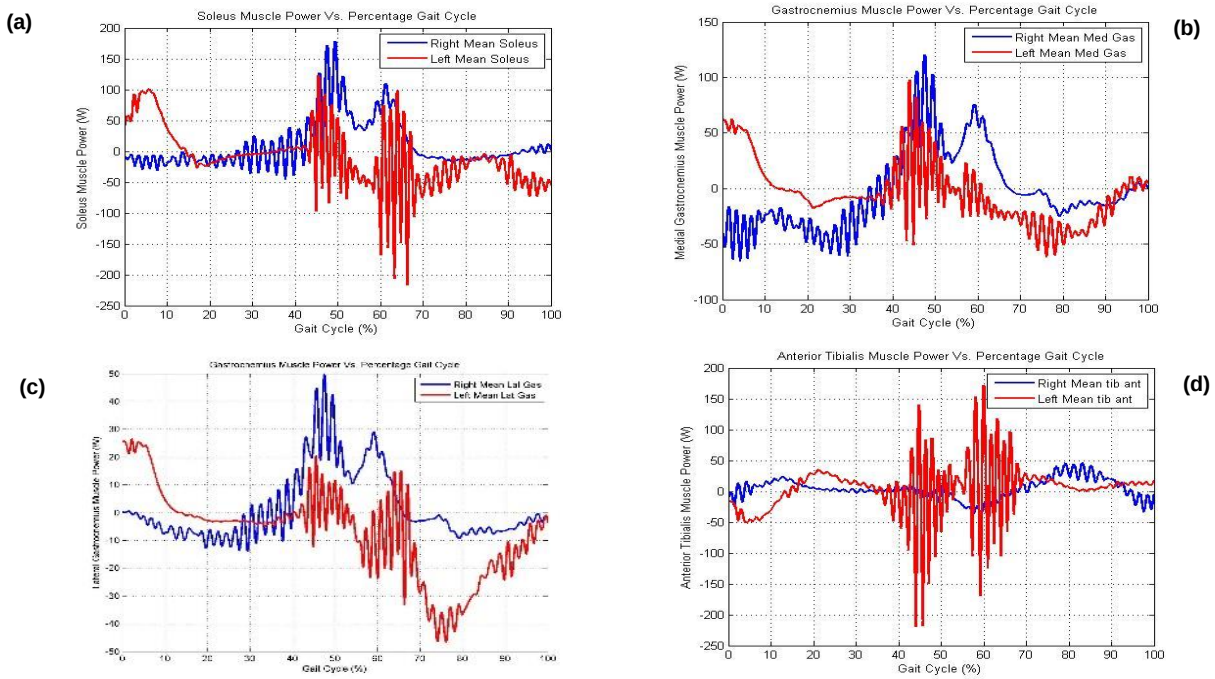

Graph 6.39 – Muscle Power of *Soleus* (a), *Medial Gastrocnemius* (b), *Lateral Gastrocnemius* (c), *Tibialis Anterior* (d) vs Gait Cycle of patient 2.

The following graphs show the force against the percentage of the gait cycle. These results obtained were compared with the literature and exhibit similar values. The *Soleus*, during the plantar flexion, assumed approximately 38.96N/kg of force and in dorsiflexion about 7.79N/kg. In the first case it is above the average as compared to values reported by Hall (Hall, 2003). Despite having the same approximate amount of power, in *Lateral* and *Medial Gastrocnemius* present different force values during the dorsiflexion movement. The first has a normalized force of about 7.14N/kg and the second of 16.88N/kg. With regard to the plantar flexion, the first assumes a force of 2.59N/kg and the second of 6.49N/kg.

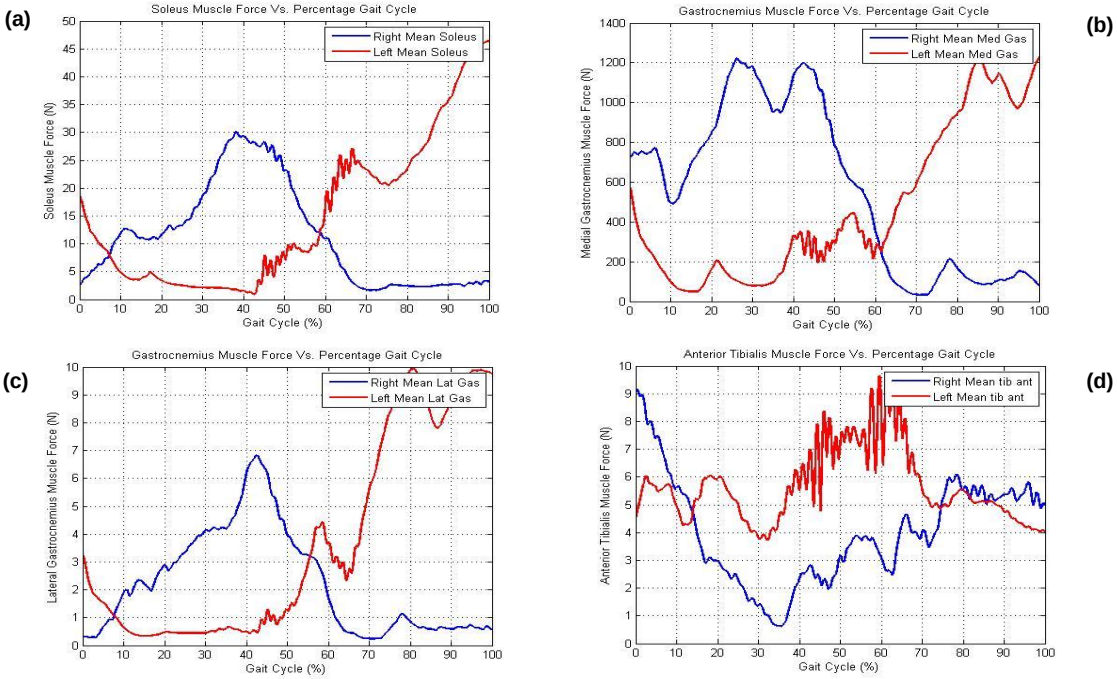

Graph 6.40 – Muscle Force of *Soleus* (a), *Medial Gastrocnemius* (b), *Lateral Gastrocnemius* (c), *Tibialis Anterior* (d) vs Gait Cycle of patient 2.

In the case of patient 3, with respect of the power, it was found that the values are below the average of the values reported by Neptune. It was also found that the values are lower in the right leg, since this was the operated leg. In this case, the *Tibialis Anterior* takes some fluctuations during the IC and midstance but its maximum power occurs near 50% of the gait cycle as reported by Neptune (Neptune & Sasaki, 2006). Regarding to force, it was found that for this patient the force is well conservative (i.e. there are not many fluctuations over time) and may be concluded that the *Soleus* assumes a normalized force of approximately 31.25N/kg in dorsiflexion and about 4.16N/kg in plantar flexion. For the *Lateral* and *Medial Gastrocnemius,* they assumed 2.08N/kg and 1.77N/kg in plantar flexion, respectively. In dorsiflexion, the values assumed are 7.29N/kg and 18.75N/kg, respectively.

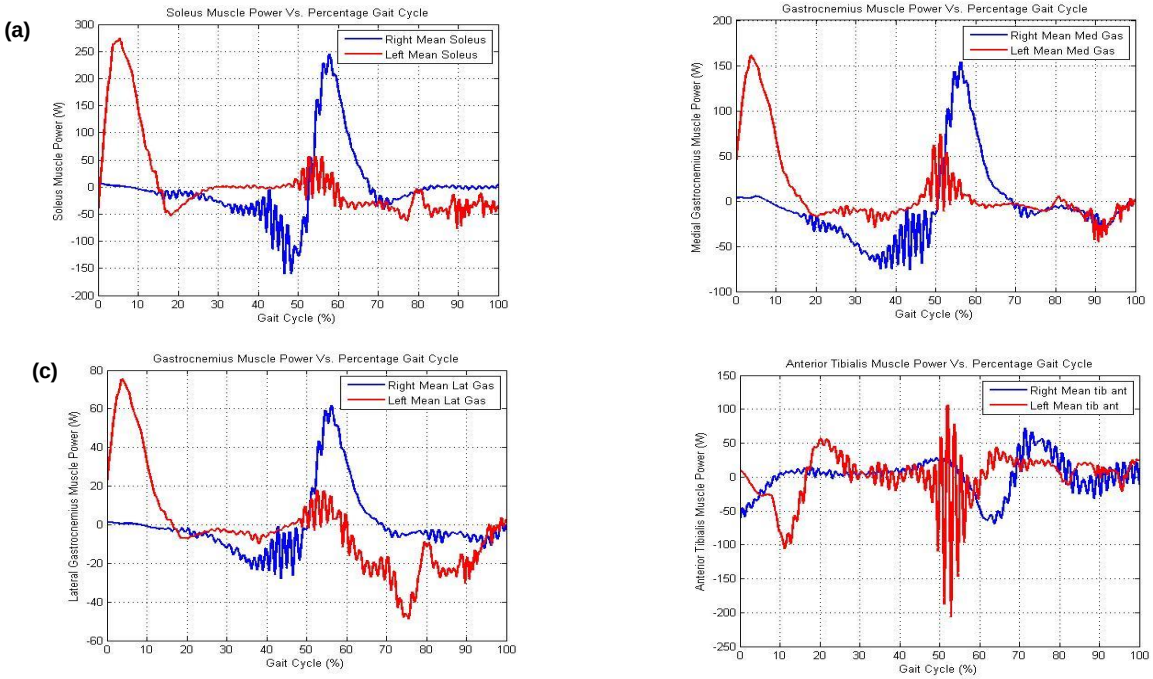

Graph 6.41 – Muscle Power of *Soleus* (a), *Medial Gastrocnemius* (b), *Lateral Gastrocnemius* (c), *Tibialis Anterior* (d) vs Gait Cycle of patient 3.

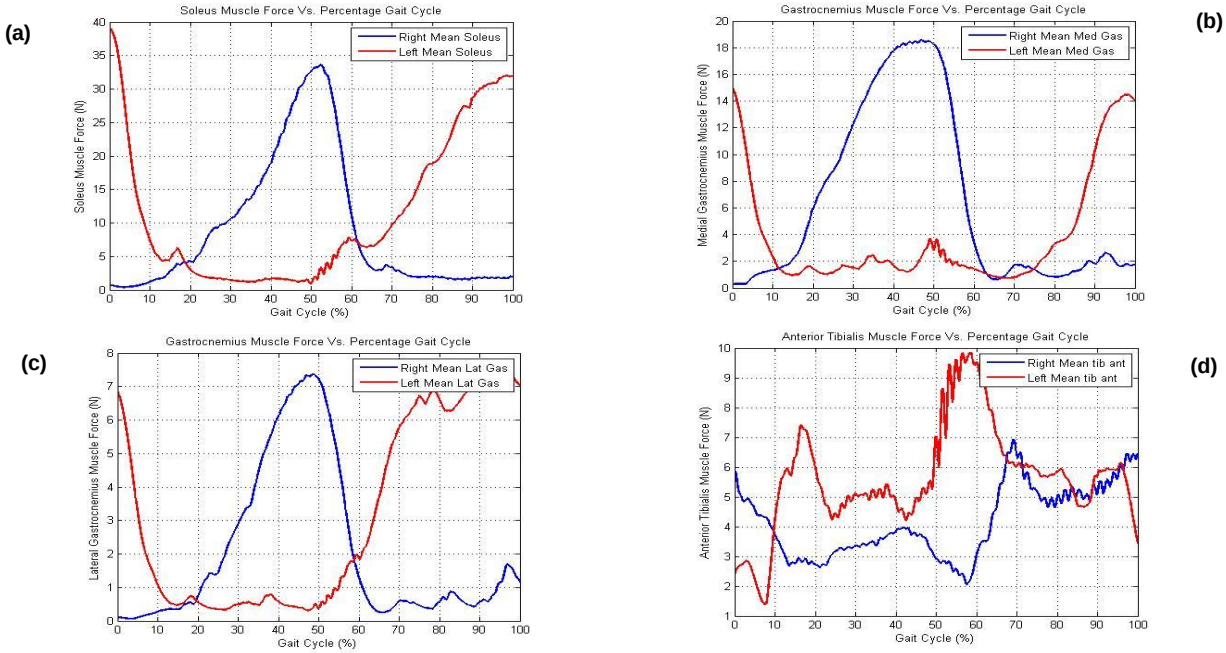

Graph 6.42 – Muscle Force of *Soleus* (a), *Medial Gastrocnemius* (b), *Lateral Gastrocnemius* (c), *Tibialis Anterior* (d) vs Gait Cycle of patient 3.

In the case of patient 4, with respect to the power, it was found that the values are below the average of the values reported by Neptune, but the results obtained are very similar to the results of control group. It was also found that the values are lower in the right leg, since this was the operated leg. In this case, the *Tibialis Anterior* takes some fluctuations during the IC and midstance but its maximum power occurs near 50% of gait cycle as reported by Neptune (Neptune & Sasaki, 2006).

Regarding the force, it was found that for this patient to the force is very well preserved (i.e. there are not many fluctuations over time) and may be concluded that the *Soleus* assumes a normalized force of approximately 43.20N/kg in dorsiflexion and about 6.17N/kg in plantar flexion. For the *Lateral* and *Medial Gastrocnemius* values of 4.93N/kg and 11.11N/kg are assumed, in plantar flexion respectively. In dorsiflexion, the values assumed are 3.70N/kg and 7.40N/kg, respectively.

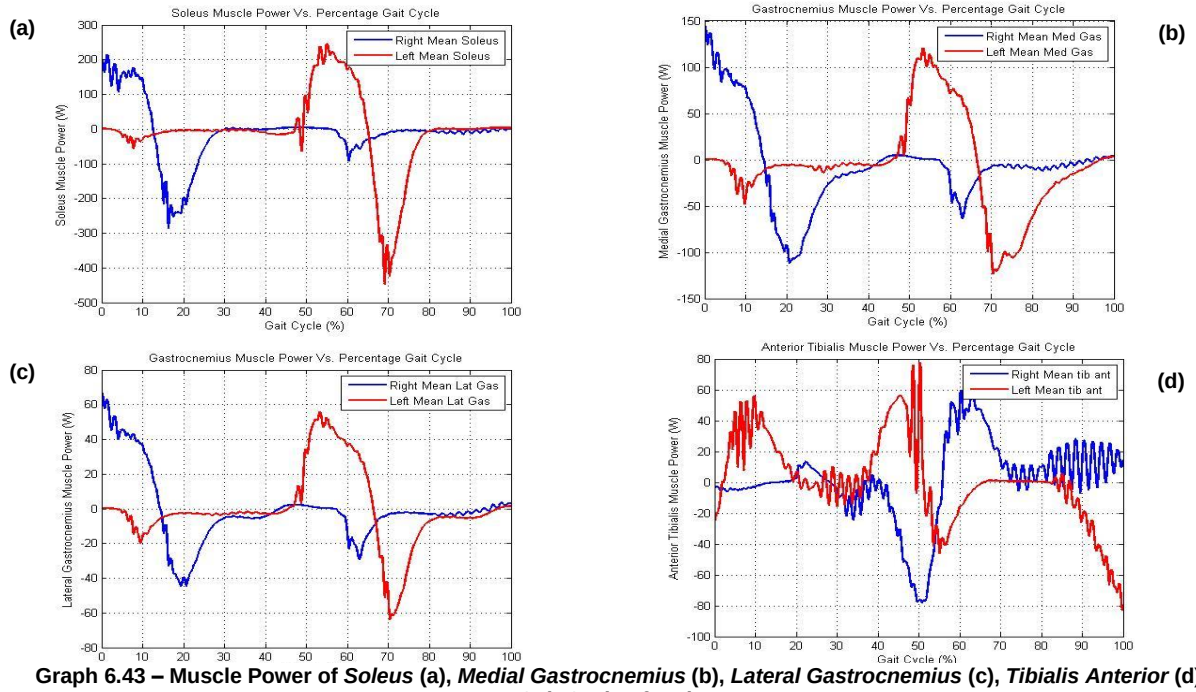

Graph 6.43 – Muscle Power of *Soleus* (a), *Medial Gastrocnemius* (b), *Lateral Gastrocnemius* (c), *Tibialis Anterior* (d) vs Gait Cycle of patient 4.

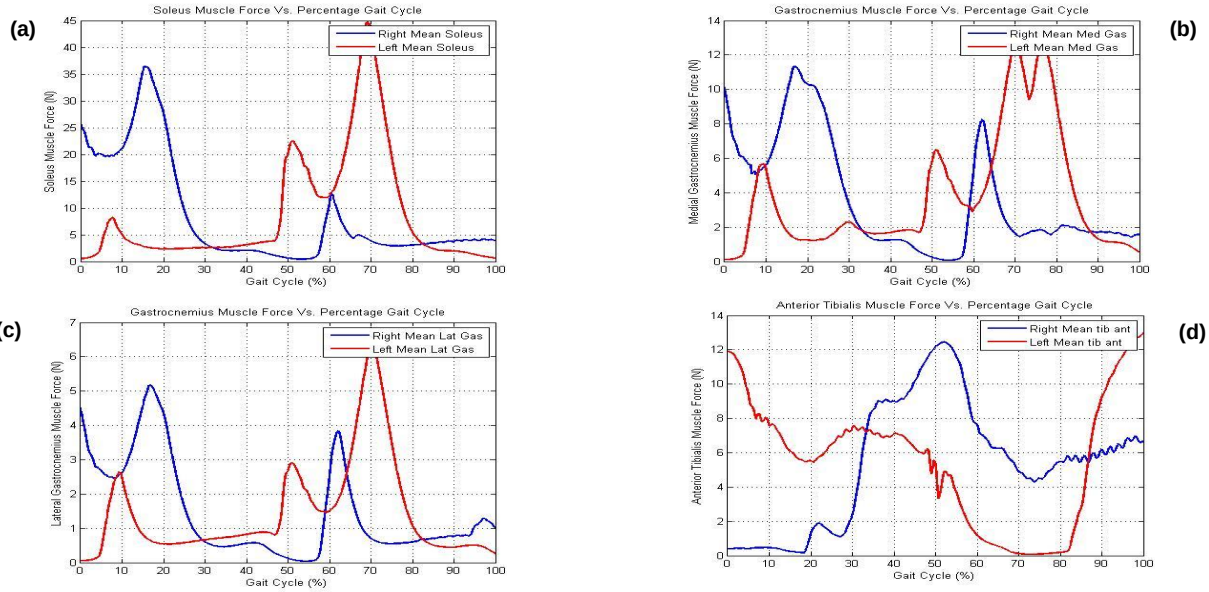

Graph 6.44 – Muscle Force of *Soleus* (a), *Medial Gastrocnemius* (b), *Lateral Gastrocnemius* (c), *Tibialis Anterior* (d) vs Gait Cycle of patient 4.

In the case of patient 5, muscle analysis is not trivial since there is no standard for the assertion that the injured leg (right). Also in this patient appears that the highest mechanical power occurs in *Soleus*. Regarding to the force it is possible concluded that this is highly conserved (i.e. takes a few peaks of variation over time). The *Soleus* assumes a normalized force during dorsiflexion of approximately 32.61N/kg, which is above the average referenced. On the other hand, the *Medial* and *Lateral Gastrocnemius* assume approximately the same value of force 17.39N/kg but Susan Hall reported that the medial force is smaller than the *Lateral* (Hall, 2003).

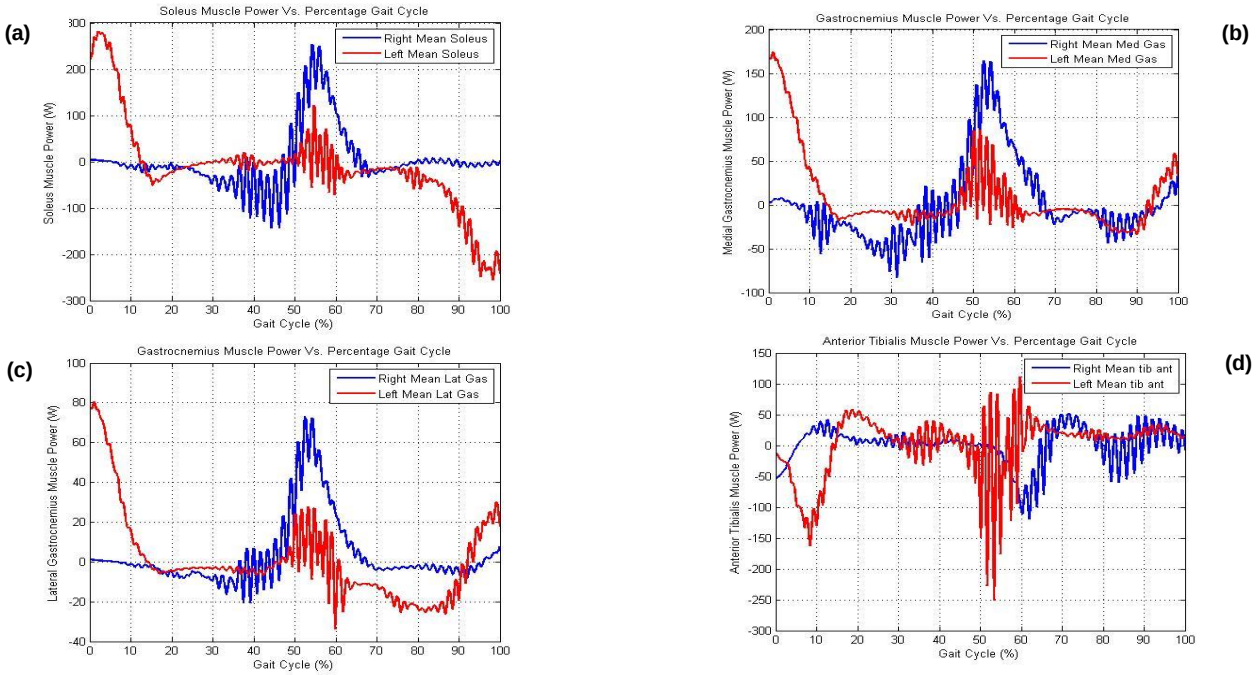

Graph 6.45 – Muscle Power of *Soleus* (a), *Medial Gastrocnemius* (b), *Lateral Gastrocnemius* (c), *Tibialis Anterior* (d) vs Gait Cycle of patient 5.

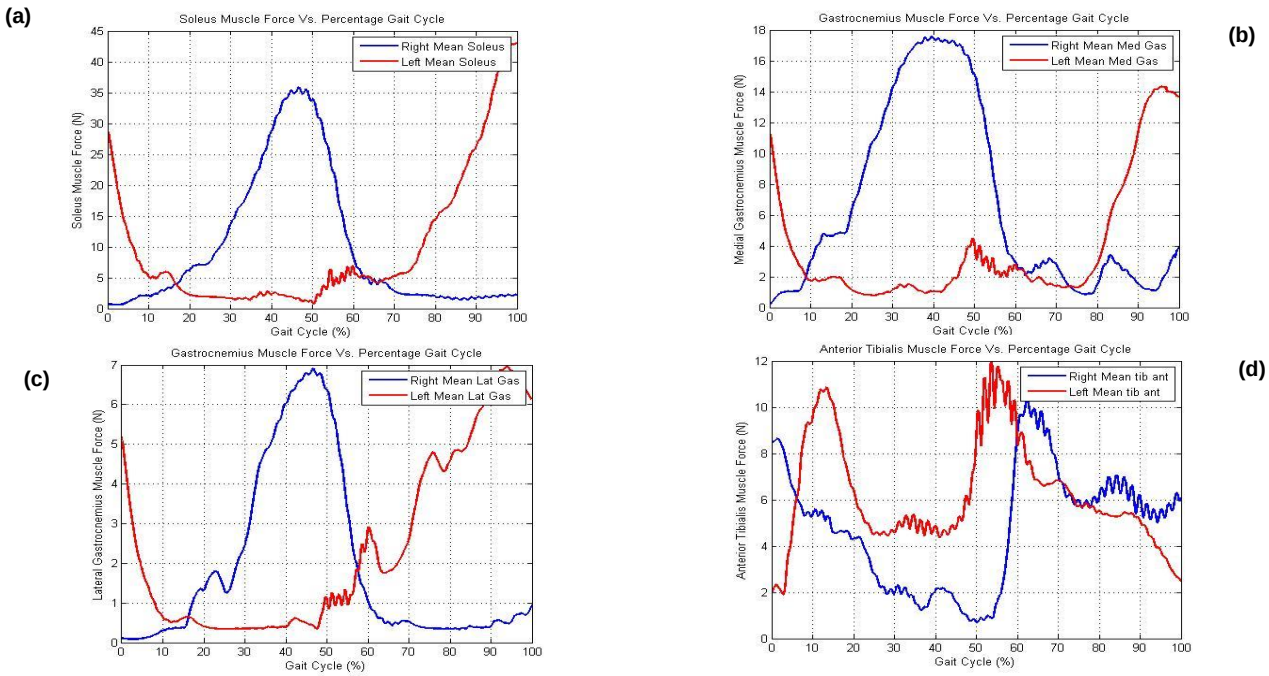

Graph 6.46 – Muscle Force of *Soleus* (a), *Medial Gastrocnemius* (b), *Lateral Gastrocnemius* (c), *Tibialis Anterior* (d) vs Gait Cycle of patient 5.

For the case of patient 6, the results compared with the reported by Neptune in 2006, and in some cases are slightly above average. The right *Soleus* assumes a maximum value of approximately 400W at terminal stance and preswing. *Lateral* and *Medial Gastrocnemius* assume similar values since they are arranged side by side. However, the pattern shown by the *Tibialis Anterior* is slightly different from those reported in the literature, because it should only be excited after 50% of gait cycle, which in this case occurs about 10% earlier. Relative of *Flexor Hallucis Longus* and the *Flexor Digitorum Longus,* these activate near TO, which makes sense because these muscles connects the toes to the metatarsal metatarsophalangeal joint through (Sasaki & Neptune, 2006). In the graphs of force the *Soleus* presents, during the plantar flexion, approximately a force of 48.38N/kg and in dorsiflexion about 8.06N/kg. In the first value it is above the average when compared to the reported values (Hall, 2003). Despite having the same approximate amount of power, in what respects muscle force the force *Lateral* and *Medial Gastrocnemius* have different values during dorsiflexion movement. The first has a normalized force of about 8.06N/kg and the second one of 19.35N/kg. With regard to the plantar flexion the first assumes a value of 3.23N/kg and the second a value of 7.25N/kg. Compared with the literature, the values for the plantar flexion movement are below of average.

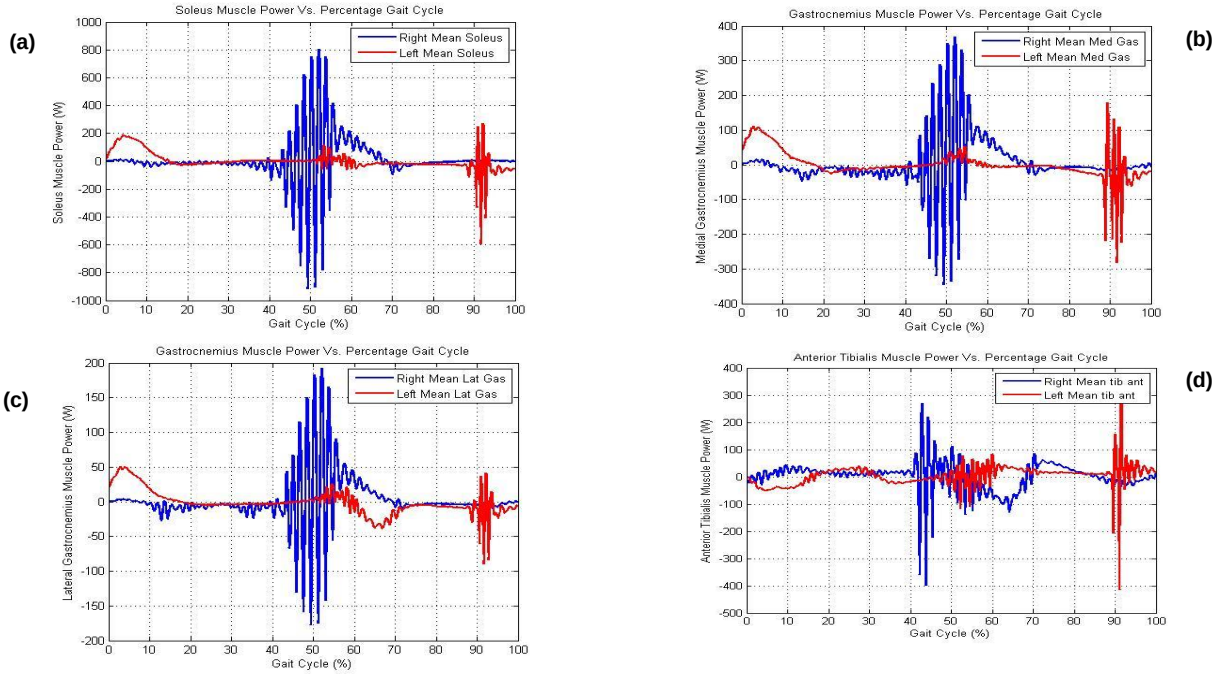

Graph 6.47 – Muscle Power of *Soleus* (a), *Medial Gastrocnemius* (b), *Lateral Gastrocnemius* (c), *Tibialis Anterior* (d) vs Gait Cycle of patient 6.

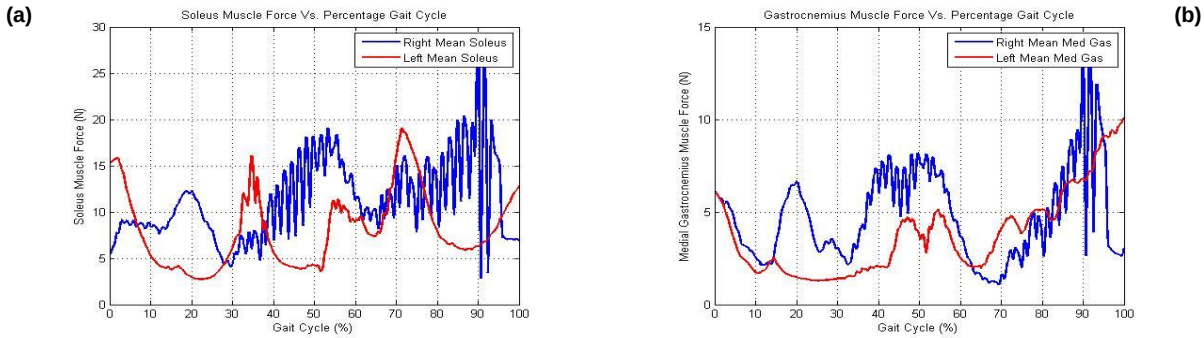

(c)

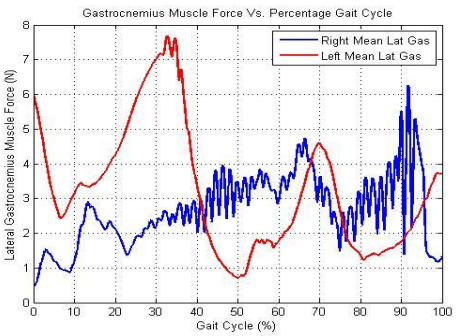

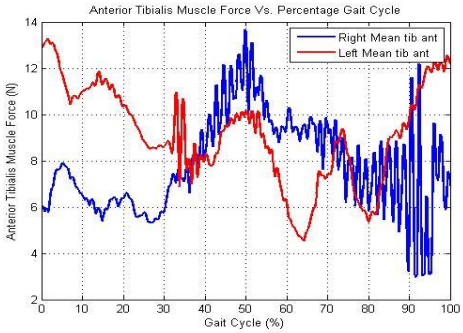

(d)

Graph 6.48 – Muscle Force of *Soleus* (a), *Medial Gastrocnemius* (b), *Lateral Gastrocnemius* (c), *Tibialis Anterior* (d) vs Gait Cycle of patient 6.

Patient 7 has essentially two peaks of higher power in *Triceps Surae* muscle at the IC and TO. While the *Gastrocnemius* and *Soleus* exhibit concentric contractions, the *Tibialis Anterior* assumes an eccentric contraction, which makes sense, since it is an antagonistic muscles. The curves for the power, presented by the foot muscles are similar. With regard to muscle force it was showed that this subject there are not many peaks of variability of the curves presented. The peaks of greatest force lie in line with the higher power. The *Soleus* has one normalized force of approximately 42.99N/kg, the *Medial Gastrocnemius* of 16.90N/kg and *Lateral Gastrocnemius* of 7.04N/kg. These values are above the average, when compared with the literature.

(a)

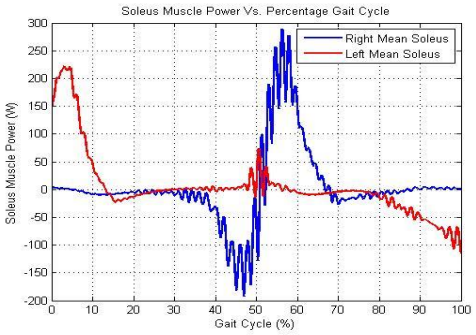

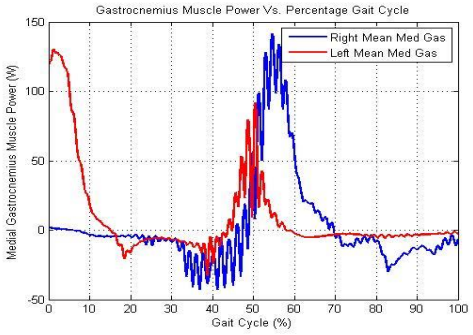

(b)

(c)

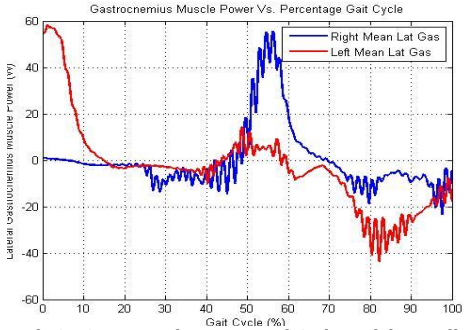

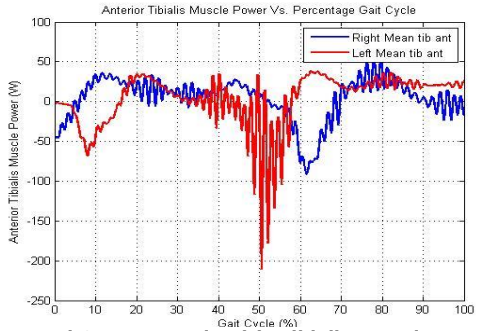

(d)

Graph 6.49 – Muscle Power of *Soleus* (a), *Medial Gastrocnemius* (b), *Lateral Gastrocnemius* (c), *Tibialis Anterior* vs Gait Cycle of patient 7.

(a)

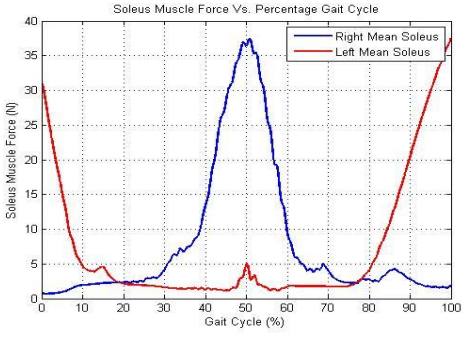

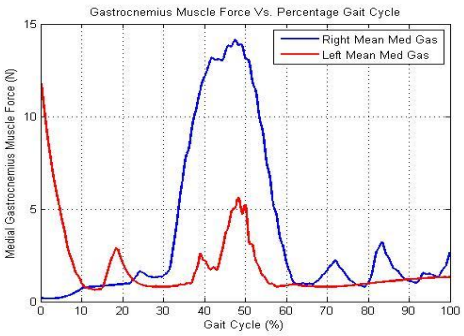

(b)

(c)

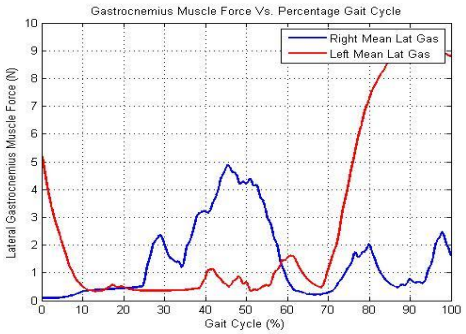

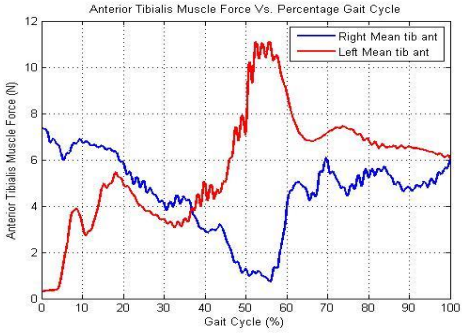

(d)

Graph 6.50 – Muscle Force of *Soleus* (a), *Medial Gastrocnemius* (b), *Lateral Gastrocnemius* (c), *Tibialis Anterior* (d) vs Gait Cycle of patient 7.

Comparing the results obtained it was found that all patients have a lower mechanical power in the *Gastrocnemius* and assume a higher force values in the muscles of *Soleus*, *Gastrocnemius* and *Tibialis Anterior* as shown in Table 6.23 and 6.24 when compared with literature. The curves in all the muscles are in agreement with those presented by Winter (Winter, 1991).

There is also is variability between patients. The peak of power and mechanical force occurs in all patients in the TO phase except in patient 1 that occurs in midstance or foot flat in both cases. When compared with the control group, it was found that the pattern of the mechanical power curve is slightly different from that obtained in the control group (view appendix III). In the TO and Terminal Stance event (≈50 % to 60% of the gait cycle) is possible to see a maximal contraction. In the case of the control group, all muscles studied, occurs in the first a concentric contraction ($P_J > 0$) and then an eccentric contraction ($P_J < 0$). For patients this pattern does not occur. Sometimes the eccentric contraction occurs before concentric contraction (patient 3, 5 and 7) or only concentric contraction occurs (patient 6). With regard to muscle force produced by the *Soleus* is superior to the control group and to the references, while one or *Lateral* and *Medial Gastrocnemius* is higher than the value obtained in the control group but lower than the one reported. For the *Flexor Digitorum Longus* and *Flexor Hallucis Longus* it was found that all patients take concentric and eccentric contractions in contrast to the control group which only takes concentric contractions (Coughlim et al., 2007; Sasaki & Neptune, 2006; Winter, 1991).

Table 6.23 – Mechanical Power of Patients.

	Mechanical Power (W)										
	1	2	3	4	5	6	7	$\bar{x}$	σ	Control Group	Reference (Winter, 1991)
Soleus	500	200	250	200	250	350	300	292.86	97.94	200	300
Lateral Gast	200	500	80	60	60	600	60	222.86	213.66	60	400
Medial Gast	200	125	150	100	150	400	150	182.14	93.27	100	300
Anterior Tibialis	200	50	75	60	100	200	50	105.00	62.16	40	50
FHL	18	5	10	6	7	80	7.5	21.00	26.73	10	3.6
FDL	20	5	6	12	10	90	5	21.14	28.54	8	1.8

Table 6.24 – Force Muscle of Patients.

Force Muscle (N/kg)											
	1	2	3	4	5	6	7	$\bar{x}$	σ	Control Group	Reference (Coughlim et al., 2007)
Soleus	18.34	38.96	31.25	43.20	32.61	43.38	42.99	35.82	8.53	30.73	29.9
Lateral Gas	5.50	7.14	4.61	4.93	17.39	8.06	7.04	7.81	4.08	3.99	5.5
Medial Gas	11.09	16.88	7.29	11.11	17.39	19.35	16.90	14.29	4.11	8.60	13.7
Anterior Tibialis	4.5	9	10	35	10	14	8	12.93	9.38	10	5.6
FHL	2	2	1.5	3	2	3	2.5	2.29	0.52	2.5	3.6
FDL	1.7	2	1.5	3	2.5	3	2	2.24	0.56	2.25	1.8

Chapter VII

7 Conclusions and Future Developments

7.1 Conclusion

The goal of the author of this work was to achieve five main objectives. The first one was to define clinical protocols and to evaluate seven pathological individuals who suffered a rupture of the Achilles tendon and were subjected to a surgery to repair this lesion. The second and third objectives were the optimization of the experimental protocols for the acquisition of the patients' experimental data at LBL and the definition of computational scripts to enable their treatment (in Matlab and OpenSim). The designed protocol should enable the analysis of kinematic and dynamic data, TDP and pedobarography, considering that it should be robust, reliable and it should not take too much time in their preparation. The fourth objective was the acquisition of the gait patterns for a population of non-pathologic and pathological subjects. Finally, the fifth objective was to proceed to the evaluation of the obtained data through the aforementioned types of analysis, performing an intra–variability analysis and a comparison with a control group.

In order to perform this work, several issues had to be considered. Initially it was necessary to develop a literature review (Chapter I), in which a brief description of the works made in this area and new ideas to innovate this type of studies were discussed. In Chapter II, some concepts of anatomy and physiology were addressed. A review of the surgeries most used by the group of orthopedics at *Hospital CUF Descobertas* was presented. In Chapter III, concepts related with gait analysis terminology were reviewed. The kinematic, kinetic and pedobarographic normal gait patterns were discussed as well as the usual theories of gait. In particular, this chapter focused on the motions in which the Achilles tendon present an important role. These two sections were very important insofar as they enabled the discussion of many concepts related with gait that were important in the following chapters. In Chapter

IV, the mathematical formulation used in multibody dynamics were presented, bearing in mind that these methodologies are the basis of analyses that are performed in the OpenSim software (IK, ID and CMC). In Chapter V, the model applied in this work was presented, taking into account its features: 18 total rigid bodies (3 rigid bodies in foot) and 76 muscles; designed protocols, in particular the anatomical landmarks considered in the definition of the movement acquisition protocol; protocols for data acquisition and finally the guidelines/steps followed during the data processing. Finally, in Chapter VI, the results obtained for each pathologic subject were discussed individually. An intra-variability analysis was performed as well as an inter-variability, allowing to study if there were differences in the patterns and stability between the non-injured and injured leg and differences between both legs and a control group. This chapter was extremely important because it allowed to withdraw diverse conclusions.

The conclusions drawn from this work, through the achievement of the objectives originally proposed, were numerous. The three questions initially proposed in this work were answered. Regarding, the quality of life of the patients, no direct changes were observed. However, some patients reported that after the rupture they changed some routines (e.g. stop playing sports). In terms of gait patterns, some changes in the amplitude of motions and torques were observed. Finally, regarding the type of surgical technique applied in the studied subjects, it has not been possible to obtain conclusions due to the low number of cases for each type.

By the analysis of the performed questionnaires, AOFAS and SF-v36, it was possible to conclude that the patients presented good physical and psychological conditions and the obtained results are within the mean values reported in the literature.

The variables measured experimentally, as the perimeter of the *Gastrocnemius,* showed that there is a decrease in the perimeter of the injured leg in all subjects. Other measured variables were the dorsiflexion and plantar flexion angles, which presented values that were within the average values reported in the literature.

In terms of time-distance parameters, such as cadence, speed, and step time, the obtained results presented values consistent with the ones observed in literature and the ones obtained for the control population.

In the case of the results of the plantar pressure analysis, it was found that there is a consistency between the data of static and the dynamic test. In almost all cases, the zone of higher pressure is located on the contralateral side of the lesion and its location varies from patient to patient. By analyzing variables such as the force/pressure and the evolution of the COP in the dynamic test of the foot, the data showed that pathological subjects tended to present a more medial progression of the COP when compared to the control population. This finding may suggest that during the IC the patients' feet tend to contact the ground in a more inverted position than the control population. Also in this type of analysis, the static force distribution showed that almost all subjects tend to distribute more force by the injured leg. This fact may be related with the type of training performed during the physical rehabilitation (physical therapy) treatments, since the usual train strategies focus on the injured led, strengthening only this leg. However, the force distribution measured for both members presented approximately the same values. The analysis of the kinematic data enabled to conclude that an intra-variability in pathological subjects exists. This variability is essentially observed on the maximum flexion during

controlled plantar flexion movements of the knee (≈10º than the values reported in the literature in almost cases) and ankle (dorsiflexion and plantar flexion during respectively the initial and final stage of the propulsion phase), which would be expected since these are two most important joints in which the Achilles tendon acts. Through these results it is possible to suggest that there was a shortening of the tendon. When compared with the control group, it was found that although the data indicated an intra-variability for some patterns, the angular ranges are within the standard deviation of this group in most of the cases.

The dynamic analysis of the patients showed patterns similar to the ones observed in the control group and the values reported in literature. The conclusions were the same as those taken in the kinematic analysis.

The data obtained for muscle activations reported patterns within the average values reported in the literature, however, in some subjects, the patterns of concentric and eccentric contractions presented slightly differences when compared to the control group. Moreover, slightly differences in the force magnitude were also observed between both legs.

The table below is a summary table that allow us to check what variables that showed significant changes. It is also possible to analyze the difference values between the both legs (in case of the perimeter of the Gastrocnemius) and between patients and control group (in case of others variables) and what percentage of decrease/increase in the injured limb.

Table 7.1 – Summary table of what variables that showed significant changes.

Variable	Decrease or Increase	Where		Quantification (values between legs OR Leg between control)		Quantification (%)	
Perimeter of Leg	Decrease	Injured Leg (Gastrocnemius)		1,36cm		3.75	
Plantar Force	Decrease	Injured Foot		0,05 N/kg		31.77	
Plantar Pressure	Decrease	Injured Foot		0,07N/cm^2		15.64	
Flexion Knee Angle	Decrease	During controlled plantar flexion		3.85º		11.24	23.29
Ankle Angle	Decrease	IC	TO	2.43º	3º	45.55	23.29
MTP Ankle		IC	TO	10.71º	6.29º	19.67	25.64
Ankle Moment	Increse/Decrease	IC	TO	0.32N/kg	0.58N/kg	35.83	24.08
MTP Moment	Decrease	Injured Foot		1.03N/kg		31.38	

Some limitations in this study can be reported, in particular the number of analyzed subjects, which did not enabled to assess whether the type of surgery may or may not influence the gait patterns. Unfortunately, not all the proposed acquisitions were performed (initially a group of 30 patients were contacted) due to lack of availability of some patients and the time available for the realization of all the analyses.

7.2 Future Developments

As future developments, the increase of the number of acquisitions of pathological subjects would be important in order to be able to more accurately validate the obtained results. Despite being a

pathology, which is predominant in the masculine gender, the evaluation of more female subjects would be important too.

The study of other hospitals and other orthopaedic teams would improve the diversity of the acquired data. In particular, the evaluation of patients from public and private hospitals can also provide relevant information (the population that have access to private health care have mostly professions that do not require great physical effort while in public hospitals all kinds of professionals are treated including those that require more effort – e.g. industry professionals). It would be important, for instance, to check the differences in gait patterns between these two types of professionals.

In order to enable more acquisitions, an optimization of the developed acquisition protocols should be considered, decreasing the time required to prepare the subjects, acquire the data and process all the data and avoiding the long acquisition periods that can cause discomfort in the patients.

Regarding the inverse dynamics software applied in this work: OpenSim, some improvements can also be made. In particular, during the performance of the CMC analysis, problems were found when the ground reaction forces were distributed by the calcaneus and the toes. For that reason, the CMC results only considered the force applied in the calcaneus segment. In order to improve the reliability of the data would also be important to perform simulations with the forces correctly applied in the different segments and analyze the differences in the results. The analysis of the CMC results can also be complemented with electromyographic data, corroborating the muscle activations obtained with this methodology.

Lastly, the routines developed in this work for processing and presenting the data can be improved to allow their use by the medical community. For instance, to detect deviations to normality or to analyze and plot automatically the minimum and maximum values of some patterns, such as joint angles, torques and forces.

References

Aes, R. M., Opin, G. C., & Verous, C. A. (2006). Is percutaneous repair of the Achilles tendon a safe technique? A study of 124 cases. *Acta Orthopaedica*, *72*, 179–183.

CIR, S. (2011). *GAITRite Manual* (Version 4.). United States. Retrieved from www.gaitrite.com

C-Motion. (2014). VISUAL 3D. Retrieved from http://www.c-motion.com/products/visual3d/

Completo, A., & Fonseca, F. (2011). *Fundamentos de Biomecânica músculo-esquelética e ortopédica*. (Publiindústria - Edições Técnicas, Ed.) (pp. 1–119). Porto.

Costa, M. L., Kay, D., & Donell, S. T. (2005). Gait abnormalities following rupture of the tendo Achillis: a pedobarographic assessment. *Journal of Bone and Joint Surgery*, *87*(8), 1085–1088.

Coughlim, M., Mann, R., & Saltzman, C. (2007). *Surgery of the foot and ankle*. (Mosby, Ed.) (Eight Edit., pp. 1221–1267). Philadelphia.

Daniel, W., & Cross, C. (2013). *Biostatistics: a foundation for anlysis in health sciences* (Tenth Edit.).

Delp, S., Habib, A., & Seth, A. (2014). OpenSim - Project Overview - website. *Neuromuscular Models Library*. Retrieved from https://simtk.org/project/xml/downloads.xml?group_id=95#package_id1084

Delp, S. L., Anderson, F. C., Arnold, A. S., Loan, P., Habib, A., John, C. T., … Thelen, D. G. (2007). OpenSim: Open-Source Software to Create and Analyze Dynamic Simulations of Movement. *IEEE Transactions on Bio-Medical Engineering*, *54*(11), 1940–50. doi:10.1109/TBME.2007.901024

Digest, S. do R. (1997). *Enciclopédia de Medicina*.

EORIF.com. (2008). Ankle-Hindfoot Scale. Retrieved from http://eorif.com/AnkleFoot/AnkleFoot Outcms.html#Anchor-AOFAS-49575

Esperança Pina, J. A. (2010). *Anatomia Humana da Locomoção*. (Lidel, Ed.) (4ª ed.).

F, N., & Simsek, A. (2005). Evaluation of the surgical results of Achilles tendon ruptures by gait analysis and isokinetic muscle strength measurements. *Acta Orthopaedica*, *39*, 1–6.

Farlex. (2014). The Free Dictionary by Farlex. Retrieved from http://medical-dictionary.thefreedictionary.com/gait+cycle

Flores, P., Ambrósio, J., Claro, J. C. P., & Lankarini, H. M. (2008). *Kinematics and Dynamics of Multibody Systems with Imperfect Joints*.

Follak, N., Ganzer, D., & Merk, H. (2002). The utility of gait analysis in the rehabilitation of patients after surgical treatment of Achilles tendon rupture. *European Journal of Orthopaedic Surgery & Traumatology : Orthopedie Traumatologie*, *12*(2), 90–95. Retrieved from http://www.ncbi.nlm.nih.gov/pubmed/24570159

Gonçalves, S. (2010). *Advanced Computer Methods for Pathological and Non-Pathological Human Movement Analysis*. Instituto Superior Técnico - Universidade Técnica de Lisboa.

Gray, H. (2013). Anatomy of the Human Body. Retrieved from http://www.bartleby.com/107/

Hall, S. J. (2003). *Basic Biomechanics* (Fourth.).

Hamner, S. R., Seth, A., & Delp, S. L. (2010). Muscle contributions to propulsion and support during running. *Journal of Biomechanics*, *43*(14), 2709–16. doi:10.1016/j.jbiomech.2010.06.025

Herr, H. (2009). *An Introduction to human Gait*. Lisbon.

Hutton, W. C., & Dhanendran, M. (1979). A study of the distribution of load under the normal foot during walking. *International Orthopaedics*, *3*, 153–157.

INTEGRA. (2010). Minimally invasive Achilles suture system. Retrieved from http://www.ilstraining.com/mid hindfoot solutions/achillon/achillon_00.html

International, Rs. (2009). *User guide: Version 7 Gait software Footwear Adviser software*. Retrieved from http://www.rsscan.com

Khan, R. J. K., Fick, D., Brammar, T. J., Crawford, J., & Parker, M. J. (2004). Interventions for treating acute Achilles tendon ruptures. *The Cochrane Database of Systematic Reviews*, (3), CD003674. doi:10.1002/14651858.CD003674.pub2

Kuo, A. (2007). The six determinants of gait and the inverted pendulum: A dynamic walking prespective. *Human Movement Science*, *26*(4), 617–656.

Kuo, A., & Donelan, M. (2010). Dynamic Principles of Gait and Their Clinical Implications. *Physical Therapysical*, *90*(2), 157–174.

Lansdaal, J. R., Goslings, J. C., Reichart, M., Govaert, G. a M., van Scherpenzeel, K. M., Haverlag, R., & Ponsen, K. J. (2007). The results of 163 Achilles tendon ruptures treated by a minimally invasive surgical technique and functional after treatment. *Injury*, *38*(7), 839–44. doi:10.1016/j.injury.2006.12.010

Leardini, a, O'Connor, J. J., Catani, F., & Giannini, S. (1999). A geometric model of the human ankle joint. *Journal of Biomechanics*, *32*(6), 585–91. Retrieved from http://www.ncbi.nlm.nih.gov/pubmed/10332622

Lynch, R. M. (2004). Achilles tendon rupture: surgical versus non-surgical treatment. *Accident and Emergency Nursing*, *12*(3), 149–58. doi:10.1016/j.aaen.2003.11.004

Malaquias, T. (2013). *Development of a Three-Dimensional Multibody Model of the Human Leg and Foot for Application to Movement Analysis*. Instituto Superior Técnico - Universidade Técnica de Lisboa.

MathWorks. (2014a). Matlab - the language of technical computing. Retrieved from http://www.mathworks.com/products/matlab/index.html

MathWorks. (2014b). SimMechanics - Model and simulate multibody mechanical systems. Retrieved from http://www.mathworks.com/products/simmechanics/

Menezes, M. (2011). *Biomechanical Analysis of Surgical Movements in Robotic Hip Resurfacing*. Instituto Superior Técnico - Universidade Técnica de Lisboa.

Metric, Q. (2014). SF-36v2 Health Survey. Retrieved from http://www.qualitymetric.com/demos/TP_Launch.aspx?SID=100

Mezzaroba, S., Bortolato, S., Fancellu, G., Marcovich, R., & Valentini, R. (2012). Percutaneous repair of Achilles tendon ruptures with Tenolig: quantitative analysis of postural control and gait pattern. *Foot (Edinburgh, Scotland)*, *22*(4), 303–309.

Murray, M. P., Drought, A. B., & Ross, K. (1964). Walking Patterns of Normal Men. *The Journal of Bone & Joint Surgery*, *46*(2).

Nordin, M., & Victor, F. (2001). *Basic Biomecanics of the Musculoskeletal System* (Third.).

OpenSim. (2012). *OpenSim User's Guide*.

Orr, J. D., McCriskin, B., & Dutton, J. R. (2013). Achillon Mini-Open Achilles Tendon Repair: Early Outcomes and Return to Duty Results in U.S. Military Service Members. *Journal of Surgical Orthopaedic Advances*, *22*(01), 23–29. doi:10.3113/JSOA.2013.0023

Orthopedics, F. (n.d.). TENOLIG - Implant for percutaneous tenosynthesis of the Achilles tendon. Retrieved from http://www.fhortho.com/sites/default/files/Tenolig.pdf

Podiatry, F. F. (2014). Feet First - Podiatry.

Qualysis. (2014). Qualysis Track Manager - website. Retrieved from http://www.qualisys.com

Raja, B., Neptune, R. R., & Kautz, S. A. (2012). Quantificable patterns of limb loading and unloading during hemiparetic gait : Relation to kinetic and kinematic parameters, *49*(9), 1293–1304.

Rodgers, M. M. (1988). Dynamic biomechanics of the normal foot and ankle during walking and running. *Physical Therapy*, *68*(12), 1822–30. Retrieved from http://www.ncbi.nlm.nih.gov/pubmed/3057519

Sasaki, K., & Neptune, R. R. (2006). Differences in muscle function during walking and running at the same speed. *Journal of Biomechanics*, *39*(11), 2005–13. doi:10.1016/j.jbiomech.2005.06.019

Saunders, J. B., Inman, V. T., & Eberhart, H. D. (1953). The major determinants in normal and pathological gait. *The Journal of Bone and Joint Surgery. American Volume*, *35-A*(3), 543–58. Retrieved from http://www.ncbi.nlm.nih.gov/pubmed/13069544

Seeley, R., Stephens, T., & Tate, P. (2008). *Anatomy & Physiology*.

Seth, A., Sherman, M., Reinbolt, J., & Delp, S. L. (2011). OpenSim: a musculoskeletal modeling and simulation framework for in silico investigations and exchange. *Procedia IUTAM*, 212–232.

Silva, M., & Ambrósio, J. A. . (2003). Solution of Redundant Muscle Forces in Human Locomotion with Multibody Dynamics and Optimization Tools. *Mechanics Based Design of the Structures and Machines*, *31*(3), 381–411.

Silva, M. T. (2003). *Human Motion Analysis using Multibody Dynamics and Optimization Tools*. Instituto Superior Técnico - Universidade de Lisboa.

Silva, M. T. (2012). Biomechatronics course unit - Master Degree in Biomedical Technologies.

Taglialavoro, G., Biz, C., Mastrangelo, G., & Aldegheri, R. (2011). The repair of the Achilles tendon rupture: comparison of two percutaneous techniques. *Strategies in Trauma and Limb Reconstruction (Online)*, *6*(3), 147–54. doi:10.1007/s11751-011-0124-1

Thelen, D. G., & Anderson, F. C. (2006). Using computed muscle control to generate forward dynamic simulations of human walking from experimental data. *Journal of Biomechanics*, *39*(6), 1107–15. doi:10.1016/j.jbiomech.2005.02.010

Vaughan, C. L., Davis, B. L., & O'Connor, J. C. (1999). *Dynamics of Human Movement*.

Whittle, M. (2001). *Gait analysis: an introduction* (Third Edit.).

Winter, D. A. (1991). *The Biomechanics and Motor Control of Human Gait: Normal, Elderly and Pathological*.

Appendix

Appendix I – Clinical rating system for the ankle and hind foot – AOFAS Score

Section 1 – Pain
None
Mild Occasional
Moderate, daily
Severe, almost always present

Section 2 – Function activity limitations/support
No limitations, no support
No limitation of daily activities, limitation of recreational activities, no support
Limited daily and recreational activities, cane
Limited daily and recreational activities, cane
Severe limitation of daily and recreational activities, walker, crutches, wheelchair, brace

Section 3 – Maximum walking distance (blocks)
Greater than 6
4-6
1-3
Less than 1

Section 4 – Walking surfaces
No difficulty on any surface
Some difficulty on uneven terrain, stairs, inclines, ladders
Severe difficulty on uneven terrain, stairs, inclines, ladders

Section 5 – Gait Abnormality
None, slight
Obvious
Marked

Section 6 – Sagittal motion (flexion plus
Normal or mild restriction (30° or more)
Moderate restriction (15° - 29°)
Severe restriction (less than 15°)

Section 7 – Hind foot motion (inversion plus
Normal or mild restriction (75% - 100%)
Moderate restriction (25% - 74% normal)
Marked restriction (less than 25% normal)

Section 8 – Alignment
Good, plantigrade foot, ankle, hind foot
Fair, plantigrade foot, some degree of ankle hind foot
Poor, nonplantigrade foot, severe malalignment.

Section 9 – Ankle hind foot stability
Stable
Definitely unstable

Appendix II – SF-v36

1. In general, would you say your health is:				
Excellent	Very Good	Good	Fair	Poor

2. Comparated to one year ago, how would you rate your health in general now?				
Much better now than one year ago	Somewhat better now than one year ago	About the same as one year ago	Somewhat worse now than one year ago	Much worse now than on year ago

3. During the past 4 weeks, how much of the time have you had any of the following problems with your work or other regular daily activities as a result of your physical health?						
		All of the time	Mosto of the time	Some of the time	A little of the time	None of the time
a)	Cut down on the amount of time you spent on work or other activities.					
b)	Accomplished less than you would like.					
c)	Were limited in the kind of work or other activities.					
d)	Had difficulty performing the work or other activities (for example, it took extra effort).					

4. During the past 4 weeks, how much of the time have you had any of the following problems with your work or other regular daily activities as a result of any emotional problems (such as feeling depressed or anxious)						
		All of the time	Mosto of the time	Some of the time	A little of the time	None of the time
a)	Cut down on the amount of time you spent on work or other activities					
b)	Accomplished less than you would you like					
c)	Did work or other activities less carefully than usual					

5. During the past 4 weeks, to what extent has your physical health or emotional problems interfered with your normal social activities with family, friends, neighbors, or groups.				
Not all	Slightly	Moderately	Quite a bit	Extremely

6. During the past 4 weeks, how much did pain interfere with your normal work (including both work outsider the home and housework)?				
Not all	A little bit	Moderately	Quite a Bit	Extremely

7. How much bodily pain have you had during the past 4 weeks					
None	Very mild	Mild	Moderate	Severe	Very severe

8. These questions are about how you feel and how things have been with you during the past 4 weeks. For each question, please give the one answer that comes closest to the way you have been feeling. How much of the time during the past 4 weeks.

		All of the time	Mosto of the time	Some of the time	A little of the time	None of the time
a)	Did you feel full of life?					
b)	Have you been very nervous?					
c)	Have you felt so down in the dumps that nothing could cheer you up?					
d)	Have you felt calm and peaceful?					
e)	Did you have a lot of energy?					
f)	Have you felt downhearted and depressed?					
g)	Did you feel worn out?					
h)	Have you been happy?					
i)	Did you feel tired?					

9. During the past 4 weeks, how much of the time has your physical health or emotional problems interfered with your social activities (like visiting friends, relatives, etc.)?

All of time	Most of the time	Some of the time	A little of the time	None of the time

10. How true or false is each of the following statements for you?

		Definitely true	Mostly true	Don't Know	Mostly False	Definitely False
a)	I seem to get sick a little easier than other people.					
b)	I am as healthy as anybody I know.					
c)	I expect my health to get worse.					
d)	My health is excelente.					

Appendix III – Static Images of Plantar Pressures of patients

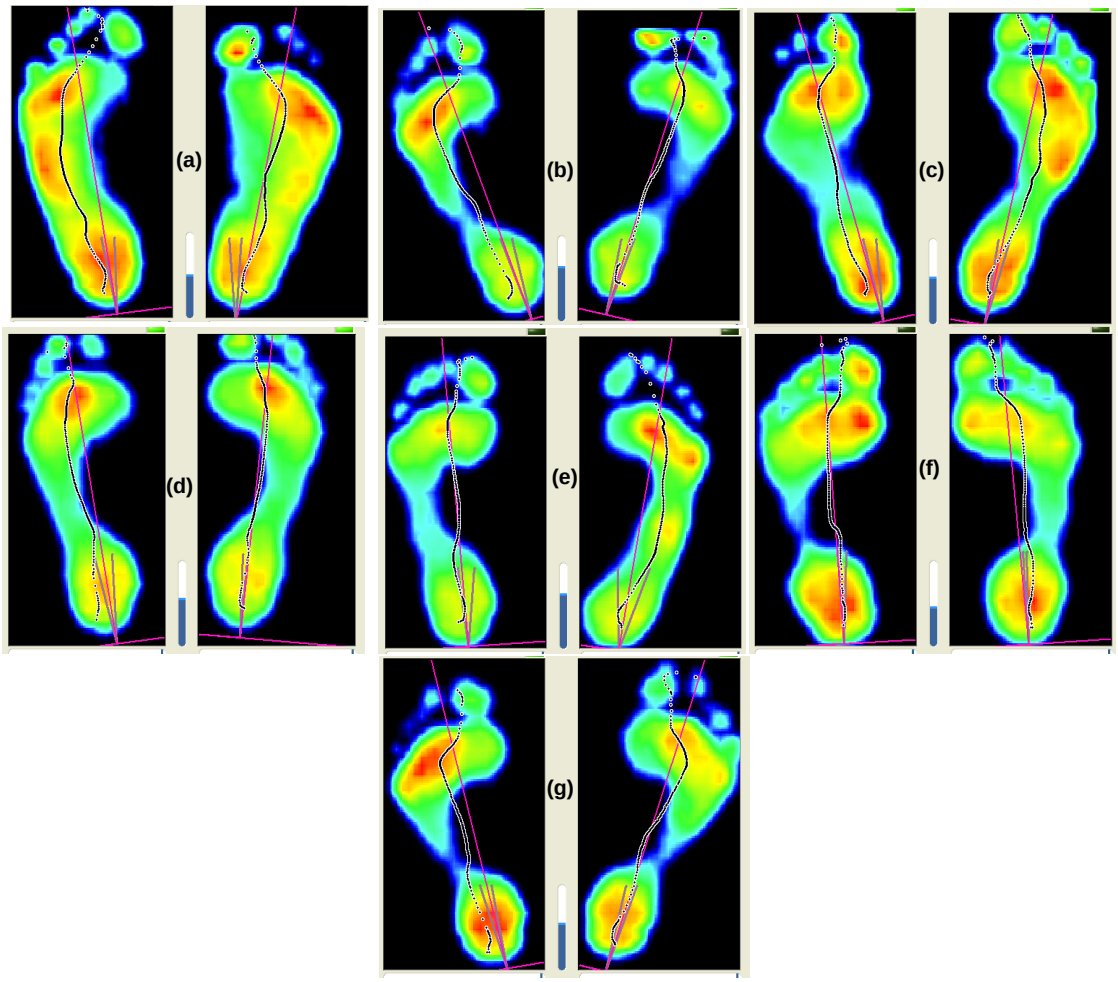

(a) Patient 1, (b) Patient 2 , (c) Patient 3, (d) Patient 4, (e) Patient 5, (f) Patient 6 and (g) Patient 7.

Appendix IV – Graphs of Control Group

IK Graphs of Control Group

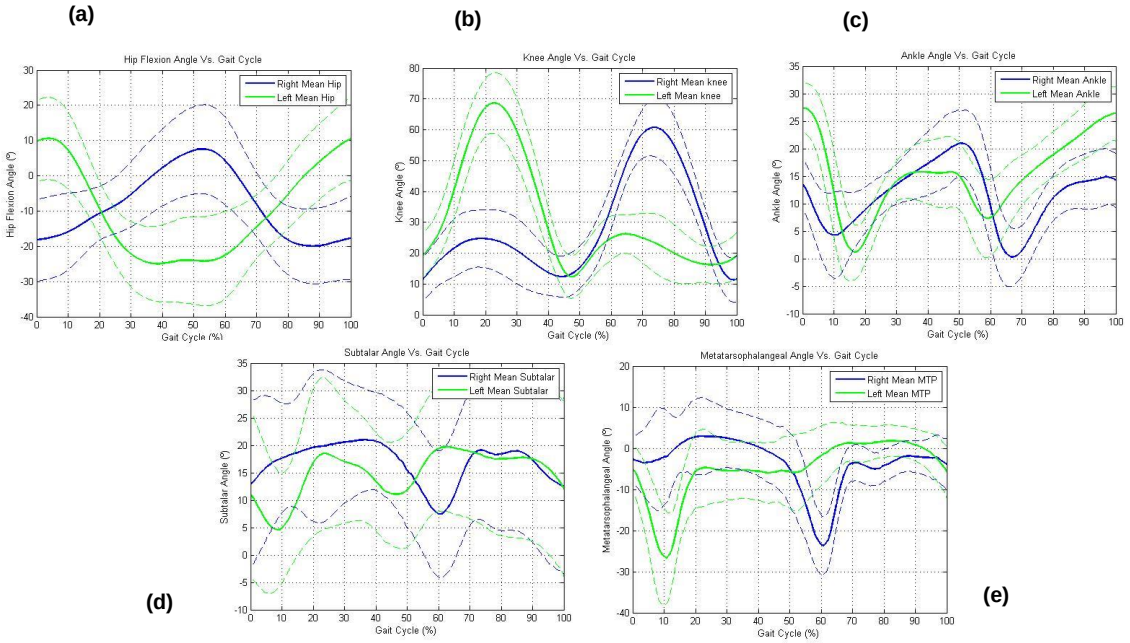

(a) Hip Flexion Angle, (b) Knee Angle, (c) Ankle Angle, (d) Subtalar Angle and (e) Metatarsophalangeal Angle.

ID Graphs of Control Group

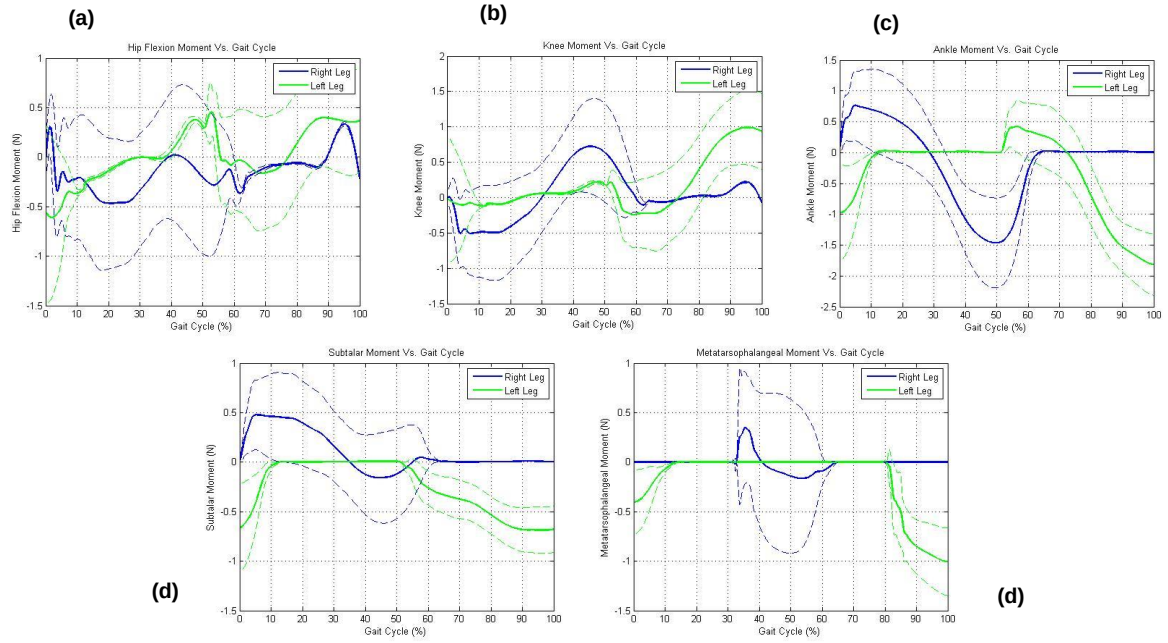

(a) Hip Flexion Moment, (b) Knee Moment, (c) Ankle Moment, (d) Subtalar Moment and (e) Metatarsophalangeal Moment.

CMC Graphs of Control Group

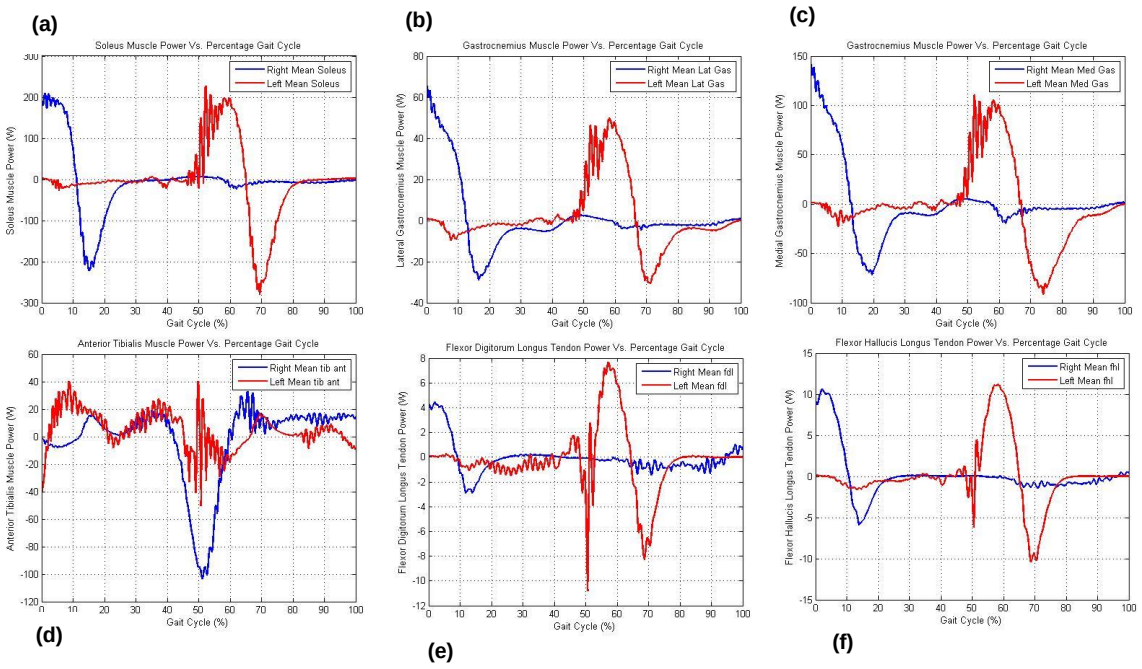

Muscle Power of *Soleus* (a), *Medial Gastrocnemius* (b), *Lateral Gastrocnemius* (c), *Anterior Tibialis* (d), *Flexor Hallucis Longus* (e), *Flexor Digitorum Longus* (f) vs Gait Cycle of Control Group.

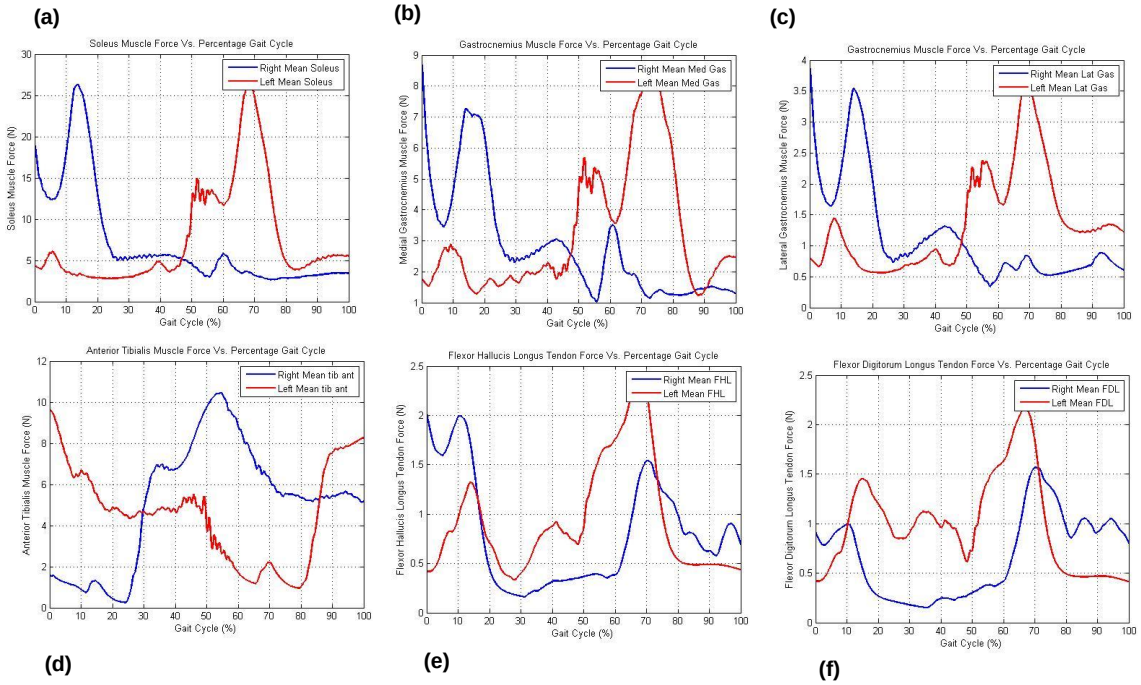

Muscle Force of *Soleus* (a), *Medial Gastrocnemius* (b), *Lateral Gastrocnemius* (c), *Anterior Tibialis* (d), *Flexor Hallucis Longus* (e), *Flexor Digitorum Longus* (f) vs Gait Cycle of Control Group.